INFORMATION TO USERS

This manuscript has been reproduced from the microfilm master. UMI films the text directly from the original or copy submitted. Thus, some thesis and dissertation copies are in typewriter face, while others may be from any type of computer printer.

The quality of this reproduction is dependent upon the quality of the copy submitted. Broken or indistinct print, colored or poor quality illustrations and photographs, print bleedthrough, substandard margins, and improper alignment can adversely affect reproduction.

In the unlikely event that the author did not send UMI a complete manuscript and there are missing pages, these will be noted. Also, if unauthorized copyright material had to be removed, a note will indicate the deletion.

Oversize materials (e.g., maps, drawings, charts) are reproduced by sectioning the original, beginning at the upper left-hand corner and continuing from left to right in equal sections with small overlaps.

ProQuest Information and Learning
300 North Zeeb Road, Ann Arbor, MI 48106-1346 USA
800-521-0600

University of Alberta

Characterization of the large mammalian Arf-GEFs: GBF1 and BIGs

by

Xinhua Zhao 

A thesis submitted to the Faculty of Graduate Studies and Research in partial fulfillment of the requirements for the degree of Doctor of Philosophy

Department of Cell Biology

Edmonton, Alberta

Fall 2005

Dedication

To my parents, Erji Zhao and Zhiyin He

for their unconditional support

To my husband, Dr. Brian Yaozhu Yu

for continued love and encouragement

To our daughter, Sabrina Fengjing Yu

for being my angel and the love of my life

Abstract

Small GTPases of the ADP-ribosylation factor (Arf) family regulate assembly of several types of coat proteins implicated in protein traffic. Arf activation is stimulated by guanine nucleotide exchange factors (GEFs) that catalyze replacement of GDP with GTP. My thesis project focused on two families of large mammalian Arf-GEFs termed GBF1 and BIG1/2 and aimed to characterize their relative sub-cellular localizations and functions. Quantitative confocal immunofluorescence microscopy with new anti-GBF1 and anti-BIG1 antibodies established for the first time that GBF1 and BIGs localize to distinct Golgi sub-compartments. Specifically, I demonstrated that GBF1 and BIG1 associate with *cis*- and *trans*- Golgi compartments, respectively, where they overlap preferentially with the COPI and clathrin coats, respectively. These observations suggest that the function of GBF1 and BIGs may not be limited to Arf activation but may also include selection of protein coats for recruitment at unique locations. Interestingly, GBF1 not only redistributed to peripheral vesicular tubular clusters (VTCs) after incubation at 15°C, but at steady-state could also be detected on peripheral structures in close proximity to endoplasmic reticulum exit sites. This result prompted me to further explore the dynamics of membrane recruitment of GBF1. I took advantage of a GFP-tagged form of GBF1 that displayed properties similar to those of the endogenous protein. Live cell fluorescence recovery after photobleaching (FRAP) analysis revealed that GBF1 rapidly cycles between the cytosol and the membranes of both juxtanuclear *cis*-Golgi and the peripheral VTCs with a $t_{1/2}$ of 16 sec. Brefeldin A (BFA) treatment blocked this dynamic exchange by stabilizing GBF1 on the membrane. The BFA-induced membrane

accumulation of GBF1 appeared to coincide with the BFA-induced membrane dissociation of COPI. The possibility that GBF1 regulates COPI membrane recruitment was confirmed by the striking result that microinjection of anti-GBF1 antibodies specifically caused dissociation of COPI, but not clathrin from the membranes. In summary, the results presented in this thesis provide the basis for a functional understanding of involvement of Arf-GEFs in distinct stages of protein traffic.

Acknowledgements

Completing a Ph.D. program indeed needs strong determination, and I would not have been able to complete this journey without the help and support of many important people in my life. First of all, I would like to extend my greatest appreciation to my supervisor, Dr. Paul Melançon. It is a big honor for me to be his 1st Ph.D. student at University of Alberta. His constant encouragement and enthusiasm have led me through the graduate program. He shows me how to be both a good scientist and a decent person. I feel extremely lucky to be his student.

I would also like to acknowledge my supervisory committee, Dr. Tom Hobman and Dr. Ellen Shibuya for their advice, comments and critical reviews of this project. Also, I would like to thank Dr. Michael Hendzel and Dr. Sergio Grinstein for being part of my thesis defense committee.

It has been a great pleasure to work with the fellow students and postdocs in the lab, both past and present, Dr. Alejandro Claude, Justin Chun, Troy Lasell, Mary Schneider and Dr. David Sheilds. I am especially grateful to the help of Florin Manolea who helped me prepare one poster until 1 am in the early morning.

I appreciate the help from our excellent technical staff, both past and present, Anita Gilchrist, Margaret Hughes, Heather Vanderthol-Vanier and Bao-Ping Zhao. I also thank the great help from our collaborators, Dr. John Presley. Extra thanks go to Honey Chan, Dr. Xue-jun Sun, Xinmei Chen and Dr. Zhixiang Wang for the great help for live cell imaging and microinjection.

I would also like to thank the Department of Cell Biology, the Faculty of Graduate Studies and Research, the CIHR and the Alberta Heritage Foundation for Medical Research for the financial support provided throughout my studies.

Finally, I am extremely grateful to my family. My parents, Erji Zhao and Zhiyin He have given me tremendous support both financially and mentally throughout my life. I especially thank my husband Dr. Brian Yu for his dearest love and support. He gave me so much encouragement. Without him, I won't finish my program. I also want to mention our lovely 1-year-old daughter Sabrina (Jingjing) who has brought to me so much joy in my life. She always gives me the strength to be the best model for her.

Table of contents

List of Tables

List of Figures

Abbreviations

AP	adaptor protein
Arf	ADP-ribosylation factor
BARS	BFA-dependent ADP-ribosyl transferase substrate
BFA	brefeldin A
BIG	BFA-inhibited GEF
CCV	clathrin-coated vesicle
CHO	Chinese hamster ovary
COP	coat protein
DCB	Dimerization / Cyclophilin Binding
DMSO	dimethyl sulfoxide
ER	endoplasmic reticulum
ERES	ER exit site
ERGIC	ER-Golgi intermediate compartment
EM	electron microscopy
FAPP	four-phosphate-adaptor protein
FBS	fetal bovine serum
FRAP	fluorescence recovery after photobleaching
GAP	GTPase activating protein
GBF	Golgi-specific BFA resistance factor
GEF	guanine nucleotide exchange factor
GFP	green fluorescent protein
GGA	Golgi-associated γ-adaptor ear homology, Arf binding proteins
HA	hemagglutinin
IF	immunofluorescence
IP	immunoprecipitation
ManII	mannosidase II
NRK	normal rat kidney
PA	phosphatidic acid
PBS	phosphate buffered saline
PH	plekstrin homology
PI	phosphoinositide
PM	plasma membrane
PtdIns(4)P	phosphatidylinositol 4-phosphate
PtdIns(4,5)P_2	phosphatidylinositol 4,5-bisphosphate
PtdIns(3,4,5)P_3	phosphatidylinositol 3,4,5-trisphosphate
Sec7d	Sec7 domain
SNARE	soluble N-ethylmaleimide-sensitive factor attachment protein receptor
tER	transitional ER
TGN	*trans*-Golgi network
VSV	vesicular stomatitis virus
VSVG	VSV-glycoprotein
VTC	vesicular tubular cluster

Chapter 1

Introduction

1.1. Endomembrane systems and the secretory pathway

Eukaryotic cells possess an elaborate endomembrane system that is responsible for the exchange of macromolecules between cells and their environment. In this system, the secretory pathway delivers newly synthesized proteins, carbohydrates and lipids to the cell surface or the outside of the cell; the lysosomal/vacuolar pathway specifically sorts lysosomal/vacuolar proteins from other secretory proteins and transports them to the lysosomes/vacuoles; and the endocytic pathway takes up macromolecules into the cell (Bonifacino and Glick, 2004; Lippincott-Schwartz, 2001).

As illustrated in Figure 1.1, the secretory membrane system consists of a number of distinct membrane-bounded organelles, including the endoplasmic reticulum (ER), vesicular tubular clusters (VTCs) (only for mammalian cells), Golgi complex, and plasma membrane (PM). These organelles function sequentially to facilitate protein secretion to the extracellular environment. In this system, secretory cargo is first synthesized and assembled in the ER, and then transported to the Golgi complex for further post-translational processing. Upon arrival at the *trans* Golgi network (TGN), it is sorted and packaged into post-Golgi carriers that move through the cytoplasm to fuse with the cell surface. This anterograde transport towards the cell surface is balanced by retrograde membrane flow, which is responsible for retrieving escaped ER-resident proteins and recycling transport components needed for ER export (Sannerud et al., 2003).

1.1.1 Protein coats and production of cargo carriers

Intracellular membrane traffic between the organelles of the secretory pathway is mediated by transport intermediates that are released from a donor organelle and fuse with an appropriate acceptor organelle (Bonifacino and Glick, 2004). The formation of

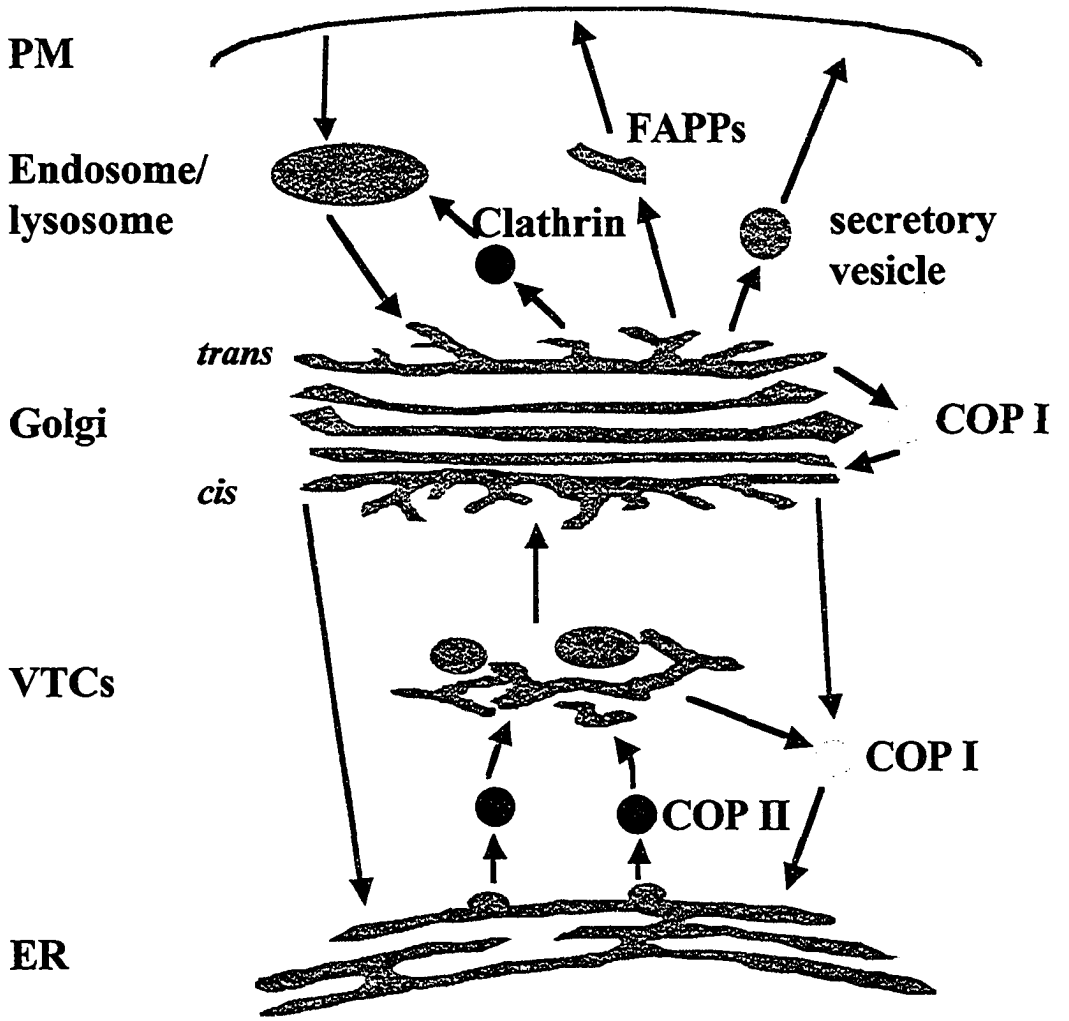

Figure 1.1. Schematic diagram of membrane traffic pathways and associated coat proteins (simplified scheme). Green and red arrows represent anterograde and retrograde transport pathways, respectively. COPII and COPI coated carriers mediate transport between the ER and *cis*-Golgi compartments, while CCVs carry cargo between the TGN and endosome/lysosomes. Secretory vesicles and the newly described FAPPs-coated carriers are responsible for regulated and constitutive transport between the TGN and the PM. Retrograde transport from the Golgi complex to the ER occurs through both COPI-dependent and COPI-independent pathways. For details see text.

transport vesicles and sorting of cargo into the vesicles are largely mediated by protein coats (Bonifacino and Lippincott-Schwartz, 2003). To date, four types of coated structures have been described (see Figure 1.1). Transport between the ER and the Golgi complex involves two types of vesicles coated with protein complexes, which are named as coat protein (COP)I and COPII. Clathrin-coated vesicles (CCVs) mediate post-Golgi and endocytic transport processes (Bonifacino and Lippincott-Schwartz, 2003). The fourth type of membrane carriers that appear coated with newly identified proteins termed the four-phosphate-adaptor proteins (FAPPs) are believed to carry cargo from the TGN to PM (Godi et al., 2004). Whether FAPP-coated structures are identical to the lace-like coated structures identified on *trans*-cisternae in tomographic studies (Ladinsky et al., 1994; Ladinsky et al., 1999) remains to be determined.

1.1.2 Tethering and fusion of cargo carriers

Specific tethering and fusion of cargo carriers to their target compartment involves several large protein families, including SNAREs (soluble N-ethylmaleimide-sensitive factor attachment protein receptors), tethering factors and Rabs. SNAREs, integral membrane proteins found in both vesicles (v-SNAREs) and target membranes (t-SNAREs), play central roles in membrane fusion. Pioneering work by the Rothman group led to the production of the SNARE hypothesis, which proposed that each type of cargo carrier contains one specific v-SNARE that binds to three cognate t-SNAREs at the target membrane (Rothman and Warren, 1994). Formation of SNARE complexes not only promotes membrane fusion itself, but also provides some level of specificity in membrane fusion (Bonifacino and Glick, 2004). Although purified SNAREs interacted promiscuously *in vitro*, SNARE pairing was almost exclusively restricted to

physiologically relevant v- and t-SNARE combinations in the presence of liposomes (McNew et al., 2000). However, the demonstration that some SNAREs participate at multiple transport steps *in vivo* indicates that SNAREs cannot be the sole determinant of specificity for membrane fusion (Waters and Pfeffer, 1999).

Tethering factors that act prior to vesicle docking provide additional specificity. They are called tethering factors because they form physical links between vesicles and target membrane that appear to facilitate the initial contact between a transport vesicle and its target membrane (Lupashin and Sztul, 2005; Pfeffer, 2001). Tether formation involves two broad families of proteins that consist of either multi-subunit complexes or long coiled-coil proteins. The first family consists of multi-component complexes that can contain as many as ten distinct subunits and function at specific steps of protein traffic (Oka and Krieger, 2005). For example, TRAPP I and DslI have been implicated in anterograde and retrograde traffic, respectively, between the ER and Golgi complex, while other complexes regulate traffic within the Golgi (COG), from the Golgi complex to the endosome (TRAPP II) or the PM (Exocyst) (Lupashin and Sztul, 2005; Oka and Krieger, 2005; Whyte and Munro, 2002). The second family consists of long coiled-coil tethers, often called golgins, which are present in the Golgi complex (Barr and Short, 2003). Golgins have been shown to interact with proteins on the vesicle and proteins of the target when a vesicle becomes tightly apposed to the target membrane (Pfeffer, 2001). For many transport steps, tethering factors are recruited onto membranes by Rab family GTPases (Guo et al., 2000). More than sixty mammalian Rabs participate in a variety of distinct membrane traffic events (Seabra and Wasmeier, 2004). The demonstration that each Rab localizes to a unique intracellular compartment suggests that Rabs collaborate

with tethers and SNAREs to provide specificity for the tethering and fusion of cargo carriers to their target membrane (Pfeffer and Aivazian, 2004).

1.2. Early secretory pathway: transport between the ER and Golgi complex

Transport between the ER and Golgi complex is the first step in protein secretion and the compartments involved in this step are always referred to as the early secretory pathway (Barlowe, 2000; Nickel and Wieland, 1998). This section describes the bi-directional protein transport between the ER and the Golgi complex, beginning with the introduction of protein export from the ER, followed by the involvement of VTCs in ER-to-Golgi transport and a description of COPI-dependent and COPI-independent retrograde transport, and finishing with a section about the role of COPI in anterograde ER-to-Golgi traffic.

1.2.1. Protein export from the ER

The export of newly synthesized proteins from the ER is mediated by COPII-coated vesicles that bud at specialized ER regions called either ER exit sites (ERESs) or transitional ER (tER). tER sites are long-lived, ribosome-free subdomains of the ER that are specialized for the production of COPII transport vesicles (Palade, 1975; Mancias and Goldberg, 2005).

The COPII coat consists of the small GTPase Sar1p, and two heterodimeric protein complexes, Sec23/Sec24p and Sec31/Sec13p (Barlowe et al., 1994). Budding of COPII coated vesicles is initiated when a transmembrane ER protein, Sec12p, converts Sar1p from the GDP-bound to GTP-bound form (Futai et al., 2004). Sar1p-GTP then tightly binds to ER membrane via a GTP-triggered membrane anchor (Bi et al., 2002).

Sar1p activation then initiates the recruitment of several proteins. First, the Sec23/24p complex is recruited. Next, Sec23/24p-Sar1p selects cargo, cargo receptor molecules and SNAREs, to form a so-called prebudding complex (Sato, 2004). Subsequently, the Sec13/31p complex binds and likely induces coat polymerization and drives membrane deformation (Matsuoka et al., 1998). In addition, the binding of Sec13/31p leads to increased Sar1p-specific GTPase-activating protein (GAP) activity mediated through the action of Sec23p (Antonny et al., 2001), which facilitates Sar1p to hydrolyse its GTP and in turn triggers coat disassembly.

A large number of cargo proteins have been demonstrated to be concentrated into COPII-coated vesicles upon ER exit (Barlowe, 2003a; Barlowe, 2003b). They bind directly to COPII (Aridor et al., 1998; Kuehn et al., 1998; Miller et al., 2003; Mossessova et al., 2003a) or indirectly via cargo receptor molecules, such as ERGIC-53 (Appenzeller et al., 1999) and p24 (Muniz et al., 2000). The Sec24p subunit of the coat has been shown to be involved in cargo binding (Miller et al., 2002). The direct binding of COPII coat and transmembrane cargo proteins or cargo receptor proteins is mediated by sorting signals that are found in the cytosolic domains of these cargo proteins. These signals are quite diverse and include di-acidic motifs, short hydrophobic motifs and dibasic motifs (Barlowe, 2003b).

1.2.2. Role of VTCs in ER-to-Golgi transport

In mammalian cells, transport of proteins from the ER to the Golgi complex involves discrete membrane-bound structures, which have been called pre-Golgi intermediates (Saraste and Kuismanen, 1992), ER-Golgi intermediate compartment (ERGIC) (Hauri and Schweizer, 1992) or VTCs (Bannykh et al., 1996). Throughout the

thesis, I refer to these structures as VTCs to emphasize their morphological properties (Bannykh and Balch, 1997).

VTCs operating in ER-to-Golgi transport have not been identified in *S.cerevisiae.* This may be a direct result of the different organization of the Golgi in these cells. A scattered Golgi in *S.cerevisiae* is in close proximity to the ER and may not require VTCs to mediate the long-range transport from peripheral ER exits sites to the juxtanuclear Golgi complex observed in mammalian cells (Stephens and Pepperkok, 2001). In animal cells, live cell imaging using a green fluorescent protein (GFP)-cargo chimera revealed that VTCs migrated towards the Golgi in a saltatory fashion at ~1 μm/s along microtubules by using the microtubule minus-end-directed dynein-dynactin motor complex (Presley et al., 1997; Scales et al., 1997). In agreement with their function, VTCs localize in both the juxtanuclear region (at the *cis*-face of the Golgi) and at the cell periphery (Klumperman et al., 1998).

The buds on VTCs display an electron-dense coat that is different from COPII. This coat, referred to as COPI, was originally identified as the proteinaceous material responsible for coating vesicles formed at the periphery of the Golgi complex (Orci et al., 1986) (Waters et al., 1991). The demonstration that treatment of cell extracts with a nonhydrolyzable analog of GTP, GTPγS led to the dramatic accumulation of coated vesicles near Golgi stacks facilitated the subsequent purification and identification of COPI (Melançon et al., 1987). The COPI coat is composed of 7 subunits, four of them have sequence homology to the clathrin-binding adaptor protein (AP) complexes (Cosson et al., 1996; Duden et al., 1991; Hoffman et al., 2003; Serafini et al., 1991). These subunits pre-assemble into a stable cytosolic protein complex termed coatomer before

they are recruited to the membrane following activation of the small GTPase Arf1 (discussed in detail in section **1.4**) (Elsner et al., 2003; Hara-Kuge et al., 1994).

The biogenesis of VTCs remains quite controversial. It has been long assumed that VTCs arise by homotypic fusion of uncoated COPII vesicles and recent experimental evidence has confirmed that COPII vesicles possess the machinery for homotypic fusion (Xu and Hay, 2004). However, this COPII-dependent mechanism has been seriously challenged by work from Mironov and colleagues (Mironov et al., 2003) who observed production of large non-vesicular carriers from the ER, next to COPII-positive ERES. This formation process is COPII-dependent but does not involve budding and fusion of COPII-dependent vesicles (Mironov et al., 2003).

Pre-formed COPI complexes are recruited from the cytosol to nascent VTCs to initiate their microtubule dependent movement toward the Golgi complex (Presley et al., 1997; Scales et al., 1997; Stephens et al., 2000). COPI also functions to mature VTCs into a polarized structure with separate COPI-rich and anterograde-cargo-rich domains as they move towards the Golgi complex (Shima et al., 1999). This is consistent with data from quantitative immuno-electron microscopy (EM) analyses demonstrating a role for VTCs in the concentration of soluble secretory proteins by exclusion from COPI-coated vesicles (Martinez-Menarguez et al., 1999; Oprins et al., 2001). In contrast to membrane proteins that were concentrated into COPII-coated carriers at ERES, the soluble secretory proteins, such as amylase and chymotrypsinogen, exhibited similar concentrations in the ER and ERES and were first concentrated in VTCs where they were excluded from COPI-coated buds (Martinez-Menarguez et al., 1999).

1.2.3. COPI-dependent and COPI-independent retrograde transport

In the secretory pathway, the anterograde membrane flow from the ER to the Golgi complex is balanced by retrograde transport, which functions to retrieve escaped ER resident proteins and lipids, as well as to recycle components of the transport machinery. As illustrated in Figure 1.1, two retrograde transport mechanisms exist in mammalian cells, one is mediated by COPI coated vesicles, and the other is independent of known coat proteins [for a review, see (Elsner et al., 2003)].

COPI plays an essential role in retrograde Golgi-to-ER transport (Letourneur et al., 1994; Orci et al., 1997). It involves the KDEL receptor that retrieves KDEL-bearing lumenal ER proteins from post-ER compartments (Majoul et al., 1998; Majoul et al., 2001). The KDEL receptor and other membrane proteins that are transported back to the ER from the Golgi contain a cytoplasmic, carboxy-terminal dilysine signal KKXX. This sorting sequence, which binds to a complex of the COPI α and β subunits, is both necessary and sufficient to direct retrograde transport of membrane proteins (Cosson and Letourneur, 1994; Velloso et al., 2002). Some type II membrane proteins are also retrieved by COPI using a di-arginine motif present at their N-terminus (Teasdale and Jackson, 1996). VTCs play an important role in COPI-dependent retrieval, which can occur from as far as TGN (Miesenbock and Rothman, 1995).

In addition to the COPI-dependent pathway, evidence suggest that certain toxins such as Shiga toxin that lack KDEL or KDEL-like motif, as well as Golgi-resident glycosylation enzymes, utilize a COPI-independent pathway (Sandvig and van Deurs, 2002; Storrie et al., 2000). Contrary to the extensively studied COPI-dependent pathway, little is known of the molecular machinery operating in the COPI-independent route,

except that it involves the function of the Rab6A GTPase (Girod et al., 1999; White et al., 1999). More recently, Rab6A was shown to interact with the microtubule dynein-dynactin motor complex, suggesting that the minus-end-directed movement could reflect a recycling process of some machinery components that function in the COPI-independent pathway (Matanis et al., 2002; Short et al., 2002).

1.2.4. Role of COPI in anterograde ER-to-Golgi traffic

COPI-coated transport carriers appear to be involved at several stages of the early secretory pathway. As mentioned above (section 1.2.3), work performed with both yeast and mammalian systems established that COPI plays an essential role in retrograde Golgi-to-ER transport (Letourneur et al., 1994; Majoul et al., 1998; Orci et al., 1997). But whether the COPI coat is directly involved in anterograde ER-to-Golgi transport or transport of cargo across the Golgi stack remains controversial. Several lines of evidence support a role for COPI in anterograde transport from the ER to Golgi complex. For example, antibodies against β–COP inhibited the transport of a temperature-restricted mutant form of the Vesicular Stomatitis Virus (VSV) Glycoprotein (VSV-G) from the ER to the Golgi complex both *in vivo* (Pepperkok et al., 1993) and *in vitro* (Peter et al., 1993). Also, a Chinese hamster ovary (CHO) cell line expressing a mutant form of ε–COP is defective in ER-Golgi transport at the non-permissive temperature (Guo et al., 1994). However, the precise molecular role for COPI in anterograde transport is far from clear. It has been suggested that soluble anterograde-moving cargo can be concentrated by exclusion from COPI-coated domains at VTCs (Martinez-Menarguez et al., 1999) (refer to section 1.2.2), or that there exists an early COPI-dependent cargo-sorting step at VTCs in mammalian cells (Stephens and Pepperkok, 2002). In agreement with such

diverse functions, COPI localizes to several compartments of the secretory pathway, with greatest abundance in VTCs and *cis*-elements of the Golgi stack (Griffiths et al., 1995; Oprins et al., 1993).

1.3. The Golgi complex

The Golgi complex in mammalian cells consists of a ribbon-like structure in which stacks of cisternae alternate with regions of tubules and vesicles; and it is often located in the juxtanuclear regions of the cell (Ladinsky et al., 1999; Marsh et al., 2001; Rambourg and Clermont, 1990). It functions to covalently modify proteins and lipids, and to sort and package these molecules for transport to their sites of function. All of these events proceed in an orderly fashion from *cis, medial* to *trans*-compartments, across the stacked Golgi membranes (Farquhar and Palade, 1998). Four aspects of the Golgi complex will be discussed in this section. I first present an overview of the molecular composition of the Golgi complex, followed by a brief summary of the two current competing models of protein transport across the Golgi stacks: vesicular transport versus cisternal maturation. I then address the properties of the TGN where cargo molecules are sorted and exit from the Golgi, and finally end with a discussion of the role of lipids within the Golgi complex.

1.3.1. Molecular composition of the Golgi complex

The Golgi complex contains thousands of different types of integral and peripheral membrane proteins (Bell et al., 2001; Wu et al., 2000). These proteins can be categorized into four classes based on their contribution to Golgi function and maintenance. These four classes are (1) processing enzymes (such as Mannosidase II

(ManII) (2) itinerant proteins (such as ERGIC53 and p24 proteins); (3) scaffold proteins (such as GRASP65 and GM130); and (4) coat proteins and other peripheral proteins (such as COPI and Arf1) (Altan-Bonnet et al., 2004; Ward et al., 2001). The first two classes are integral membrane proteins; and the last two are peripheral membrane proteins. Surprisingly, fluorescence recovery after photobleaching (FRAP) experiments revealed that no classes of Golgi proteins stably associate with the Golgi membranes, supporting the view of the Golgi complex as a dynamic, steady-state organelle (Presley et al., 2002; Ward et al., 2001; Zaal et al., 1999). The residency times as measured by FRAP vary enormously: processing enzymes stay within the Golgi complex for up to 60 min, while itinerant proteins transit within 10 min and most other peripheral proteins exchange extremely rapidly with half-time of 1 min or less (Presley et al., 2002; Ward et al., 2001).

1.3.2. Protein transport across the Golgi stacks: vesicular transport versus cisternal maturation

Two conflicting models represented in a diagram form in Figure 1.2 have been proposed for transport of cargo through the Golgi complex. One is the vesicular transport model, and the other is cisternal maturation model.

The vesicular transport model proposes that each Golgi cisterna constitutes a separate compartment of distinctive composition and that cargo travels from the *cis* to the *trans* region of the Golgi complex in vesicles that release from one cisterna and fuse with the next (Farquhar and Palade, 1981; Rothman, 1994). This model arose from the early EM studies of G. Palade (Palade, 1975), and gained wide support from experimental results obtained using *in vitro* systems, especially *in vitro* vesicular transport experiments

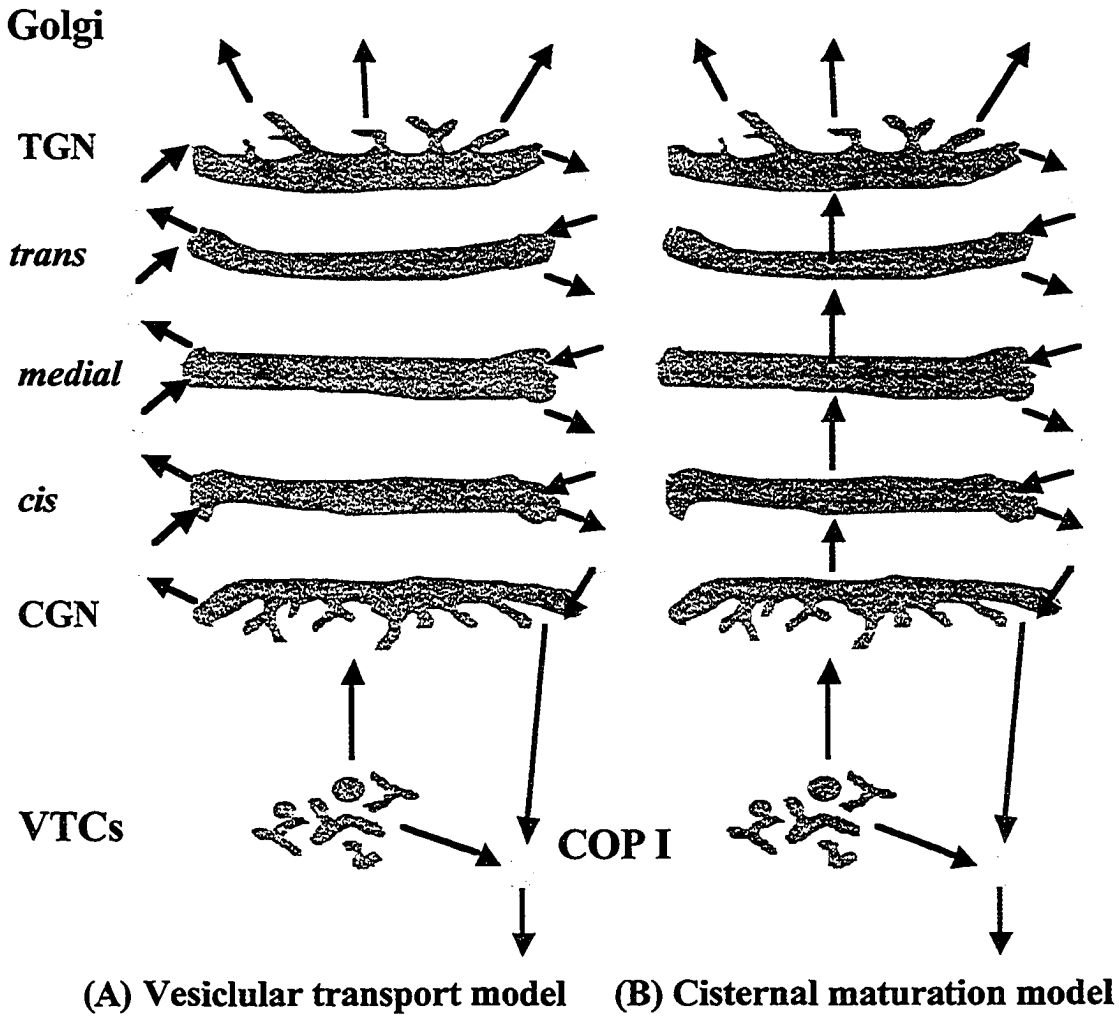

Figure 1.2. Two models explaining protein transport across the Golgi stack. (A) In the vesicular transport model, Golgi cisternae are static organelles, which contain a distinctive complement of resident enzymes. The transport of molecules through the Golgi stacks is accomplished by forward-moving transport vesicles, which release from one cisterna and fuse with the next in a *cis*-to-*trans* direction. **(B)** According to the alternative cisternal maturation model, anterograde protein transport is not mediated by vesicles, but by cisternal maturation. As each Golgi cisterna migrates from *cis* to *trans* through a stack, it matures by accepting Golgi resident enzymes moved backward (*trans* to *cis*) from later cisternae through COPI-coated vesicles. For details see text.

performed by Rothman and coworkers (Rothman, 1994; Rothman and Orci, 1992; Rothman and Wieland, 1996).

Recently, however, the vesicular transport model has been seriously challenged as the result of the failure to detect secretory proteins in Golgi vesicles (Martinez-Menarguez et al., 2001; Orci et al., 1997) and the difficulties in explaining the transport of macromolecular complexes such as algal scales (Becker et al., 1995) and procollagens (Bonfanti et al., 1998), which are too large to fit into standard transport vesicles. Consequently, the cisternal maturation model became the favored model for transport through the Golgi complex. To accommodate the new information briefly mentioned above, the modified maturation model is different from the original maturation model introduced in the 1950s (Grasse, 1957) in a way that it is actually a hybrid between the maturation and vesicular transport models. As shown in Figure 1.2, it proposes that anterograde transport occurs by whole cisternae maturation from *cis* to *trans* coupled with retrograde vesicular transport of Golgi proteins from *trans* to *cis* to maintain Golgi architecture (Pelham, 2001). Evidence has been provided that not only larger structures (such as procollagens (Bonfanti et al., 1998)), but also small cargo (such as VSV-G) is largely excluded from the vesicles (Mironov et al., 2001). The work of Martinez-Menarguez (Martinez-Menarguez et al., 2001) provide independent evidence in favor of cisternal maturation, by showing that COPI vesicles in the vicinity of the Golgi complex lacked cargo, such as VSV-G, but instead contain Golgi enzymes, such as ManII.

Nevertheless, neither the vesicular transport model nor the modified maturation model for anterograde transport is completely proven and the mechanism of transport across the stack remains controversial (Marsh and Howell, 2002). It has even been

proposed that under some conditions, secretory traffic occurs through formation of transient tubular continuities across Golgi sub-compartments (Trucco et al., 2004).

1.3.3. TGN: sorting and exit from the Golgi

The compartment for sorting cargo for exit from the Golgi was defined as the TGN, in which cargo are sorted for delivery to various cellular destinations: the cell surface (apical and basolateral in polarized cells), secretory granules in endocrine cells, or the endosome/lysosome system. It was believed that TGN is the single *trans*-most cisterna of the Golgi and the network that extends from it (Orci et al., 1987). However, EM tomographic studies revealed that the sorting and exit site from the Golgi comprised not one but two to three distinct *trans*-cisternae (Ladinsky et al., 1994; Ladinsky et al., 2002; Mogelsvang et al., 2004). The 3D structure of the Golgi ribbon from EM tomography is of such high resolution that clathrin-coated profiles can be identified in the tomograms. Surprisingly, clathrin-coated buds were only found on the *trans*-most cisterna of the Golgi (Mogelsvang et al., 2004), indicating a unique site for the sorting of cargo destined for the lysosomal pathway. These observations further suggest that cargos targeted to the PM must exit from the two previous *trans*-cisternae.

Detailed analysis of the mechanism for clathrin-mediated transport from the TGN to the endosomal/lysosomal pathway has been complicated by the presence of several adaptor complexes (AP-1;3;4) (Robinson, 2004) and adaptor-like molecules including GGAs (Golgi-localized, γ-ear-containing, Arf-binding proteins) (Bonifacino, 2004). Whereas AP-1 is highly enriched in purified CCVs, other adaptor proteins were not detected on purified CCVs (Robinson, 2004). Both AP-1 and GGAs have been suggested to regulate selective transport of mannose 6-phosphate receptors and associated cargos

from the TGN to endosomes (Doray et al., 2002; Puertollano et al., 2001a; Zhu et al., 2001), but whether they act sequentially, on parallel trafficking pathways, or on opposite trafficking pathways remains controversial (Bonifacino, 2004).

A new family of proteins, called FAPPs, has been implicated in formation of membrane carriers at the TGN and in controlling Golgi-to-cell-surface membrane traffic. In the same study, it was found that FAPPs regulated post-Golgi carrier formation through interactions with phosphatidylinositol 4-phosphate [PtdIns(4)P] and Arf1 (Godi et al., 2004). The discovery of protein modules that bind selectively to specific phosphoinositides also highlighted the importance of lipid-protein interactions in membrane trafficking at the Golgi complex (Itoh and De Camilli, 2004; Shin and Nakayama, 2004).

1.3.4. Lipids and the Golgi complex

Golgi membranes contain many lipid species, including cholesterol and phosphoinositides (PIs), which will be taken as two examples to discuss the important roles lipids play in membrane trafficking through the Golgi complex.

Cholesterol is an essential lipid constituent in the membranes of mammalian cells with unique properties and cellular distribution. Cholesterol preferentially associates with sphingolipids, which bear long unsaturated fatty acid chains, resulting in thicker bilayers that can segregate from bulk phospholipids to form small "lipid rafts" (Holthuis and Levine, 2005; Munro, 2003). The tight regulation of cholesterol subcellular traffic results in a concentration gradient along the secretory pathway, with low concentrations of cholesterol in the ER and high concentrations at the PM (van Meer, 1998).

Several years ago, Bretscher and Munro proposed that the cholesterol gradient

and resulting variations in lipid bilayer thickness across the Golgi stack and PM, played a critical role in the retention of Golgi resident proteins in this organelle (Bretscher and Munro, 1993). This model was based on the observations that (Brugger et al., 2000; Holthuis and Levine, 2005) Golgi enzymes generally have shorter transmembrane domains than PM proteins, and that lengthening of the trans-membrane region leads to appearance of Golgi enzymes in the thicker bilayer of the PM (Munro, 1995). However, a molecular mechanism to explain the bilayer-thickness sorting remained unavailable.

COPI vesicles may play an important role in generating the cholesterol gradient and facilitating the retention of Golgi enzymes in the cisternae (Holthuis and Levine, 2005). This possibility was first raised by the demonstration that COPI-coated vesicles generated from Golgi membranes contain lower levels of sphingolipids and cholesterol than the Golgi membrane from which they bud (Brugger et al., 2000). This lipid segregation, whether it occurred before budding or during budding (Holthuis and Levine, 2005), would ensure efficient retrograde movement of phospholipids and cause progressive accumulation of sphingolipids and cholesterol at the *trans*-cisternae in comparison to the *cis*-cisternae (Holthuis and Levine, 2005). Furthermore, enrichment of Golgi resident proteins in phospholipid-rich domains would ensure their capture in COPI vesicles and their return to cis-compartments. This model is supported by recent studies demonstrating that anterograde transport at the Golgi is sensitive to changes in the cholesterol concentration, probably because this leads to improper segregation of lipids and proteins (Stuven et al., 2003; Ying et al., 2003).

One unique feature of phosphatidylinositol is that it undergoes independent phosphorylation at positions 3, 4, and 5 on its inositol ring. Phosphatidylinositol and its

phosphorylated derivatives altogether are called PIs. Different types of PIs are concentrated on distinct organelle membranes. Whereas PtdIns(4)P is concentrated in the Golgi complex, phosphatidylinositol-4,5-bisphospate [PtdIns(4,5)P_2] is barely detectable in this compartment (Watt et al., 2002). PtdIns(4)P acts as a targeting signal for proteins that associate with the Golgi complex. Indeed, AP-1(Wang et al., 2003) and FAPPs (Godi et al., 2004) have been recently found to associate with Golgi membranes via interactions with PtdIns(4)P.

1.4. Arf: small GTPases that regulate coat assembly and cargo sorting

The ADP-ribosylation factors (Arfs) are a family of ~20 kDa Ras-like guanine nucleotide-binding proteins that were first identified as cofactors for cholera toxin-catalyzed ADP-ribosylation of Gsα (Kahn and Gilman, 1984). Later, Arfs were found to be important regulators of membrane traffic and dynamics within eukaryotic cells and therefore have been extensively studied [reviewed in (Donaldson, 2003; Moss and Vaughan, 1998; Nie et al., 2003; Randazzo et al., 2000)]. This section starts with the introduction of regulators and effectors of the Arfs, follows by a description of their diverse functions in membrane traffic, and ends with a model for COPI coat assembly controlled by Arf and its regulators.

1.4.1. Regulators and effectors of the Arfs

Arfs are found in all eukaryotic organisms examined to date and are highly conserved. There are six Arfs (Arf 1-6) in mammals and three (Arf1p-Arf3p) in the yeast *S. cerevisiae*. Mammalian Arfs are structurally categorized into three classes: class I, Arf

1–3; class II, Arf4-5; and class III, Arf6 (Boman and Kahn, 1995; Pasqualato et al., 2002).

Analogous to other Ras-like proteins, Arfs work as molecular switches and cycle between an inactive GDP-bound form and active GTP-bound form. Two families of proteins regulate this cycle (Donaldson and Jackson, 2000; Nie et al., 2003). The activation of Arfs (i.e. from Arf-GDP to Arf-GTP) is stimulated by Arf guanine nucleotide exchange factors (Arf-GEFs) that will be described in detail in section **1.5**. The inactivation of Arfs is promoted by Arf GAPs that induce the hydrolysis of GTP to GDP. Among the sixteen mammalian Arf GAPs that have been identified, some are implicated in Golgi function (Donaldson and Jackson, 2000; Randazzo and Hirsch, 2004). For example, Arf GAP1 has been shown to bind to Golgi membranes through interaction with KDEL receptor, a transmembrane protein that cycles between the ER and Golgi complex (Aoe et al., 1997; Aoe et al., 1999). Arf GAP1 stimulates the GTPases activity on Arf1, and on the basis of previous in vitro experiments was thought to promote COPI coat protein dissociation. However, it now turns out that Arf GAP1 enhances vesicle formation. The involvement of Arf GAP1 in COPI coat formation will be discussed further in section 1.4.3. ARAP1 is another Arf GAP found associated with the Golgi complex. The morphology of the Golgi complex is affected by overexpression of ARAP1, supporting a role of ARAP1 in Golgi function (Miura et al., 2002).

In its GTP-bound active state, Arf interacts with a variety of effector proteins, which are categorized into three groups (Nie et al., 2003): Group I are vesicle coat proteins and adaptors, including COPI (Zhao et al., 1997), AP1/3/4, and GGA1/2/3 (Puertollano et al., 2001b); Group II are phospholipid-metabolizing enzymes, such as

phospholipase D (Brown et al., 1993) and phosphatidylinositol 4 kinase (PI4-kinase)(Godi et al., 1999); and Group III are those proteins that bind to Arf-GTP but with unknown functions, such as Arfophilins (Shin et al., 2001) and Arfaptin2 (Shin and Exton, 2001).

1.4.2. Arfs: their diverse functions in membrane traffic

Arf-GTP bound to effector proteins mediates the physiological functions of Arf. Consistent with the diverse group of effectors, Arfs have diverse cellular functions, including the regulation of membrane traffic through the recruitment of cytosolic coat proteins onto membranes to facilitate sorting and vesicle formation, and the modulation of actin structures (Nie et al., 2003).

Among the six mammalian Arfs, Arf1 is the best understood one and has been implicated in ER-to-Golgi transport, function of the Golgi complex, transport from the TGN, transport in the endocytic pathway through regulating the assembly of several types of vesicle coat complexes including COPI on Golgi, AP1, GGAs on the TGN and AP3 on endosomes (Lippincott-Schwartz et al., 1998). In each case, Arf1 has been found to bind the coat protein directly. Little is known about the function of class-II Arfs. Arf6, the only class-III Arf, has been suggested to regulate endocytosis, phagocytosis, receptor recycling and the formation of actin-rich protrusions and actin-rich membrane ruffles (Donaldson, 2003). In agreement with their function, Arf1 and Arf3, as well as Arf5, have been localized to Golgi membranes (Hosaka et al., 1996; Stearns et al., 1990; Tsai et al., 1992). In contrast, Arf6 associates primarily with the PM and endosomes (Cavenagh et al., 1996; Peters et al., 1995).

Arf-GTP binds to and activates PI4-kinase (Godi et al., 1999) and phospholipase D (Brown et al., 1993), leading to the production of PtdIns(4,5)P_2 and phosphatidic acid (PA). PtdIns(4,5)P_2 and PA are likely to contribute to the effects of Arf in both actin and membrane remodeling (Roth, 1999).

1.4.3. Control of COPI coat assembly by Arf and its regulators

The mechanism of Arf regulation of COPI coat assembly is reasonably well understood relative to our current knowledge of Arf regulation of its many other effectors. Analogous to the dependence of Sar1-GTP for COPII binding, COPI coat assembly begins through activation of Arf1 GTPase catalyzed by an Arf GEF. Unique to Arfs, the GDP to GTP exchange reaction is coupled with membrane recruitment of Arfs through a now well-described series of conformational changes. Four domains display dramatic changes in conformation in response to GTP binding and hydrolysis, including two loops called switch 1 and switch 2 that interact with several effectors. The region between switch 1 and switch 2 called the interswitch as well as a myristoylated N-terminal 17-residue amphipathic helix also play a critical role in Arf activation. In the GDP-bound conformation, the myristate group of the N-terminal helix is thought to lie in a hydrophobic groove on the Arf surface but can be readily exposed to interact with the phospholipid bilayer. This weak but measurable membrane association is completely abolished if myristoylation is abrogated (Franco et al., 1995; Franco et al., 1996). The Arf-membrane interaction is stabilized in the GTP-bound form by a conformational change in the interswitch, which abolishes the hydrophobic groove and renders the membrane insertion of the N-terminal helix irreversible (Antonny et al., 1997; Goldberg, 1998).

Once on the membrane, Arf-GTP provides a direct binding site for COPI through its β and γ subunits (Zhao et al., 1997), which then acts as a "priming complex" for further coat assembly (Springer et al., 1999). Although activated Arf1 is essential to the recruitment of the ~700 kDa heptametrical COPI complex from the cytosol (Orci et al., 1993), additional interactions between COPI and cargo receptor proteins such as the p24 family may facilitate the membrane association of COPI as well (Dominguez et al., 1998).

The formation of COPI vesicles *in vitro* requires only Arf1 and coatomer when a non-hydrolysable GTP derivative, GTPγS, is used (Ostermann et al., 1993; Spang et al., 1998). However, the incorporation of cargo proteins requires GTP hydrolysis by Arf1 (Lanoix et al., 1999; Nickel et al., 1998; Pepperkok et al., 2000). Consistent with the idea that GTP hydrolysis is required for cargo sorting, recent observations have shown that Arf GAP1 promotes coat formation and has even been detected in COPI vesicles (Poon et al., 1999; Rein et al., 2002; Yang et al., 2002). These results are really surprising since GAP activity had been predicted to antagonize the recruitment of coat proteins and consequently stop vesicle formation based on previous findings that GTP hydrolysis was required for COPI vesicle uncoating (Bremser et al., 1999). Then how is the coat maintained to yield productive vesicles in the presence of Arf GAPs that catalyze hydrolysis of Arf-GTP and releases Arf from the membrane? One elegant mechanism to restrict Arf GAP activity to late in the budding process to prevent premature uncoating is suggested by a very recent observation in which the activity of Arf GAP1 is stimulated by an increase in membrane curvature (Bigay et al., 2003). Alternatively, coat protein

dissociation might be regulated by a mechanism that is independent of Arf (Randazzo and Hirsch, 2004).

1.5. Arf-GEF: sec7 domain-containing proteins that activate Arfs

Although the existence of GEF activity in Golgi membranes was first demonstrated in 1992 (Donaldson et al., 1992a; Helms and Rothman, 1992), the first Arf GEFs were not identified until 1996 when human ARNO (Chardin et al., 1996) and yeast Gea1p (Peyroche, 1996) were shown to promote guanine-nucleotide exchange on Arfs. Since then, a large and surprisingly diverse family of Arf-GEFs have been identified (Cox et al., 2004). In eukaryotic cells, 6 subfamilies with established Arf GEF activity are currently identified with size ranging from small (~40-80 kDa, including CYH and EFA6) to intermediate (~100-150 kDa, including BRAG and SYT1) and large (~160-230 kDa, including GBF/GEA and BIG/SEC7) (Cox et al., 2004; Mouratou et al., 2005; Niu et al., 2005) (Figure 1.3). This section begins with a description of the structure of Sec7 domain (Sec7d), followed by a summary of the properties of small and intermediate-sized Arf-GEFs, as well as large-sized Arf-GEFs.

1.5.1. Structure of the Sec7 domain

All Arf GEFs share one common feature, a region of roughly 200 amino acids with strong homology to the yeast protein Sec7p, which is called the Sec7d (Jackson and Casanova, 2000). The first hint of the relationship between Arf and the Sec7d was presented about the middle of 1996; Franzusoff and colleagues reported that overexpression of not only yeast Arf1p and Arf2p but also human Arf4 rescued the yeast sec7 mutant (Deitz et al., 1996). Subsequent studies established that Sec7d itself was

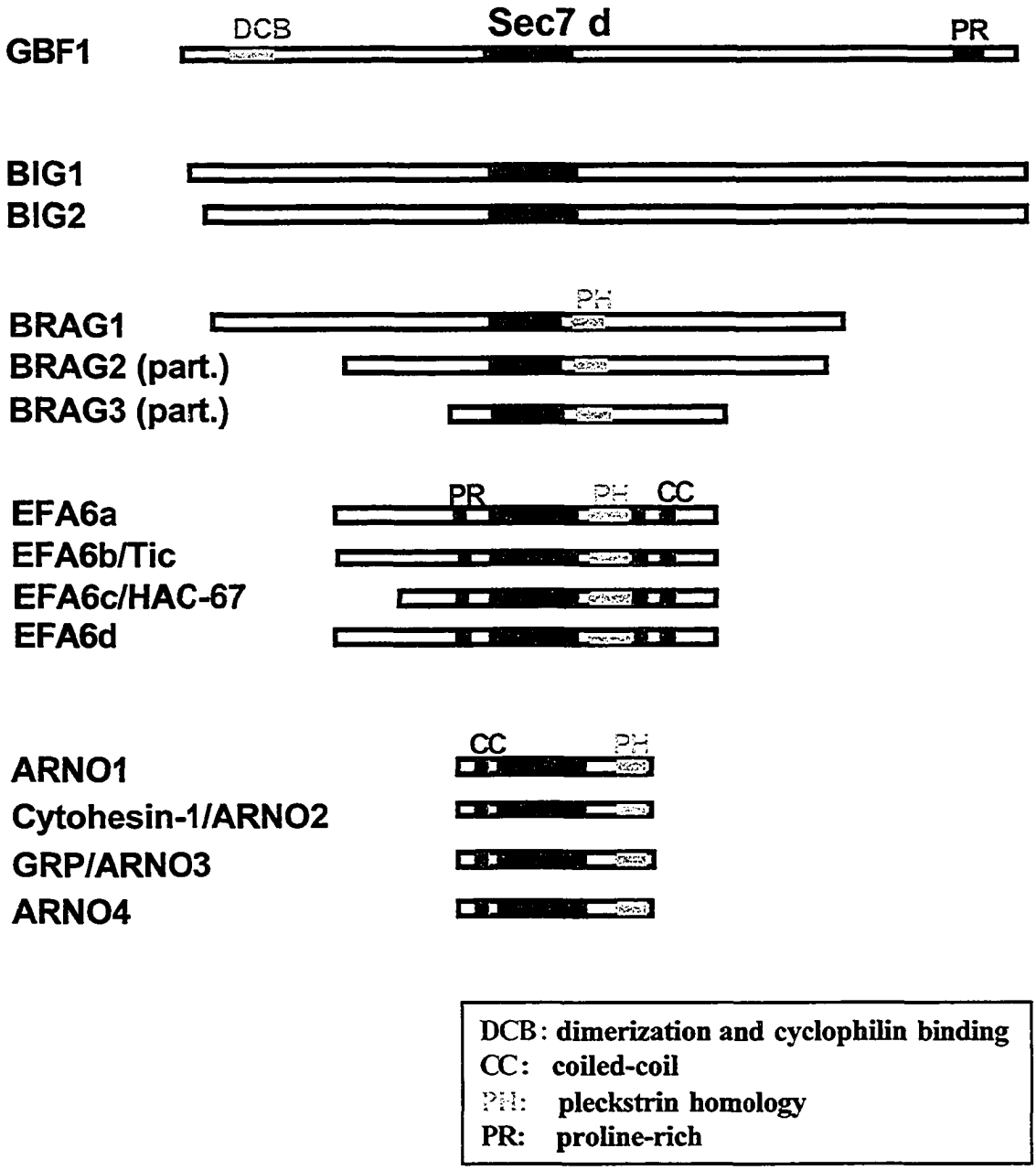

Figure 1.3. Mammalian members of the Arf-GEF family. Representative members of five different subfamilies of mammalian Arf-GEFs are shown, with colored bars representing various domains shared by some or all members.

sufficient to promote nucleotide exchange (Chardin et al., 1996; Mansour et al., 1999; Sata et al., 1998).

Several groups (Cherfils et al., 1998; Mossessova et al., 1998; Renault et al., 2002) have determined the crystal structures of the Sec7d of different Arf-GEFs. It consists of ten α-helices arranged in an elongated cylinder. A hydrophobic groove contains the two most highly conserved sequence stretches (Cherfils and Chardin, 1999; Goldberg, 1998). The first one, termed motif 1, contains a critical glutamic acid residue (also called 'glutamate finger') which inserts into the nucleotide binding fold of the Arf and perturbs the Mg^{2+} and phosphates, thereby facilitating GDP release (Beraud-Dufour et al., 1998) (Goldberg, 1998). Substitution of an aspartate residue for the conserved glutamate reduces the rate of exchange nearly 20 fold. In contrast, a charge-reversal mutation in the glutamate residue introduced into the sec7d of several Arf-GEFs reduces exchange activity to background levels (Beraud-Dufour et al., 1998). The second more degenerate stretch, termed motif 2, displays several hydrophobic residues implicated in substrate binding (Cherfils and Chardin, 1999; Goldberg, 1998).

1.5.2. Low and intermediate molecular weight Arf GEFs

Unlike the large-sized Arf GEFs discussed in the next section, the small and intermediate-sized Arf GEFs are not present in all eukaryotes. Mammals express at least one member of the CYH, EFA and BRAG subfamilies, while yeasts express the SYT1 (Cox et al., 2004). Also in contrast with large Arf- GEFs, all small and intermediate-sized Arf GEFs contain a plekstrin homology (PH) domain (Cox et al., 2004; Mouratou et al., 2005). This PH domain appears to mediate membrane recruitment of these proteins by binding to PIs (Hemmings, 1997), which enhances GEF activity by concentrating the

reactants at the membrane surface (Paris et al., 1997). The various PH domains have been shown to have different preferences for PIs (Harlan et al., 1995). For example, while the PH domains of the CYHs bind specifically to phosphatidylinositol-3,4,5-trisphospate [PtdIns(3,4,5)P_3] (Klarlund et al., 1997), EFA6 PH domain has an equivalent affinity for both PtdIns(3,4,5)P_3 and PtdIns(4,5)P_2 (Brown et al., 2001). The relative abundance of PtdIns(4,5)P_2, even in resting cells, might therefore explain why EFA6 appears to be constitutively membrane bound, in contrast to CYHs, which are largely cytoplasmic in resting cells, but are recruited to the PM upon PI-3 kinase stimulation (Brown et al., 2001; Nagel et al., 1998; Venkateswarlu et al., 1998).

Another feature common amongst the small and intermediate-sized Arf GEFs is that, with the exception of the yeast-specific SYT1(Jones et al., 1999), all Arf GEFs can catalyze nucleotide exchange on Arf6 *in vitro* (Franco et al., 1999; Frank et al., 1998; Langille et al., 1999) (Chen et al., 2003). EFA6 activates Arf6 preferentially *in vitro* (Franco et al., 1999) and *in vivo* (Derrien et al., 2002). Through yet poorly understood mechanisms, activated Arf6 regulates endocytic and recycling processes, as well as the remodeling of actin cytoskeleton in the endosomal-PM system (Derrien et al., 2002; Donaldson, 2003).

In contrast to the situation with EFA6, the actual substrate specificity for CYH members such as ARNO, cytohesin1, GRP1 and cytohesin4, remains controversial. For example, while some groups have shown that ARNO and GRP1 activate Arf6 at the PM following stimulation (Frank et al., 1998; Langille et al., 1999), others observed that ARNO, cytohesin-1 and GRP1 catalyze exchange more efficiently on class I Arfs *in vitro* (Jackson and Casanova, 2000; Meacci et al., 1997). Complicating matters, these CYH

members were localized by one research group to the Golgi complex (Lee et al., 2000; Lee and Pohajdak, 2000). Furthermore, recent studies revealed that both Arf6 and Arf1 can be activated by ARNO in response to cell-surface signaling events (Macia et al., 2001). Interestingly, the presence of PH domains with different specificities may provide an explanation to these apparent discrepancies. Indeed, it is possible that the PH domain determines the specificity of the small and intermediate-sized Arf GEFs towards Arf6 indirectly, by recruiting these GEFs to the PM where Arf6 resides (Cox et al., 2004; Derrien et al., 2002; Franco et al., 1999; Jackson and Casanova, 2000; Macia et al., 2001)

There is not much published work about BRAGs, except that human BRAG1 displayed more active GEF activity towards Class I Arfs that appeared BFA resistant using *in vitro* exchange assay (Melançon et al., 2004); human BRAG2 (also called ArfGEP100) was suggested to localize to an endosomal compartment (Someya et al., 2001) by activating Arf6; and Drosophila BRAG1 (also called loner) was required for myoblast fusion by activating Arf6 (Chen et al., 2003). The *S.cerevisiae* SYT1 represents a novel subfamily (Jones et al., 1999), but its localization and function remain unknown.

1.5.3. High molecular weight Arf GEFs

The high molecular weight Arf GEFs are present in all eukaryotes, lack PH domains and include two subfamilies: GBF/GEA and BIG/SEC7 (Cox et al., 2004).

The GBF/GEA subfamily includes yeast Gea1p and Gea2p, Arabidopsis GNOM/Emb30p, and mammalian Golgi-specific BFA resistance factor (GBF)1 (Cox et al., 2004). In *S.cerevisiae*, Gea1p and Gea2p proteins share 50% identity and appear to be functionally redundant, since yeast cells lacking either gene showed no apparent growth or secretion defect, whereas a strain lacking both genes is unviable (Peyroche, 1996).

Gea1/2p have been localized to the Golgi complex and play an important role in the structure and function of the Golgi complex in yeast (Peyroche et al., 2001). Recent studies have also suggested a role for Gea1/2p in the organization of the actin cytoskeleton (Zakrzewska et al., 2003).

Arabidopsis GNOM/Emb30p protein can restore growth to a *gea1tsgea2*Δ mutant, suggesting that it is a functional orthologue of the Gea1 and Gea2 proteins (Steinmann et al., 1999). However unlike its homologues, yeast Gea1/2p and mammalian GBF1 that localize to the Golgi complex (Claude et al., 1999; Peyroche et al., 2001), this protein was found to associate with endosomes and suggested to be required for recycling of auxin transport components (Geldner et al., 2003). However, the localization and function of two GNOM related proteins called GNOM-like 1 (GNL)-1 and GNL-2 remain unknown (Mouratou et al., 2005). Located in the N-terminal of GNOM, a domain ~250 residues is involved in dimerization and possibly binding to cyclophilin5 and therefore was named the Dimerization/Cyclophilin Binding (DCB) domain (Grebe et al., 2000). This domain is among the 5 out-of-sec7d domains that conserved by GBF/GEA and BIG/SEC7 subfamilies (Mouratou et al., 2005). GBF1 (Claude et al., 1999) was originally identified in our laboratory in an attempt to clone the factor responsible for the Brefeldin A (BFA) (a fungal metabolite that block protein transport, see section 1.6) resistance of a mutant CHO cell line, BFY1 (Yan et al., 1994). Unexpectedly, analysis of cDNAs recovered from wild type (wt) CHO cells and BFY1 cells established that transcripts in these cells had identical sequence. Although overexpression of GBF1 in mammalian cells confers resistance to the growth inhibition and Golgi disassembly caused by BFA treatment of the cells, GBF1 is expressed at identical levels in both wild

type and mutant cell lines, suggesting that GBF1 is not the factor responsible for the BFA resistance observed in BFY1 cells (Claude et al., 1999). GBF1 has been localized to the Golgi complex based on colocalization with β-COP (Claude et al., 1999). Interestingly, while Golgi-enriched membrane fractions from cells transfected with GBF1 showed a BFA-resistant GEF activity toward class I Arfs, partially purified His6-tagged GBF1 exhibited *in vitro* GEF activity that is specific towards Arf5 at physiological Mg^{2+} concentration: partially purified GBF1 failed to catalyze GDP-GTP exchange on class I Arfs, but acted robustly on purified Arf5 when the Mg^{2+} concentration was raised above 1mM (Claude et al., 1999).

The Sec7/BIG subfamily includes yeast Sec7p and mammalian BFA-inhibited GEF (BIG)1 and BIG2. Sec7p was first identified by Novick and Schekman in a selection for *S.cerevisiae* secretion-defective mutants (Novick et al., 1980), and its function is essential in yeast (Achstetter et al., 1988). Sec7p, like Gea1/2p, is localized to the Golgi complex (Franzusoff et al., 1991; Mogelsvang et al., 2003). However, the *SEC7* gene is unable to rescue a *gea1*Δ*gea2*Δ strain (Spang et al., 2001), indicating that Sec7p is functionally different from Gea1/2p (Jackson and Casanova, 2000).

BIG1 (also called p200-GEP) and BIG2 were initially co-purified from bovine brain cytosol as a >670 kDa macromolecular complex based on their BFA-inhibited GEF activity (Morinaga et al., 1996). They show highest sequence similarity to each other and yeast Sec7p. Co-immunoprecipitation (IP) analysis using tagged forms of BIG1 and BIG2 established that greater than 75% of these two GEFs exist as hetero-dimers (Yamaji et al., 2000) that localize to the Golgi complex at the light microscope level (Mansour et al., 1999; Yamaji et al., 2000). However, pools of homodimers with distinct functions

appear to exist as well (section 5.4.3). Only 75% of BIG1 can be immunoprecipitated with BIG2 antibodies and vice versa under conditions where IP is quantitative. I conclude from this that 25% of protein is homodimer. BIG1 and BIG2 catalyze nucleotide exchange most efficiently on class-I Arfs in vitro and are also active on Arf5 but do not use Arf6 as a substrate (Jackson and Casanova, 2000; Morinaga et al., 1999; Togawa et al., 1999).

1.6. BFA is a powerful tool to understand regulation of protein transport

BFA, a fungal fatty acid metabolite, is a potent inhibitor of protein secretion in eukaryotic cells. BFA has dramatic effects on the structure and function of intracellular organelles, particularly the Golgi complex (Klausner et al., 1992). Therefore, BFA has been widely used as a drug for studying protein transport. The main cellular target of BFA has been identified as a subset of the Arf GEFs (Cox et al., 2004; Donaldson et al., 1992a; Helms and Rothman, 1992; Randazzo et al., 1993). This section begins with a description of the effects of BFA on the secretory pathway, follows with a description of the primary cellular targets and mechanism of action of BFA and ends with the poorly understood impact of BFA-induced ADP-ribosylation of CtBP3/BARS.

1.6.1. BFA effects on the secretory pathway

The drug BFA has a profound effect on the secretory pathway in a wide range of cell types. BFA was initially shown to reversibly block secretion of proteins such as VSV-G in mammalian cells (Misumi et al., 1986). Subsequent studies revealed that BFA caused the complete disassembly of the Golgi complex, and the redistribution of Golgi enzymes to the ER. This effect is very rapid, with complete loss of the Golgi complex

within minutes of BFA treatment (Lippincott-Schwartz et al., 1990; Lippincott-Schwartz et al., 1989). This BFA induced relocalization is mediated by membrane tubules extended out of the Golgi complex along microtubules in BFA treated cells (Lippincott-Schwartz et al., 1990; Sciaky et al., 1997). Although the molecular mechanism of BFA induced Golgi membrane tubulation is unknown, subsequent studies demonstrated that it required the dissociation of coatomer from the membrane (Scheel et al., 1997). COPI dissociation from the Golgi membrane has been shown to be the earliest effect of BFA treatment, which occurs after less than 1 min of drug exposure (Donaldson et al., 1990; Orci et al., 1991). Arf1 is also rapidly released from membranes upon BFA treatment (Donaldson et al., 1991; Robinson and Kreis, 1992). In agreement with the role of Arf1 in recruiting several coat proteins, subsequent studies demonstrated that a number of proteins were rapidly released from Golgi and endosomal membranes upon BFA treatment, including AP-1/3/4 and GGAs (Robinson, 2004).

As a result of inhibited formation of CCVs on the TGN, BFA treatment affects not only the Golgi complex, but also other organelles in the endocytic pathway. For example, BFA causes fusion of the TGN with the early (sorting) endosomes (Lippincott-Schwartz et al., 1991), and their clustering around the microtubule organizing center (Lippincott-Schwartz et al., 1991; Wood et al., 1991). BFA treatment of particular cell types also causes tubulation of lysosomes and blocks certain transport steps within this system (Lippincott-Schwartz et al., 1991).

1.6.2. BFA targets the sec7 domains of sensitive GEFs and acts as an uncompetitive inhibitor

A major breakthrough in understanding the molecular action of BFA came with

the discovery that it specifically inhibits a Golgi-associated GEF activity for Arf1 (Donaldson et al., 1992b; Helms and Rothman, 1992). In agreement with this observation, it has been demonstrated that cells expressing the dominant negative mutant (constitutively GDP-bound form) of Arf1 had a phenotype indistinguishable from that of BFA treated cells (Dascher and Balch, 1994; Ward et al., 2001). Subsequently, a number of Arf GEFs (including Gea1p and Gea2p, GNOM/Emb30, Sec7p, BIG1 and BIG2) have been identified with an in vitro exchange activity that is sensitive to BFA. However, BFA has little effect on the in vitro exchange activity of a subset of some other Arf GEFs (including ARNO, cytohesin-1, GRP1 and GBF1) (Cox et al., 2004; Jackson and Casanova, 2000).

In agreement with the discovery that the isolated Sec7d of BIG1 (Mansour et al., 1999) or Sec7p (Jones et al., 1999; Sata et al., 1998) is a direct target of BFA, substitution of the sec7d of the BFA-sensitive Gea1p and Sec7p with that of the BFA-resistant ARNO rendered these GEFs resistant to BFA whether assayed *in vitro* or *in vivo* (Peyroche et al., 1999). Furthermore, kinetic analyses have suggested that BFA did not compete with Arf for interaction with BIG1, but rather acted as an uncompetitive inhibitor that stabilizes a normally very-short-lived Arf-GDP-Sec7d protein complex (Mansour et al., 1999). Jackson and colleagues obtained similar results with the Sec7d of a BFA sensitive form of ARNO and succeeded in isolating a ternary BFA-Arf-Sec7d complex by chromatography (Peyroche et al., 1999). Recent crystallographic studies of the Arf-GDP-Sec7d-BFA complex have established that BFA binding interferes with the closure of the Sec7d groove, trapping the Arf-GDP-Sec7d complex before the nucleotide-release stage (Mossessova et al., 2003b; Renault et al., 2002; Renault et al., 2003).

Detailed mutagenesis studies of Sec7d identified five amino acids within the Sec7d that convert a BFA sensitive Arf-GEF into a BFA resistant one, or vise versa, both *in vitro* and *in vivo* (Baumgartner et al., 2001; Peyroche et al., 1999; Sata et al., 1999). These studies define the BFA sensitivity consensus motif as YS-M-D-M (Cox et al., 2004). Interestingly, the five amino acids of this consensus are positioned on one surface of the Sec7d (Suh et al., 2002), and two of them, Y- and M interact directly with BFA (Mossessova et al., 2003b; Renault et al., 2003).

1.6.3. BFA and ADP-ribosylation of CtBP3/BARS

Most of the effects of BFA can be explained by the inhibition of Arf-GEFs; however, Sec7d-Arf complex is not the only target of BFA within the cell. At least in mammalian cells, BFA induces mono-ADP ribosylation of cytosolic proteins of 38 and 50 kDa (De Matteis et al., 1994). Interestingly, the ligand selectivity and the levels of BFA needed to induce ADP-ribosylation and block Arf activation were found to be similar. Further characterization of this reaction established that whereas the substrates are primarily cytosolic, the modifying enzyme is membrane-associated. The enzyme fractionated preferentially with Golgi membranes but retained its sensitivity to BFA even when assayed after Triton-solubilization and partial purification (Di Girolamo et al., 1995; Weigert et al., 1997). These observations as a whole suggest that BFA does not induce ADP-ribosylation indirectly through changes in membrane-associated Arfs or COPI, but rather targets the ADP-ribosyl transferase directly. Despite significant efforts, the enzyme responsible for this unusual modification remains unknown.

Characterization of one of the **B**FA-dependent **A**DP-**r**ibosyl transferase **s**ubstrates, or BARS, proved more productive and established that ADP-ribosylation

contributes significantly to the cellular effects of BFA. The 38 kDa ADP-ribosylated protein turned out to be glyceraldehyde 3-phosphate dehydrogenase, or GAPDH. Modification of this abundant metabolic enzyme is very inefficient (usually less than 3%), and its significance was not further elucidated (De Matteis et al., 1994).

The 50 kDa protein, referred to as BARS-50 (De Matteis et al., 1999) or CtBP3/BARS (Spano et al., 1999) turned out to be a novel protein with an important function in Golgi membrane dynamics. Initial characterization by Mironov and colleagues first established that its NAD-dependent ADP-ribosylation, although not sufficient, was clearly required to observe dispersal of the Golgi complex upon BFA treatment (Mironov et al., 1997). The importance of ADP-ribosylation in mediating the cellular effects of BFA was subsequently confirmed by the demonstration that addition of excess unmodified recombinant CtBP3/BARS could actually prevent BFA-induced Golgi dispersal (Spano et al., 1999).

Current evidence suggests that CtBP3/BARS-dependent production of PA is critical to membrane scission events at several stages of protein traffic. Initial work with recombinant protein revealed that addition of CtBP3/BARS led to a significant increase in number of constrictions in tubular regions of Golgi cisternae (Weigert et al., 1999). This morphological transformation required the presence of palmitoyl-CoA and further work established CtBP3/BARS as an enzyme that can convert lyso-PA into PA using acyl-CoA as the acyl donor (Weigert et al., 1999). ADP-ribosylation causes apparent dimerization of the enzyme (Spano et al., 1999) and abolishes this activity (Spano et al., 1999). The ability of excess CtBP3/BARS to prevent BFA-dependent Golgi dispersal in semi-intact cells could therefore arise from increased membrane scission and a reduction

in number of intact tubules that make contact with the ER. More recently, the role of CtBP3/BARS in intracellular transport was examined *in vivo*, and it was found to control membrane fission of transport carriers in both endocytic and exocytic pathways (Bonazzi et al., 2005). CtBP3/BARS has also been shown to mediate mitotic Golgi partitioning (Hidalgo Carcedo et al., 2004).

1.7. This Project: Research Rationale

Since the first identification of Sec7d-containing Arf GEFs (Chardin et al., 1996), much progress has been made in understanding their functions in recruiting coat proteins to form transport intermediates by activated Arfs. However, how Arf1 could regulate the assembly of so many coats (COPI; AP-1/3/4 and GGA1-3) (Nie et al., 2003), or how assembly of one particular coat, COPI, could be required for both anterograde and retrograde protein transport (Nickel and Wieland, 1998) remains a mystery. Our working hypothesis is that the combination of Arfs and their activator GEFs play an essential role in providing selectivity to the process of coat recruitment, and ultimately cargo sorting into different types of transport carriers.

The aim of this project was to test this hypothesis by studying the subcellular localization and function of large Arf GEFs, and more specifically, two subfamilies of large Arf-GEFs: GBF1 and BIG1/2. In Chapter 3, I provide novel information concerning the distinct sub-compartments of the Golgi complex localization of GBF1 and BIGs, which are recruited to the *cis*- and *trans*-Golgi, respectively. Furthermore, I identify that the N-terminal third of BIG1 and BIG2 contains sufficient information for localization to the TGN. Chapter 4 focuses more specifically on GBF1 function, investigating the

dynamic recruitment of GBF1 to various membranes in the early secretory pathway and the functional involvement of GBF1 in ER-to-Golgi protein transport. In summary, the data presented in this thesis provide novel information about GBF1 and BIGs localization and function.

Chapter 2

Materials and Methods

2.1. Reagents

Media and culture reagents were purchased from Invitrogen Canada Inc. (Burlington, ON, Canada) Disposable plasticware and six-well culture plates were purchased from BD Biosciences (Mississauga, ON, Canada). BFA and nocodazole were purchased from Sigma-Aldrich (St. Louis, MO, US), dissolved in dimethyl sulfoxide (DMSO) and stored at –20°C as stock solutions of 10 mg/ml and 5 mg/ml, respectively. Geneticin (G418 sulfate) and zeocin were obtained from Invitrogen Canada Inc.. Geneticin was dissolved in water and stored at 4°C as a stock of 40 mg/ml. Zeocin was obtained as a 100 mg/ml solution and stored at –20°C.

2.2. Cell culture

The following cell lines were used in this thesis: Hela cells (ATCC CCL-2); COS-1 cells (ATCC CRL-1650); BHK-21 (obtained from Dr. Thomas Hobman, University of Alberta); Normal rat kidney (NRK) cells (ATCC CRL-1571); and NRK cells expressing GFP tagged GBF1 (described in section 2.5). Monolayers of all cell lines were maintained in DMEM supplemented with 10% fetal bovine serum (FBS) (Sigma), 100 μg/ml penicillin G, 100 μg/ml streptomycin and 2 mM glutamine at 37°C in a 5% CO_2 incubator. For incubations at 15°C, NRK cells were transferred to DMEM lacking HCO_3^- that was supplemented with 20 mM HEPES, pH 7.4. For live cell imaging, NRK cells expressing GFP tagged GBF1 were grown in CO_2 independent DMEM (Gibco Laboratories, Grand Island, NY) plus 10% FBS in a Delta T open dish (Bioptechs, Butler, PA).

2.3. Antibodies

2.3.1 Preparation of antibodies

The rabbit polyclonal antibody H154 (1:500 dilution), raised against the C-terminal peptide of GBF1, has been described previously (Claude et al., 1999).

Polyclonal antibodies against BIG1, named 9D3, as well as polyclonal antibodies against GBF1, named 9D2 and 9D5, were raised in rabbits according to standard procedures (Harlow and Lane, 1988). Recombinant proteins that encompass fragments of either human BIG1 or GBF1 were injected into rabbits as immunogens. For 9D3, the plasmid used for recombinant expression encoded a hexa-histidine-tagged form of the sec7d of human BIG1 (termed M1) that was constructed by Dr. Sam Mansour (Mansour et al., 1999). For 9D2 or 9D5, the plasmid used for recombinant expression encoded a hexa-histidine-tagged form of the N- terminal fragment of human GBF1; it was constructed by Baoping Zhao by inserting the 5' Ssp1-Nhe1 fragment of human GBF1 cDNA at the Nhe1 site of pRSET A (Invitrogen). The recombinant proteins that encompass either residues 560-890 of hBIG1(M1) or residue 5-621 of hGBF1 were expressed and purified by Baoping Zhao as described (Mansour et al., 1999).

Antibodies to BIG1 (9D3) were affinity-purified against strips of nitrocellulose onto which the recombinant M1 had been transferred following SDS-PAGE. Bound antibody was recovered by acid elution as described (Harlow and Lane, 1988) and used at 1:50 dilution for immunofluorescence (IF) study. Comparison of signal obtained with equivalent dilutions of crude and affinity-purified serum confirmed that affinity purification yielded a significant increase in specificity with total recovery of approximately 30% of the initial BIG1 binding antibody (see Figure 3.2).

Anita Gillchrist affinity-purified antibodies to GBF1 (9D2 and 9D5) using an Affigel-10 column (Bio-Rad Laboratories, Mississauga, Ontario, Canada) onto which the recombinant GBF1 N- terminal fragment had been conjugated according to manufacturer's instructions. Bound antibody was recovered by acid elution as described (Harlow and Lane, 1988) and used at 1:50 dilution for IF. The yield and increase in specificity were determined by immunoblot and IF, as before for anti-BIG1 antibodies.

Alexa488-labeled anti-BIG1 (9D3) antibodies and Alexa488-labeled anti-GBF1(H154) antibodies were prepared according to manufacturer's instructions by using Alexa Fluor™ 488 Protein Labeling Kit (A-10235) (Molecular Probes, Eugene, OR). IgG fractions purified from crude serum by chromatography on protein A Sepharose following ammonium sulphate precipitation were used for this purpose. The specificity of these antibodies was confirmed by immunoblot and IF. Alexa488-labeled anti-BIG1(9D3) antibodies were used at 1:10 dilution for IF and Alexa488-labeled anti-GBF1(H154) antibodies used at 1:100 dilution for IF.

2.3.2. Monoclonal and polyclonal antibodies from other sources

Several primary antibodies were obtained either commercially or from other laboratories. The source and working IF dilutions for monoclonal and polyclonal antibodies are indicated in Table 2.1 and Table 2.2, respectively.

2.3.3. Secondary antibodies

The following fluorescent secondary antibodies were used: FITC-conjugated goat anti-rat antibody (Jackson ImmunoResearch Laboratories) at 1:100; Alexa594-conjugated goat anti-rabbit and Alexa488 conjugated goat anti-mouse antibodies (Molecular Probes, Eugene, OR) at 1:600.

Table 2.1 Monoclonal antibodies used for IF

Antibodies	Source	IF dilution
anti- hemagglutinin (HA) (clone 3F10, rat)*	Roche Diagnostics Canada (Laval, QC, Canada)	1:50
anti-p115 (clone 3A10)[1]	a kind gift of Dr. G. Waters (Merck, New Jersey)	1:1000
anti-p58 (clone 7DB2)	a kind gift of Dr. L. Hendricks (Centocor, PA)	1:150
anti-Man II (clone 53FC3)[2];	a kind gift of Dr. B. Burke (University of Florida, Gainesville, FL)	1:50
anti-α-tubulin (clone no. B-5-1-2)	Sigma-Aldrich	1:4000
anti-β-COP (clone M3A5)[3]	1. a kind gift of Dr. T. Kreis (University of Geneva, Geneva, Switzerland) 2. Sigma-Aldrich	1:300
anti-clathrin (clone X22)	1. a kind gift of Dr. S. Sorkin (University of Colorado Health Science Center, Denver, CO) 2. ABR-Affinity BioReagents (Golden, CO)	1:200
anti-VSV-G (clone P5D4)[4];	a kind gift from Dr. Dr. T. Kreis (University of Geneva, Geneva, Switzerland)	1:100

* This is a rat monoclonal antibody; all others are mouse monoclonal antibodies

References: 1. (Waters et al., 1992); 2. (Burke et al., 1982); 3. (Allan and Kreis, 1986); 4. (Kreis and Lodish, 1986)

Table 2.2 Polyclonal antibodies used for IF

Antibodies	Source	IF dilution
anti-TGN38	a kind gift of Dr. J. Barasch (Columbia University, New York, NY)	1:2000
anti-p58 (Molly 6) [1]	a kind gift of Dr. J. Saraste (University of Bergen, Bergen, Norway)	1:100
anti-Man II	a kind gift of Dr. K. Moremen (University of Georgia, Athens, GA)	1:2000
anti-GFP	a kind gift from Dr. L.G. Berthiaume, (University of Alberta, Edmonton, AB, Canada)	1:500
anti-sec31 [2]	a kind gift from Dr. B.L. Tang (Institute of Molecular and Cell Biology, Singapore, Republic of Singapore)	1:500

References: 1. (Saraste et al., 1987); 2. (Tang et al., 2000)

2.4. Plasmids construction

2.4.1. HA-tagged BIG1 fragments

Five HA-tagged truncated fragments of hBIG1 covering amino acid residues 2-559, 2-890, 560-1849, 891-1849, and 560-890 were generated by Dr. Sam Mansour (Mansour et al., 1999).

2.4.2. BIG2 N-terminal fragment

Troy Lasell generated a plasmid encoding a tagged-form of the N-terminus of BIG2 by PCR from a yeast two-hybrid human pancreatic library (Clontech) using the Expand High Fidelity PCR kit (Boehringer Mannheim) and primers F1 5'-CGAGATCTTCTAGACAGGAGAGCCAGACCAAGAGCATGTTCG- 3' and R1A 5'-CTTCCTCGAGTCATGTCATTCCCAGCTCATGTCCACTTCTTCC-3'. Troy cloned this fragment, which encodes residues 2-552 of hBIG2, directionally into a pCEP4 derivative, pMCL, that yields fusion proteins with a hemagglutinin (HA) tag (MAYPYDVPDYASGT; underlined residues) at the N terminus (Mansour et al., 1999). Briefly, the insert in pMCL-HA-N2 was excised with Nhe1 and Xho1, and replaced with the PCR fragment using the XbaI and XhoI sites engineered into F1 and R1A, respectively. Several clones from two distinct PCR reactions were sequenced on both strands to ensure construct fidelity. This analysis revealed a two-nucleotide difference (^{619}GA instead of ^{619}AG) from the sequence of BIG2 published by Vaughan and colleagues (Togawa et al., 1999), leading to a change from Arg to Glu at position 207. This corrected sequence matches the published human genomic sequence on the NCBI site (accession # NT_011361.3).

2.4.3. N- or C- terminal GFP tagged GBF1

Dr. Alex Claude constructed plasmids encoding GBF1 tagged with EGFP at either the N terminus or C terminus. To generate N-terminal GFP tagged GBF1 (GFP-GBF1), pCEP4-GBF1 (also called clone 32) that contains the cDNA of CHO cell line GBF1 (Claude et al., 1999) was digested with EcoRV and SacII. This fragment was then inserted into pEGFP-C1 (Clontech, Palo Alto, CA) digested with SmaI and SacI, downstream of the EGFP cDNA. This ligation created a GFP-GBF1 fusion gene with a linker of 111 nucleotides encoding 37 amino acids between EGFP and GBF1 (Figure 2.1A). Subsequently, the GFP-GBF1 encoding fragment was recovered by digestion with NheI and NotI and subcloned into the corresponding sites of the mammalian expression vector pIND (Invitrogen, Carlsbad, CA) to yield pIND-GFP-GBF1.

To generate C terminal GFP tagged GBF1, pCEP4-GBF1 was first digested with Bspm1 to liberate the 3'end. After filling-in the Bspm1 site with *Taq* polymerase (Invitrogen), the plasmid was digested again with SacII to liberate the 5'end. This fragment was ligated into pEGFP-1(Invitrogen) cut with Sma1 and Sac II upstream of the EGFP gene. In this case the construction caused loss of the last 45 amino acid residues of GBF1. The GBF1-GFP encoding fragment was recovered by digestion with NheI and NotI and subcloned as before to generate pIND-GBF1-GFP.

2.5. Isolation of NRK cell lines expressing GFP tagged GBF1

To generate stable lines, pIND-GBF1-GFP and pIND-GFP-GBF1 were separately electroporated into NRK cells in the presence of a plasmid encoding the hormone receptor pVgRXR (Invitrogen). Transfectants harboring both plasmids were selected by

growing cells in the presence of 400 μg/ml G418 and 200 μg/ml zeocin. Colonies were picked as they appeared, expanded under selection conditions and stored in liquid nitrogen until needed. Upon subsequent thawing and expansion, fluorescence microscopy revealed that only a subset of selected clones expressed GFP tagged GBF1, and in these only a fraction of the cells gave GFP signal. The clone with the largest fraction of GFP-positive cells expressed was chosen for further analysis. Two rounds of fluorescent activated cell sorting with GFP-specific filter settings yielded a population with a greatly increased fraction (~70%) of stably expressing cells relative to the original population (~30%). These cells, termed NRK-GFP-GBF1 remained heterogeneous and expressed varied levels of GFP-GBF1. Approximately 70% of GFP-positive cells express weak to moderate levels (1-1.5 times over endogenous level), which produce enough GFP signal for fluorescence microscopy.

Several lines of evidence demonstrate that the GFP-GBF1 used in our studies has properties indistinguishable from those of the endogenous protein and can be used to examine the properties of GBF1 in living cells. Foremost, GFP-GBF1, like endogenous GBF1 (refer to Figure 4.1), localized to a juxta-nuclear structure, and also to small peripheral punctae (Figure 2.1B arrowheads). More specifically, GFP-GBF1 colocalized very well with the *cis*-Golgi localized protein, p115, and remained separate from the TGN localized protein, BIG1 (Figure 2.1B), as will be described for endogenous GBF1 (refer to Figure 3.4). Additional observations further suggested that GFP-GBF1 remained functional: (1) GFP-GBF1, like the endogenous protein, accumulated on peripheral punctae within 30 sec but redistributed to the ER shortly thereafter in response to BFA treatment (Figure 2.2), and (2) as observed with full-length GBF1 (Claude et al., 1999),

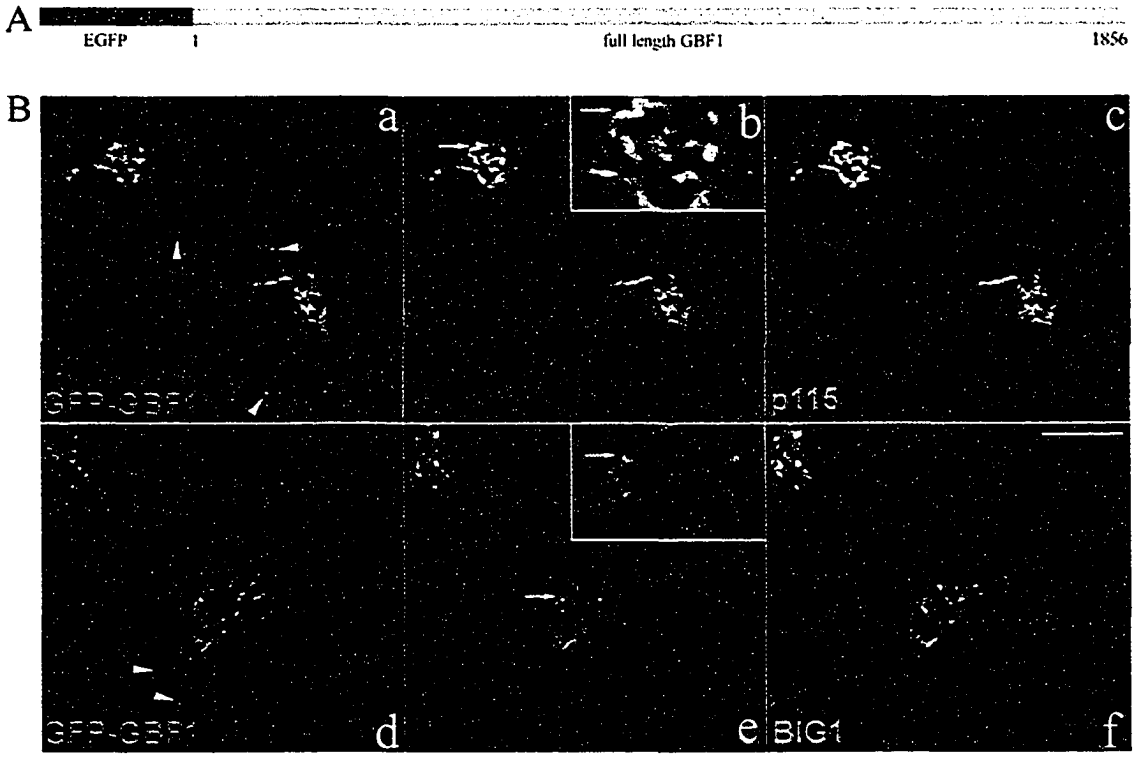

Figure 2.1. GFP-GBF1, like endogenous GBF1, localizes to membranes of the *cis*-Golgi and peripheral VTCs. **(A)** Schematic representation of GFP-GBF1: EGFP (green rectangle) was fused in frame with full length GBF1 (orange rectangle) at its N terminus. Chimera also contains additional residues (blue rectangle) encoded by plasmid-derived and GBF1 5'UTR sequences. **(B)** NRK cells stably expressing GFP-GBF1 were fixed and processed for either double-label IF by staining with affinity purified polyclonal antibody against GFP (a) and monoclonal antibody against p115 (3A10) (c), or single-label IF by staining with polyclonal antibody against BIG1 (9D3) (f). Peripheral punctae revealed by GFP fluorescence (d), or labeling with polyclonal antibodies against GFP (a) are indicated by arrowheads. Shown are single slice confocal images. Middle panels (b and e) show merged left and right images. The inset shows a threefold magnification of the area indicated by the arrow. Bar, 10 μm.

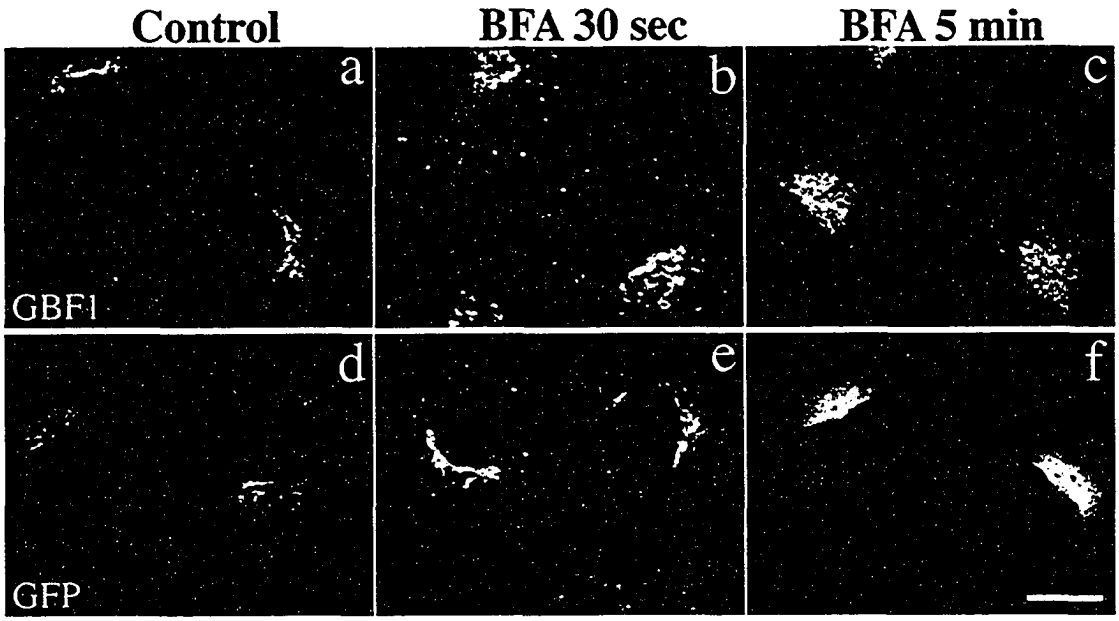

Figure 2.2. GFP-GBF1, like endogenous GBF1, accumulates on peripheral punctae prior to dispersal into the ER upon BFA treatment. NRK cells, either wt (a-c) or stably expressing GFP-GBF1, were treated with DMSO (Control, a and d) or 5 μg/ml BFA for 30 sec (b and e) or 5 min (c and f) before fixation. Cells were then processed for single-label IF using antibodies against GBF1 (a-c). Images d-f show GFP fluorescence. Images were obtained by standard epifluorescence microscopy. The smoother appearance of image f relative to image c likely resulted from direct imaging with GFP. Bar, 10 μm.

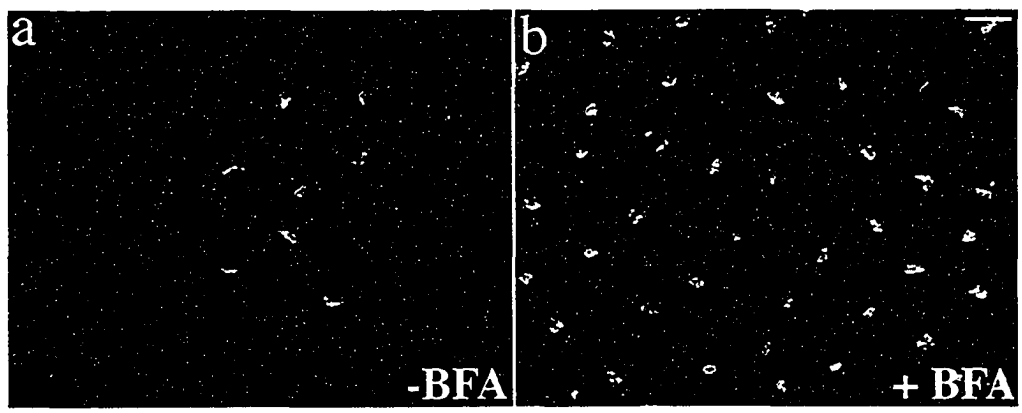

Figure 2.3. Overexpression of GFP-GBF1 enables NRK cells to grow in the presence of BFA at a concentration that kills wt parental cells. NRK cell clone obtained by antibiotics selection of cells transfected with GFP-GBF1 plasmid (see texts for details) was cultured in the presence of either DMSO ("-BFA", a) or 0.2 μg/ml BFA ("+BFA", b) for 72 hours. Cells were then fixed and processed for IF staining by using antibody against GFP. Although transfectants harboring GFP-GBF1 plasmid have been selected by growing cells in the presence of appropriate antibiotics, somehow a large fraction of cells did not give recognizable GFP signals and these cells were killed by BFA treatment. Bar, 20 μm.

overexpression permitted growth in the presence of BFA. For example, selection of the original population with ~30% expressing GFP-GBF1 (Figure 2.3a) in media containing 0.2μg/ml BFA yielded a cell population with increased fraction of positive cells that could grow in the presence of BFA (~90% Figure 2.3b). I did not perform further experiments with this BFA-resistant GFP-GBF1 population because of potential concerns with additional unforeseen adaptive changes in response to BFA.

2.6. Transient Expression in BHK-21 cells

For transient expression from plasmids encoding HA-tagged BIG1 or BIG2 fragments, BHK-21 cells grown on coverslips at 60% confluency were transfected with designated plasmids using FuGENE 6 transfection reagent according to manufacturer's instructions (Roche Molecular Biochemicals) and cultured for 20-24 h prior to fixation.

2.7. Immunofluorescence staining

Cells grown on glass coverslips were washed once in phosphate-buffered saline (PBS) and fixed with either methanol (–20°C, 6 min) or 3% paraformaldehyde in PBS (room temperature, 20 min). Double labeling with mouse and rabbit antibodies was performed as described before (Mansour et al., 1999). For double labeling with two rabbit primary antibodies, cells were first decorated with one unlabelled polyclonal antibody for 90 min, followed by Alexa594 labeled anti-rabbit IgG for 60 min. Cells were then incubated a second time for 60 min with the same unlabelled polyclonal antibody, prior to final labeling for 60 min with Alexa488-labelled BIG1 antiserum (9D3) or Alexa488-labelled GBF1 antiserum (H154). This precaution minimized potential labeling of the

9D3 or H154 antibodies with Alexa594 anti-rabbit IgG remaining in the sample. Several control experiments confirmed the lack of cross-reaction.

2.8. Epifluorescence microscopy and confocal microscopy

2.8.1 Epifluorescence microscopy

For Figures 2.2; 2.3; 2.4; 3.1B; 3.2C; 3.9; 4.1c-f; 4.8A; 4.9 and 4.10, mounted coverslips were viewed with an Axioskop microscope (Carl Zeiss, Thornwood, NY) equipped with a Spot 1.1 digital camera (Diagnostic Instruments). Images were taken with a 63× objective (NA=1.4). To minimize misalignment between channels, merged images were acquired using a dual-band filter set that can capture signals from red and green fluorophores simultaneously. This filter set (51004v2; Chroma Technologies) contains excitation bandpass filters of 470-490nm and 540-565nm and emission bandpass filters of 500-530nm and 580-620nm.

2.8.2 Confocal microscopy

For the remaining fluorescent micrographs, 8-bit confocal images were obtained with a LSM 510 microscope (Carl Zeiss) equipped with a 63× objective (NA=1.4) using 488 nm laser excitation and a 500-550 nm bandpass filter for Alexa488 and GFP, 543 nm laser excitation and a 560 nm longpass filter for Alexa594. When two markers were imaged in the same cells, each fluorophore was excited and detected sequentially (multitrack mode) to avoid channel bleed-through. Laser intensity, amplifier gain and image offset were adjusted to give maximum signal but avoid saturation (grayscale intensity of 255). Tests confirmed that under our detection conditions, images obtained in the red and green channels were in register to within 60 nm. To acquire single focal

plane images of identical thicknesses in each channel (0.8 μm), the pinhole diameter was adjusted to 1 or 1.05 for red and green channels, respectively.

For Figure 3.3, a through focus series of z sections was collected and displayed as orthagonal slices in LSM510 software provided with the microscope. For Figure 3.8, a through focus series of z sections was collected at 0.2 and 0.3 μm intervals and used to generate projections that better reveal peripheral structures.

2.8.3 Live cell time-lapse imaging

Living NRK-GFP-GBF1 cells were maintained at 37°C and imaged on the temperature-controlled stage of a Zeiss LSM510 confocal laser scanning microscope (see 2.8.2). Uniform and stable temperature was maintained with the aid of the Delta T system, supplemented with a heated lid and objective heater (Bioptechs). The LSM510 software was used to control image acquisition and manipulation. Unless otherwise indicated, fluorescent structures were viewed in a single image plane with the pinhole fully opened to maximize signal capture. Images were then exported either as still time point images or as QuickTime movies.

2.8.4. FRAP

FRAP experiments were performed on the temperature-controlled stage of a Zeiss LSM510 confocal microscope as described above (section 2.8.3). The region of interest (ROI) (outlined in figures) within a cell was bleached 30 times at 100% laser power (488nm line); recovery of fluorescence into the bleached area was monitored at 2 sec (for cytosolic FRAP) or 5 sec intervals by scanning at 1% laser power. No significant focal level change or photo-bleaching was observed during recovery.

2.9. Confocal images quantitation

2.9.1. Quantitation of double IF images

Quantitation of IF images was performed using either NIH image (version 1.62 downloaded from http://rsb.info.nih.gov/nih-image) or Metamorph (version 4.5r5 Universal Imaging Corporation). Our approach to quantify the degree of overlap of GBF1 and p115 in peripheral structures (Figure 3.8) was based on that described by Glick and colleagues (Hammond and Glick, 2000). Briefly, NRK cells incubated at 15°C for 2 hours were co-stained with H154 (anti-GBF1) and 3A10 (anti-p115). NIH image was then used to generate separate masks for the green and red signal using a range of threshold values that retained all discernable peripheral structures. For practical reasons, analysis was confined to smaller peripheral structures (<0.7 μM) with clearly identifiable centers; the number of structures eliminated from analysis was less than 5% of total. Two peripheral structures were defined as co-localized if their geometric centers (ultimate points in NIH image) were within three pixels (0.2 μm) from each other. Results are expressed as percentage of total spots chosen for analysis in the green mask that were concentric with spots in the red mask. A total of 7 cells (521 peripheral structures) were analyzed. Comparison of masks generated with various threshold values established that the choice of parameter did not significantly alter the outcome.

The extent of overlap between GBF1, BIG1 and several other markers in the perinuclear Golgi area (Figure 3.11) was quantitated as follows. Single focal plane images were used for this purpose. Pixels of interest were first identified by generating a mask for each channel to eliminate background signal resulting from non-specific binding or out-of-focus signal. The perinuclear region is the thickest portion of the cell

where intensity measurement errors due to out of focal plane fluorescence is most pronounced. Using Metamorph software, we overcame this problem by defining a threshold value in red and green channels separately that includes only the brighter labeled structures. Image capture conditions had been optimized to yield intensity values near the maximum 255, while avoiding over-saturation. For such images, preliminary studies established that threshold values near 100 were necessary to retain fine structure within the Golgi complex. For a few weaker samples, the maximum value was less than 255 and in those cases, an equivalent threshold value was defined as 40% of the maximum intensity. This procedure ultimately yielded binary "masks" that had values of 1 for the pixels with intensity above threshold value and 0 for all others. Shared pixels between the red and green masks were then identified with the "AND" function.

Rather than simply comparing the "number" of shared pixels to the total, overlap was defined as the percent of total signal "intensity" present in shared pixels. This approach yields a more accurate estimate of overlap since it weighs preferentially those pixels with greater intensity. To do this, we first had to recover the pixel intensity value information lost during processing. The binarized masks obtained above, were modified using a combination of subtract and multiply functions in Metamorph to regain the green and/or red intensity values above threshold. To calculate overlap for the green signal, we then used the ratio of the average intensity of the green pixels in the "AND" mask over that of the green mask. The converse calculation was performed for the red signal using the red mask and the "AND" mask modified with red pixel values. To eliminate contribution from peripheral staining, the analysis was restricted to the perinuclear Golgi

structure using Metamorph to select identical measurement areas in all three images (red, green, AND). For any given pair of markers, several cells were analyzed.

The validity of our quantitation method was established using two pairs of markers known to overlap either well or poorly. Images taken from NRK cells that were transfected with HA-tagged N1 fragment of BIG1 and doubly stained with anti-BIG1 and anti-HA antibodies were used as positive control (Figure 3.2C). By using the above quantitation method, 85% of BIG1 signal overlaps with HA-positive structures, while 90% of HA signal overlaps with BIG1 positive structures. Images taken from NRK cells doubly stained for TGN38 and p115 were used as negative control (Figure 3.4, a-c). We found that 29% of the TGN38 signal overlaps with p115 and 15% of p115 signal overlaps with TGN38. The small overlap between p115 and TGN38 likely results from the limitation of the IF confocal microscopy; however, we cannot exclude a partial colocalization of these two proteins.

2.9.2. FRAP Quantitation analysis

Quantitative analysis of recovery kinetics of GFP-GBF1 signal in the ROI (juxtanuclear Golgi region in Figures 4.2B; 4.2D and 4.6A; cytoplasm in Figures 4.2A and 4.6B) was performed using the ratios of the whole cell signal present in the ROI at each time point. Ratios at each time point were expressed as a fraction of the initial value before bleach (set as 1) and plotted against time, setting time zero as equal to the first time point after bleach. The data was then fit to the general equation for a single exponential $y = a\,(1 - e^{-bx}) + c$ using KaleidaGraph (version 3.6.1, Synergy Software, Reading, PA). Note that the first two time points after bleach that correspond to fast diffusion of free cytosolic GFP-GBF1 were excluded from the analysis to obtain fits to a

single exponential. The recovery half time ($T_{1/2}$) can be calculated from b as: $T_{1/2}$= ln2/b. The mobile fraction (R) can be determined by comparing the relative ROI / total cell ratio after full recovery (a) with the relative ratio before bleaching (1) and just after bleaching (Y_0) as: R=(a- Y_0)/(1- Y_0).

2.9.3. Diffusion coefficient

Diffusion coefficients of GBF1 in ER or in cytosol were determined by photobleach and computer analysis as described in (Siggia et al., 2000) and (Sciaky et al., 1997). Briefly, circular regions 3 microns in diameter located within flat regions of living cells and avoiding the nucleus were photobleached followed by acquisition of a time-lapse series. Total fluorescence within the photobleached region was acquired as a function of time. Dr. John Presley (McGill University, Montreal, Quebec) determined diffusion coefficients by comparing the actual recovery curve to a simulated recovery curve in which the immediate post-bleach image relaxed into the pre-bleach configuration, and appropriately scaling the temporal axis for a least-squared best fit of the curves. This was done using the algorithms and procedures described in detail in (Siggia et al., 2000) with spatial units provided in microns/pixel. The entire procedure including the curve fit was completely automated using computer software provided by Dr. E. Siggia. An important advantage of this method is that it does not require detailed knowledge of the geometry of the photobleached region and can be used even when the photobleached area is large compared to the size of the cell.

2.10. Nocodazole Treatment

We used a modified procedure to examine the microtubule requirement for

Figure 2.4. Incubation of cells for 2 h at 15°C in the presence of nocodazole causes complete depolymerization of microtubules. **(A)** NRK cells incubated for 2 h in a 15°C water bath were transferred to ice and incubated for another 15 min in the presence of either 0.1% DMSO vehicle control (DMSO) or 5 μg/ml nocodazole (NOZ). Cells were either immediately fixed (0 min) or quickly transferred to 37°C water bath and incubated for an additional 1 min before fixation. Coverslips were processed for double-label IF using polyclonal anti-GBF1 (a-b and e-f) and monoclonal anti-tubulin (c-d and g-h). **(B)** NRK cells were transferred to DME containing HEPES (pH 7.4) and either 0.1% DMSO vehicle control (DMSO) or 5 μg/ml nocodazole (NOZ), and then incubated in a 15°C water bath for 2 hours. Cells were quickly transferred to 37°C water bath and incubated for an additional 1 min before fixation. Coverslips were processed for IF using monoclonal anti-tubulin (i and j). Images presented were obtained by standard epifluorescence microscopy. Bar, 20μm.

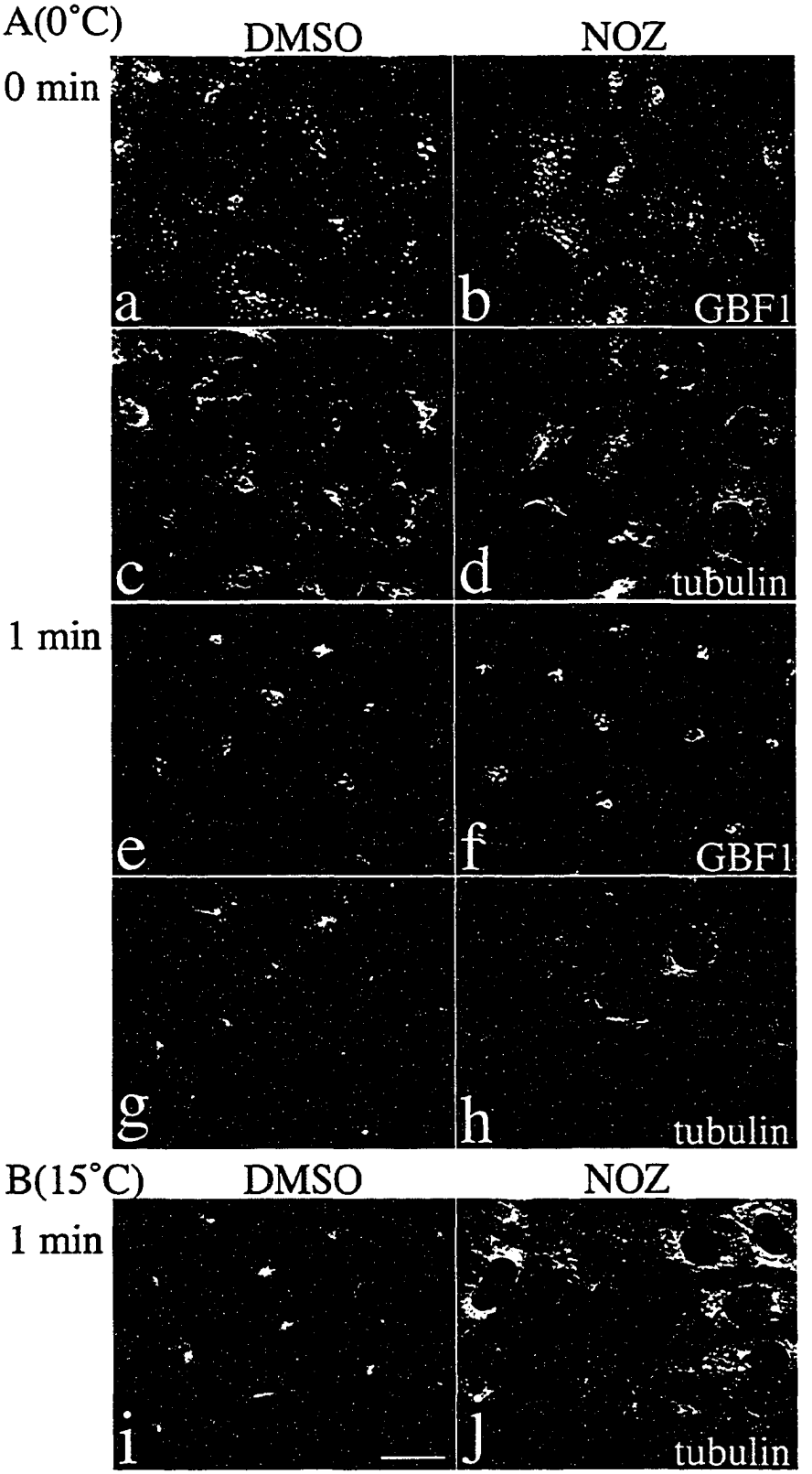

movement of VTCs. Preliminary experiments established that we could not use the standard approach of a brief incubation at 4°C with nocodazole before warm-up. Under these conditions, within 1 min of warm-up, depolymerization was incomplete (Figure 2.4A, image h) and sufficient microtubules remained to facilitate fast movement of GBF1 from peripheral structures to the perinuclear area (Figure 2.4A, image f). To solve this problem, we included 5 μg/ml nocodazole during the 2 h at 15°C (Figure 2.4B). Staining with anti-α-tubulin antibody confirmed that this method caused a complete loss of the microtubule array (Figure 2.4B, image j). The presence of nocodazole during the 15°C incubation neither prevented redistribution of GBF1, nor caused redistribution of Golgi resident enzymes such as Man II (refer to Figure 3.9).

2.11. BFA recruitment assays

BFA-mediated membrane recruitment of GBF1 was assayed using 3 x 150 mm plates of confluent NRK cells as starting material. Following trypsinization to release cells, media was added to neutralize the trypsin and cells were pelleted by centrifugation at 1000 g for 1 min at 4°C. Cells were washed in buffer (10 mM Tris pH 8, 150 mM NaCl, protease inhibitor cocktail (Roche), pepstatin A and O-phenanthroline), containing either 0.5 μg/ml or 5 μg/ml BFA, or vehicle control (DMSO). Pelleted cells were resuspended in 5 volumes of wash buffer containing either 0.5 μg/ml or 5 μg/ml BFA, or vehicle control (DMSO). Following 5 min incubation on ice, samples were homogenized by 15 passages through a 23 gauge needle and the homogenates were subjected to low speed centrifugation (1000 g for 1 min at 4°C). The low speed supernatant (usually 100 μl) was subsequently centrifuged at 115,000 g for 5 min at 4°C. The resultant

supernatant (cytosol) was retained and NP40 was added to a final concentration of 1%. An equivalent volume of wash buffer containing 1% NP40 was used to resuspend the high speed pellet (microsomes) for SDS-PAGE analysis.

2.12. Immunoblot analysis

Equivalent amounts of the cytosolic and microsomal fractions were separated by Tris-Glycine SDS-polyacrylamide electrophoresis, on 5% polyacrylamide gels calibrated with prestained molecular weight standards (Bio-Rad). Following electrophoresis, proteins were transferred to nitrocellulose membranes and immunoblotted with primary antibodies at the indicated concentration. Protein-antibody complexes were detected by enhanced chemiluminescence with horseradish peroxidase-conjugated secondary antibody using the ECL-plus western blot detection system (Amersham Pharmacia Biosciences) as directed. Digital images were captured using a FluorChem 8000 imaging system (AlphaInnotech Corp, San Leandro, CA).

2.13. VSVtsO45 infection

COS-1 cells were grown to confluence on glass coverslips in a tissue culture dish. Cells were infected with VSVts045 in CO_2-independent DMEM without FBS at 32°C for 1 h with occasional rocking at 10-15 min intervals. The infected cells were then incubated at the restrictive temperature (40.5°C) for 3 h post-infection in DMEM with 10% FBS to accumulate newly synthesized G-protein in the ER. ER-restricted VSVG protein was released by incubation at the permissive temperature (32°C) for various time periods. Cells on the coverslips were then fixed and processed for IF as described above.

2.14. Microinjection

Before microinjection, affinity purified anti-GBF1 antibodies to be used were concentrated to ~20 mg/ml in PBS by membrane ultrafiltration (Centricon and Microcon, 30 kDa for NMWL) (Millipore, Billerica, MA) and cleared by passage through a 0.22 um filter. Hela cells were grown to ~80% confluence on glass coverslips in 35 mm tissue culture dishes, and antibodies were injected into the cytoplasm of cells with an Eppendorf semi automated microinjector and Femtotip needles (Brinkmann Instruments Inc., Westbury, NY). Injections were performed on a Nikon TE300 inverted microscope by Dr. Sun. After microinjection, cells were returned to the incubator and then fixed and processed for IF as described above 2 h later.

Chapter 3

Localization of large Arf-GEFs to different Golgi compartments: Evidence for distinct functions in protein traffic

Figure 3.1 was published in " Mansour, S.J., J. Skaug, X.H. Zhao, J. Giordano, S.W. Scherer, and P. Melançon. 1999. p200 ARF-GEP1: a Golgi-localized guanine nucleotide exchange protein whose Sec7 domain is targeted by the drug brefeldin A. *Proc Natl Acad Sci U S A.* 96:7968-73". Most of the remaining figures presented in this chapter were published in "Zhao, X., T.K. Lasell, and P. Melançon. 2002. Localization of large ADP-ribosylation factor-guanine nucleotide exchange factors to different Golgi compartments: evidence for distinct functions in protein traffic. *Mol Biol Cell.* 13:119-33.".

3.1. Overview

As introduced in Chapter 1, the two major coat proteins of the Golgi complex, COPI and clathrin, localize to *cis*- and *trans*-side of this organelle, respectively. We hypothesized that Arf-GEFs may help determine when and where these different coat proteins are recruited. This hypothesis was based on the expectation that localization of Arf-GEFs should determine when and where Arfs are activated, and activated Arfs subsequently determine when and where distinct coated membrane carriers are formed. We tested this hypothesis by investigating the detailed subcellular localization of GBF1 and BIGs. GBF1 and BIGs belong to the GBF/GEA and BIG/SEC families (Cox et al., 2004). Although previous observations suggested that GBF1 and BIGs differ in Arf substrate specificity and BFA sensitivity, these two families of large mammalian GEFs both localized to the Golgi complex in intact cells.

In this chapter, I demonstrate that GBF1 and BIGs can be further distinguished by their predominant localization to *cis*- and *trans*-elements of the Golgi complex, respectively. These observations suggest that Arf-GEFs may participate in coat selection. Furthermore, our observation that GBF1 is the only identified *cis*-Golgi localized mammalian Arf-GEF challenges current thinking that GBF1 is a BFA-resistant Arf-GEF (Claude et al., 1999) since this *cis*-Golgi localized Arf-GEF should be responsible for the BFA sensitivity of the early secretory pathway.

3.2. Endogenous BIG1 localizes to the Golgi complex through sequences present in the N-terminal third of the protein

Our previous localization studies of BIG1 revealed that full-length HA-tagged

BIG1 is targeted to the Golgi complex (Mansour et al., 1999). To identify domains involved in Golgi localization of BIG1, plasmids encoding five truncations of BIG1 with a HA tag at the N-terminus (Figure 3.1A) constructed by Dr. Sam Mansour were transfected into BHK-21 cells. The results presented in Figure 3.1B revealed that truncations N1 and N2 localize to a juxtanuclear structure reminiscent of the Golgi complex. Costaining with an antibody that recognizes Man II, a transmembrane Golgi marker, confirmed this assignment. The remaining three truncations lacking the amino-terminal third appeared diffuse, and in the case of M1, even localized in the nucleus. This demonstrated that the N-terminal region is required and sufficient for localization of BIG1 to the Golgi complex.

To further investigate BIG1 localization under physiological conditions, we examined the localization of endogenous BIG1. To achieve this goal, antibodies were raised by immunizing rabbits with recombinantly produced fragments of BIG1 (see section 2.3.1). One serum (9D3) that recognizes a truncation containing the Sec7d termed M1 worked best for IF and was therefore chosen for further analysis. When assayed by immunoblotting, affinity-purified 9D3 showed greater specificity than crude serum, and labeled specifically a protein of 208 kDa, the size predicted from the cDNA (Figure 3.2A). When used for IF, both 9D3 crude serum and affinity-purified 9D3 gave nearly identical perinuclear signals with little cytoplasmic staining (Figure 3.2B). Addition of excess immunizing protein (M1) eliminated perinuclear staining (Figure 3.2B). Theneutralization of perinuclear staining by excess antigen was specific to BIG1, since it had no effect on the co-staining with monoclonal antibodies against p115 (figure 3.2B).

After we established that the N-terminal third fragment of BIG1 (N1-BIG1) is

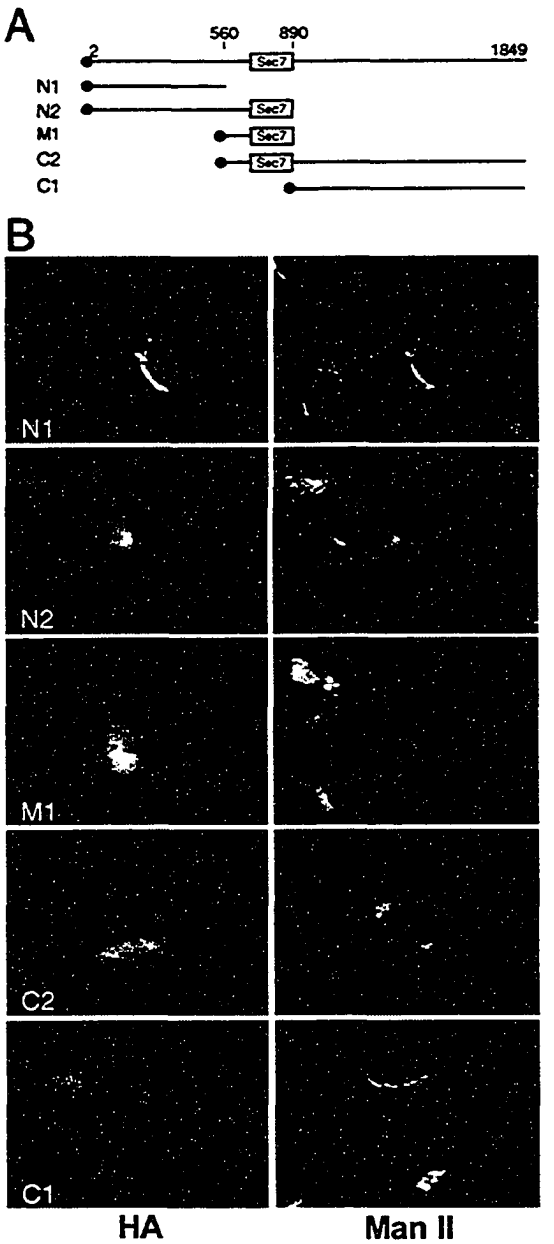

Figure 3.1. N-terminal region is required and sufficient for localization of BIG1 to the Golgi complex. **(A)** Schematic representation of HA-tagged truncations in reference to full-length protein. Numbers refer to the position of amino acids in the full-length polypeptide; the filled circle symbolizes the HA tag. **(B)** BHK-21 cells were transiently transfected with plasmids encoding HA-tagged truncations of BIG1 and processed for IF using antibodies against the HA epitope (3F10) and Man II. Each horizontal pair of panels corresponds to a field of view seen with different filters. These results were reproduced in several independent transfections.

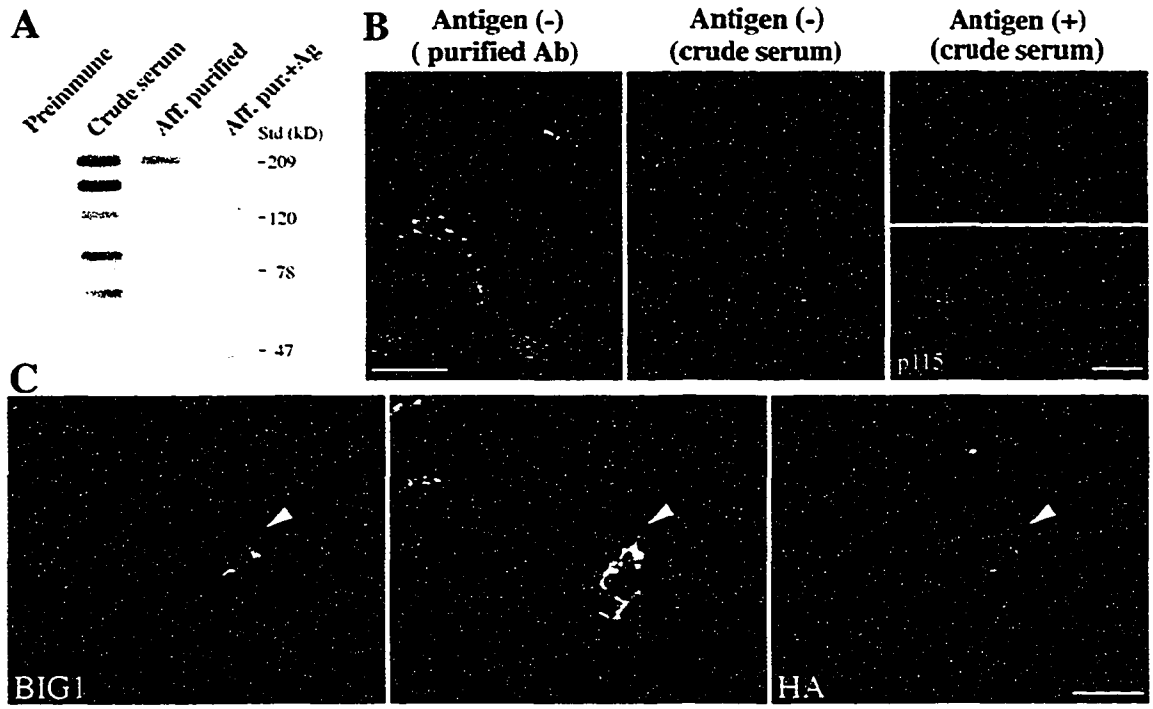

Figure 3.2. Endogenous BIG1 localizes to the Golgi complex through sequences present in the N-terminal third of the protein. **(A)** Both crude and affinity purified 9D3 serum (anti-BIG1) label a protein of 208 kDa, the size predicted from the cDNA of hBIG1. NRK cell lysates (400 μg) were loaded into the wide lane (7.3 cm) of an 8% gel, separated by SDS-PAGE, and then transferred to a nitrocellulose membrane. Narrow membrane strips (~0.5cm) were incubated with the indicated sera at equivalent dilutions and processed for enhanced chemi-luminescence. One strip was incubated with antibody in the presence of 2 μg antigen, as indicated. The position of molecular weight standards run in parallel is shown on the right side. Shown are representative data from two experiments with similar results. **(B)** Both crude and affinity-purified 9D3 serum specifically localize endogenous BIG1 to a perinuclear structure by IF. NRK cells were fixed and processed for either single-label IF using 9D3 sera (crude serum or affinity-purified antibody) or double –label IF using monoclonal anti-p115 and 9D3 crude serum in the presence of the immunizing antigen (1 μg). Shown are single slice confocal images. **(C)** N-terminal third truncation of BIG1 (N1-BIG1) is recruited to the same sub-compartment within the Golgi complex as full length endogenous BIG1. NRK cells were transiently transfected with constructs encoding HA-tagged N1 truncation of BIG1 and processed for IF by incubation with rabbit serum 9D3 and monoclonal anti-HA 3F10. Transfected cell is indicated by arrowhead. Images were obtained by standard epifluorescence microscopy because the low transfection efficiency made confocal microscopy impractical in this case. The middle image was taken using a dichroic filter to simultaneously capture the signal from both the red and green fluorophores. Bars (B and C), 10μm.

required and sufficient for localization of BIG1 to the Golgi complex (Figure 3.1B), we next determined whether N1-BIG1 was recruited to the same sub-compartment within the Golgi complex as full length endogenous BIG1. Our new serum, 9D3, which specifically recognizes the endogenous BIG1, but not N1–BIG1 that lacks the Sec7d, allowed us to address this question. NRK cells were transfected with a vector encoding HA-N1-BIG1 and then double-stained with anti-HA and 9D3 (Figure 3.2C). The representative images presented in Figure 3.2C revealed that overexpressed exogenous N1-BIG1 colocalizes extensively with endogenous BIG1. These results not only confirmed the perinuclear Golgi localization obtained with overexpressed HA-tagged forms (Mansour et al., 1999), but also provided additional evidence for the specificity of our new 9D3 serum. More importantly, these observations demonstrated that the targeting information in the N-terminal third of the protein is sufficient to localize the protein to the correct Golgi sub-compartment. Whether this region contains a targeting signal, or is involved in dimerization to a full-length molecule with the targeting signal remains unclear.

3.3. GBF1 and BIG1 are recruited to different compartments of the Golgi complex

Experiments with BHK cells over-expressing HA-tagged BIG1 first revealed that both GBF1 and over-expressed tagged BIG1 localized primarily to perinuclear structures but overlapped with each other to a very limited extent (see Figure 3.3a). Analysis of red and green signal along the Z-axis confirmed the extent of signal separation (side panels in Figure 3.3a). To establish that the lack of overlap did not result from the use of an over-expressed tagged protein, we further compared the localization of endogenous BIG1 and GBF1. Since the only antibodies available against these two GEFs were polyclonal, one

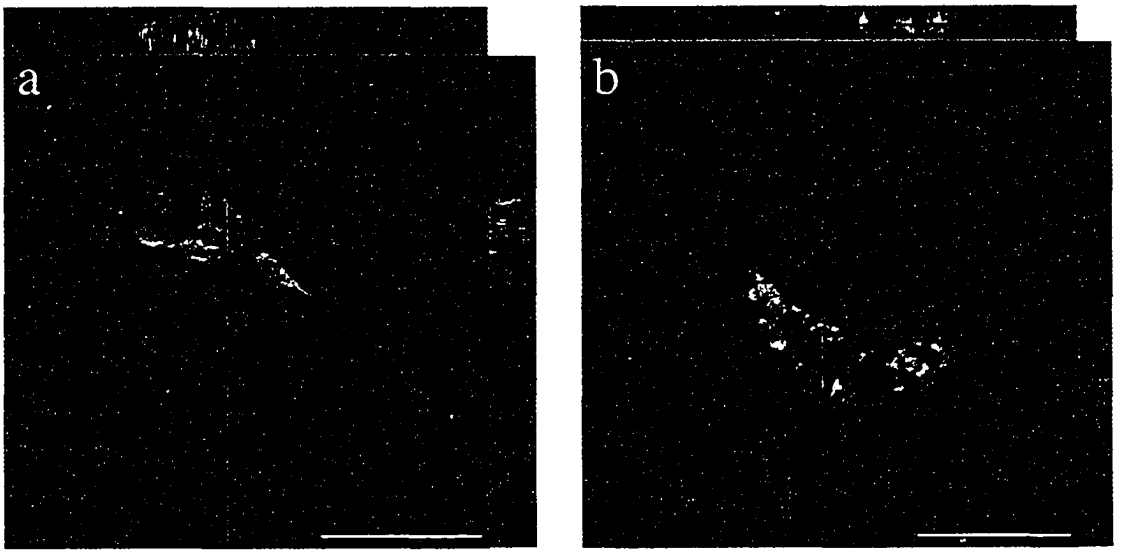

Figure 3.3. GBF1 and BIG1 are recruited to different compartments of the Golgi complex. (a) BHK-21 cells were transiently transfected with a plasmid encoding HA-tagged full length BIG1 and processed for IF using antibodies against the HA epitope (3F10/Fluorescein) and GBF1 (H154/ Texas red). **(b)** NRK cells were fixed and processed for IF using antibodies against GBF1 (H154/Alexa594) and BIG1 (Alexa488-conjugated 9D3). Both images (a and b) were obtained by collecting stacks of optical sections (3.2μm in thickness for BHK-21 cell (a) and 2.0μm for NRK cell (b)) using a confocal microscope. Shown in the center is an X-Y slice. Above and to the right are slices through the stack that reveal the distribution in the X-Z and Y-Z planes at the position indicated by the magenta and green lines, respectively. Bars, 10μm. Similar results were obtained from at least three independent experiments.

of them (anti-BIG1 rabbit serum, 9D3) was conjugated with the fluorophore Alexa-488. Double staining of NRK cells with this antibody and a previously characterized anti-GBF1 polyclonal serum (H154) confirmed that GBF1 and BIG1 do not overlap (see Figure 3.3b). Although usually in close proximity, the BIG1 and GBF1 signals not only remained clearly separate from each other, but also often took on very different patterns. Quantitative analysis discussed in more detail in Figure 3.11 confirmed this interpretation.

3.4. GBF1 and BIG1 localize to *cis*- and *trans*-compartments of the Golgi complex, respectively

Double staining of NRK cells with antibodies for two well characterized markers of the *cis*-Golgi and TGN, p115 and TGN38, respectively, confirmed the feasibility of distinguishing *cis*-Golgi and *trans*-Golgi proteins by IF at light microscopy level in these cells (Figure 3.4, a-c). NRK cells decorated separately with antibodies raised against either GEF and each co-stained for the common *cis*-marker p115 revealed that GBF1 largely co-localized with p115 (Figure 3.4, d-f). In contrast, the staining for BIG1 appeared largely distinct from that observed for p115 (Figure 3.4, g-i). Identical results were obtained with another *cis*-Golgi marker, p58 (Figure 3.5). These results indicated that GBF1 associates primarily with early compartments of the Golgi complex and confirmed our initial observation of distinct localization for GBF1 and BIG1 (Figure 3.3). In addition, they suggested that BIG1 might localize to *trans*-elements of the Golgi complex. This possibility was tested directly by comparing the localization of BIG1 and TGN38 using Alexa488-labeled BIG1 antibody and a polyclonal serum to TGN38.

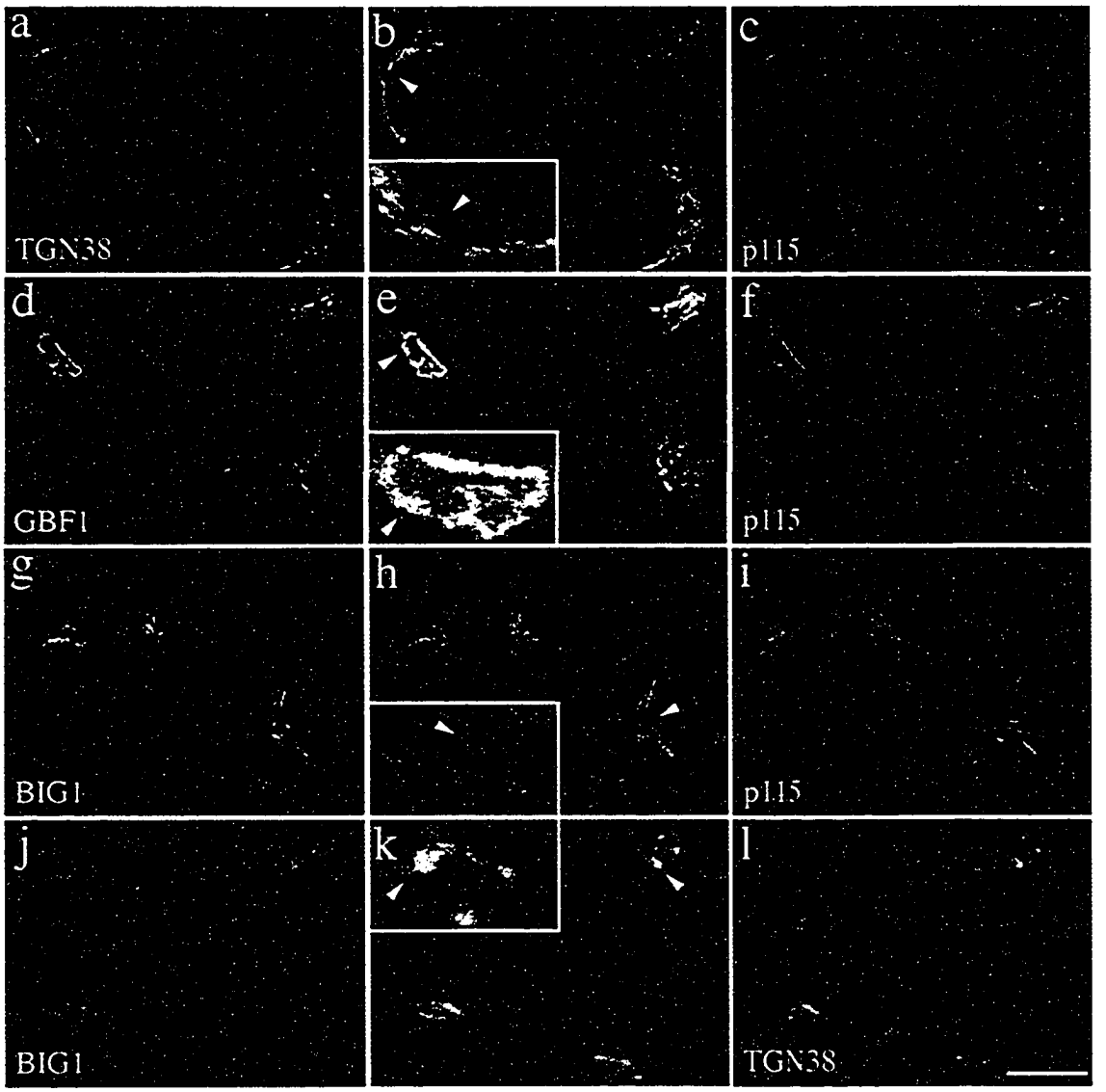

Figure 3.4. GBF1 and BIG1 localize to *cis* and *trans*-compartments of the Golgi complex, respectively. NRK cells were fixed and processed for double-label IF using either polyclonal anti-TGN38 (a), anti-GBF1 (d) or anti-BIG1 (g), and monoclonal anti-p115 (c, f and i), or two polyclonal antibodies: Alexa488-conjugated 9D3 (anti-BIG1, j) and anti-TGN38 (l). Shown are single slice confocal images. Middle panels (b, e, h and k) show merged left and right images. The inset shows a 3-fold magnification of the area indicated by an arrowhead. Bar, 10μm. Shown are representative data from at least three experiments with similar results.

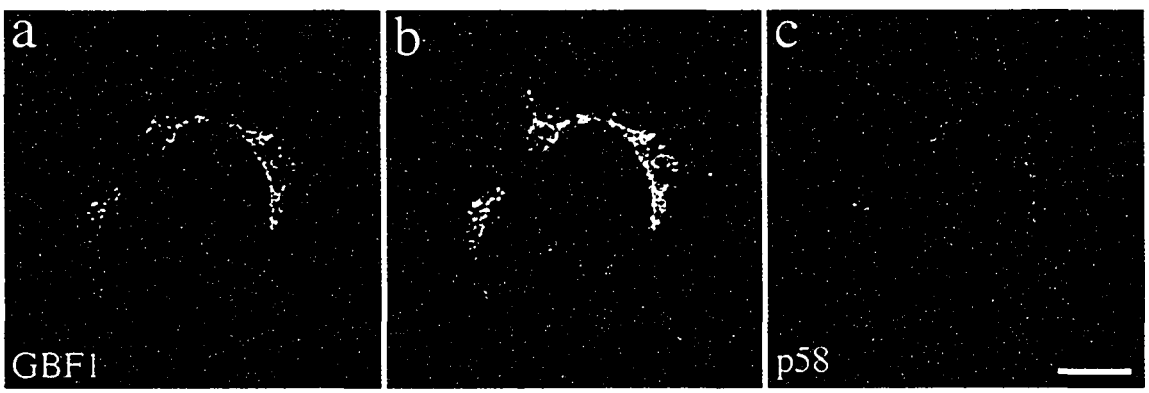

Figure 3.5. GBF1 extensively colocalize with the *cis*-Golgi marker p58. BHK-21 cells were fixed and processed for double-label IF using polyclonal anti-GBF1 (a) and monoclonal anti-p58 (c). Shown are single slice confocal images. Middle panels (b) show merged left and right images. Bar, 10μm.

These experiments established that BIG1 largely overlapped with TGN38 (Figure 3.4, j-l). Higher magnifications of selected regions of merged images are presented in boxed insets to better illustrate the relative localization of the GEFs. We conclude that GBF1 and BIG1 localize to *cis* and *trans*-elements of the Golgi complex, respectively. Quantitative analysis described in more detail in Figure 3.10 clearly supported this interpretation.

Previous work by Vaughan and colleagues predicts that BIG2 should have a distribution nearly identical to that of BIG1 and thus be distinct from that of GBF1: Co-IP studies established that the bulk of BIG1 and BIG2 exist as a complex, and initial IF studies suggested extensive colocalization of these two GEFs (Yamaji et al., 2000). Since our attempts to generate antibodies that recognize endogenous BIG2 were unsuccessful, we chose to investigate the relative distribution of BIG2 and GBF1 by constructing a series of HA-tagged fragments containing the N-terminal domain of BIG2 (constructed by T. Lasell; see section 2.4.2). As was the case for BIG1, a fragment containing the N-terminal third of BIG2 (HA-N-BIG2) localized to a perinuclear structure, which resembled that observed with several Golgi markers. More detailed analysis demonstrated that the staining pattern of BIG2, although perinuclear, remained quite distinct from that of the *cis*-Golgi marker p58 (Figure 3.6, a-c). More importantly, double staining of BHK cells overexpressing HA-N-BIG2 for HA and GBF1 confirmed that there is little overlap between GBF1 and BIG2 (Figure 3.6, d-f). Higher magnifications of selected regions of merged images are presented in boxed insets to better illustrate the relative localization of exogenously expressed HA-N-BIG2. We

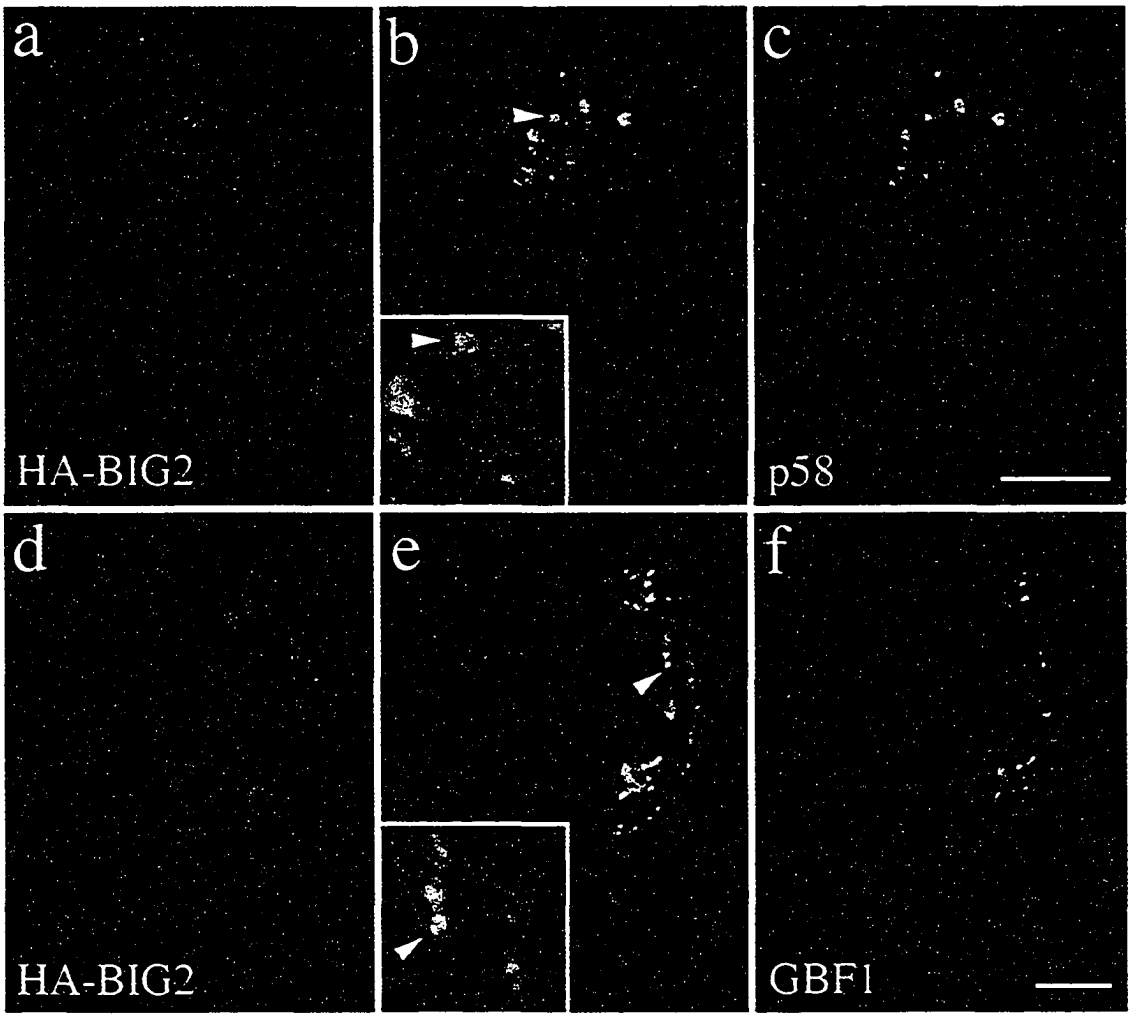

Figure 3.6. N terminus of BIG2, like BIG1, does not colocalize with GBF1 and the *cis*-Golgi marker p58. BHK-21 cells were transiently transfected with a plasmid encoding HA-tagged N-BIG2 and processed for double-label IF using monoclonal anti-HA and polyclonal antibodies against either p58 (a-c) or GBF1 (d-f). Shown are single slice confocal images obtained with the indicated antibody. Middle panels (b and e) show superimposed left and right images. The inset shows a 3-fold magnification of the area indicated by an arrowhead. Bars, 5μm. Distinct staining for HA-BIG2 and GBF1 was observed in each of four experiments.

conclude that the two Arf-GEF families localize and function in distinct regions of the Golgi complex.

3.5. GBF1 and BIG1 redistribute to distinct structures in response to BFA

To further test the behavior of GBF1 and BIG1 as proteins of *cis*- and *trans*-Golgi compartments, we examined the effect of the fungal metabolite BFA on their distribution (Figure 3.7). In most animal cells, BFA treatment will induce extensive tubulation of both the TGN and central stack of the Golgi complex, and cause their resident enzymes to redistribute to distinct compartments. BFA-induced tubules from the main Golgi stack eventually fuse with the ER. In contrast, tubulation of *trans*-cisternae leads to formation of a hybrid organelle with the endosomal system that clusters near the microtubule-organizing center (Klausner et al., 1992). Double staining of NRK cells treated with 10 μg/ml BFA for either 10 or 30 min at 37°C prior to fixation, established that the two GEFs eventually moved to distinct structures following prolonged BFA treatment (Figure 3.7, e and f). While GBF1 redistributed to a diffuse ER pattern similar to that observed with ManII (Figure 3.7, e and g), BIG1 appeared in a dense collection of fine punctate structures near the nucleus reminiscent of that observed with TGN38 (Figure 3.7, f and h).

3.6. GBF1, but not BIG1, redistributes from the Golgi complex to peripheral VTCs at 15°C

The *cis*-Golgi localization of GBF1 suggests that it regulates events at the interface between the ER and Golgi complex. To test this possibility, we examined the

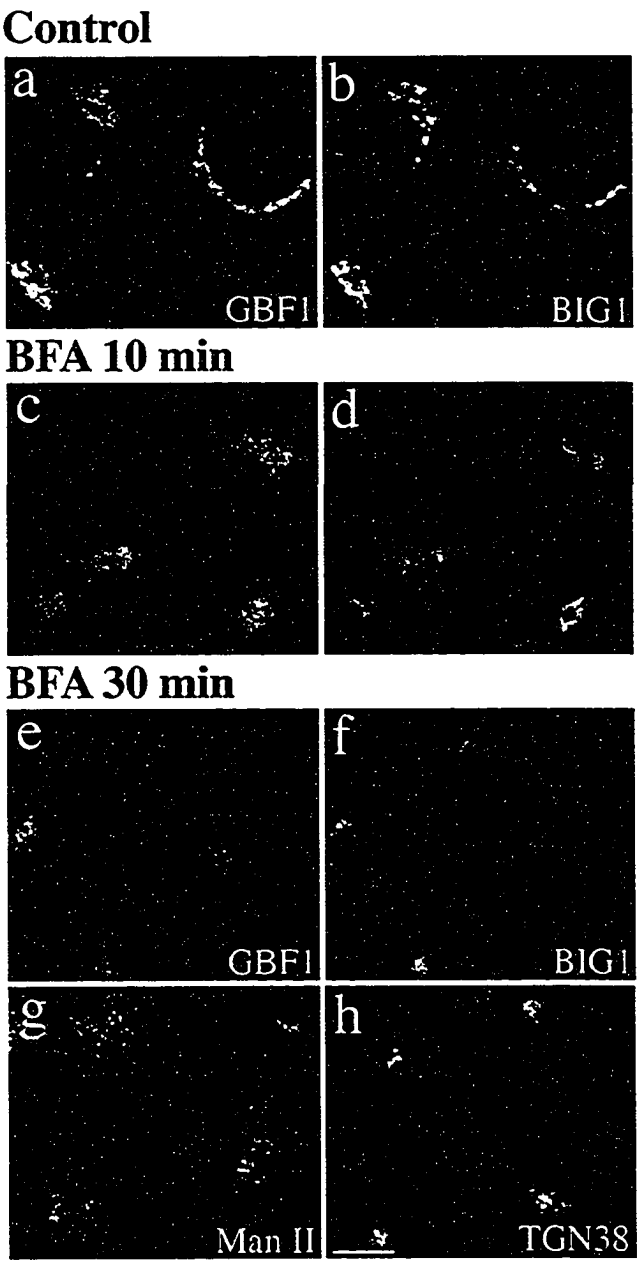

Figure 3.7. GBF1 and BIG1 redistribute to distinct structures in response to BFA. NRK cells were treated with either 0.1% DMSO (**Control**) for 30 min or 10 μg/ml BFA for either 10 min (**BFA 10 min**) or 30 min (**BFA 30 min**) at 37°C prior to fixation and processing for IF. Cells were either double-stained using two polyclonal antibodies (a-f) against GBF1 (H154/Alexa594; a, c and e) and BIG1 (Alexa488-conjugated 9D3; b, d and f), or singly stained using polyclonal antibodies against Man II (g) or TGN38 (h). Shown are single slice confocal images. Bar, 10μm. Similar results were obtained from at least two independent experiments.

effect of incubation at lower temperature on the subcellular localization of GBF1. Protein traffic between the ER and Golgi stack in animal cells is temperature sensitive and blocked at temperatures below 15°C. Under these conditions, cargo accumulates in small punctate peripheral structures called VTCs (Saraste et al., 1986). Proteins that shuttle between the *cis*-Golgi and VTCs, p115 and KDEL receptor for example, also accumulate in peripheral VTC structures during prolonged incubation at 15°C (Alvarez et al., 1999). To examine how GBF1 and BIG1 react during treatment at lower temperature, NRK cells either kept at 37°C or incubated at 15°C for 2 h prior to fixation were processed for IF using antibodies that recognize p115, endogenous GBF1 or endogenous BIG1. As shown in Figure 3.8, GBF1, like p115, largely redistributed to peripheral punctate structures during the 15°C block (Figure 3.8, a-c). In contrast, BIG1 remained in a tight ribbon-like perinuclear structure under conditions where p115 clearly redistributed throughout the cell (Figure 3.8, d-f).

The appearance of GBF1 in peripheral structures suggested that GBF1 might function to regulate Arf activation during formation and/or maturation of VTCs. Extensive colocalization of p115 and GBF1 in merged images indeed suggests that GBF1 associates with p115 positive structures at reduced temperatures (Figure 3.8b). Additional experiments confirmed the expected presence of COPI in those peripheral structures (Figure 3.8, g-i). Quantitative analysis of Figure 3.8b and several similar images established that 88 ± 2% of peripheral structures examined (7 cells / 521 structures) stain for both GBF1 and p115 (see section 2.9.1). As predicted from the range of color (orange-yellow-lime) in the merged images, the ratio of green to red signal within these overlapping peripheral structures was quite variable. In spite of this

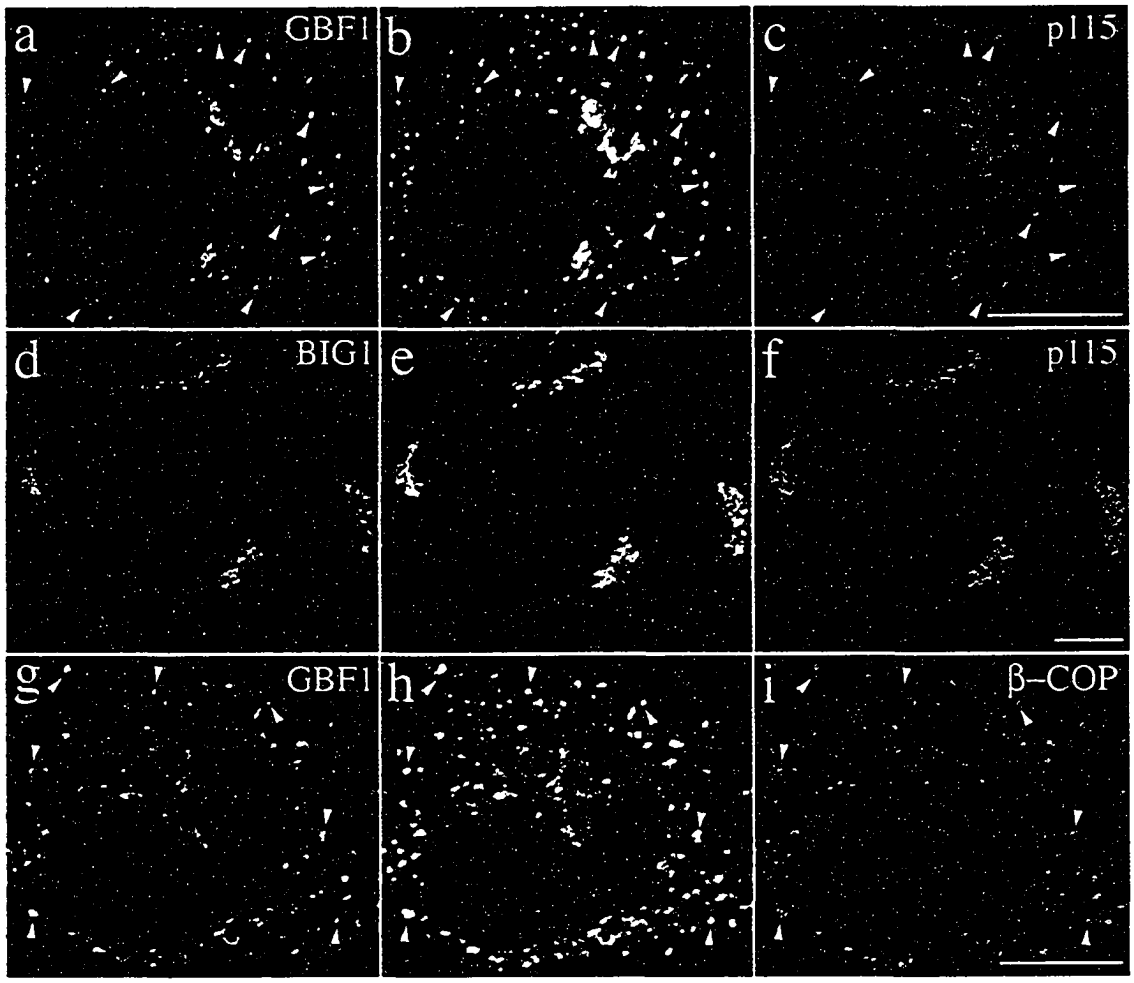

Figure 3.8. GBF1, but not BIG1, redistributes from the Golgi complex to peripheral VTCs at 15 °C. NRK cells incubated for 2 hours in a 15°C water bath prior to fixation were processed for double-label IF using monoclonal antibodies against either p115 (c and f) or β-COP (i) and polyclonal antibodies that recognize either GBF1 (a and g) or BIG1 (d). To better reveal small peripheral structures, projections of several confocal slices are shown. Middle panels (b, e and h) show superimposed left and right images. As indicated by arrowheads in image b and h, the peripheral GBF1 and p115 or β-COP staining patterns are almost identical. Peripheral structures appear as either yellow or orange dots depending on the relative intensity of red and green signals. The apparent partial overlap between BIG1 and p115 in perinuclear area shown in image e is due to the overexposure of perinuclear signals in order to better display small peripheral structures. Bars, 10μm. The distinct response to temperature shift for GBF1 and BIG1 was observed in each of at least three separate experiments.

unexplained variation, the presence of p115 in GBF1-positive peripheral structures clearly suggests a function for GBF1 at early stages of exocytosis.

To further test the functional significance of GBF1 in peripheral structures, we determined whether this redistribution was readily reversible upon warm-up. Previous studies established that cargo accumulated in peripheral structures at 15°C migrates towards the Golgi stack at speeds about 1 μm / s, and does so in a microtubule-dependent manner (Presley et al., 2002; Scales et al., 1997). We found that GBF1 accumulated in peripheral structures at 15°C does return to perinuclear localization upon warm-up to 37°C. This redistribution was extremely rapid and complete in less than one minute (Figure 3.9, left, DMSO). This result is consistent with previous estimates of migration rates for ER-Golgi transport intermediates mentioned above. In contrast, GBF1 remained in peripheral structures when incubations were performed under conditions where microtubules have been disrupted with nocodazole (Figure 3.9, right, NOZ). Significant amounts of GBF1 remained in peripheral structures even after a 10-min incubation in the absence of microtubules (Figure 3.9j). Under these conditions, ManII, a Golgi resident enzyme of medial cisternae clearly did not redistribute to peripheral structures (Figure 3.9l). The observation that GBF1 associates with peripheral structures clearly distinct from the perinuclear structures positive for Man II further strengthens our conclusion that GBF1 is involved in traffic between the ER and Golgi complex.

3.7. GBF1, but not BIG1, overlaps significantly with COPI

Several studies established that COPI components associate primarily with VTCs and *cis*-compartment of the Golgi complex (Griffiths et al., 1995; Oprins et al., 1993).

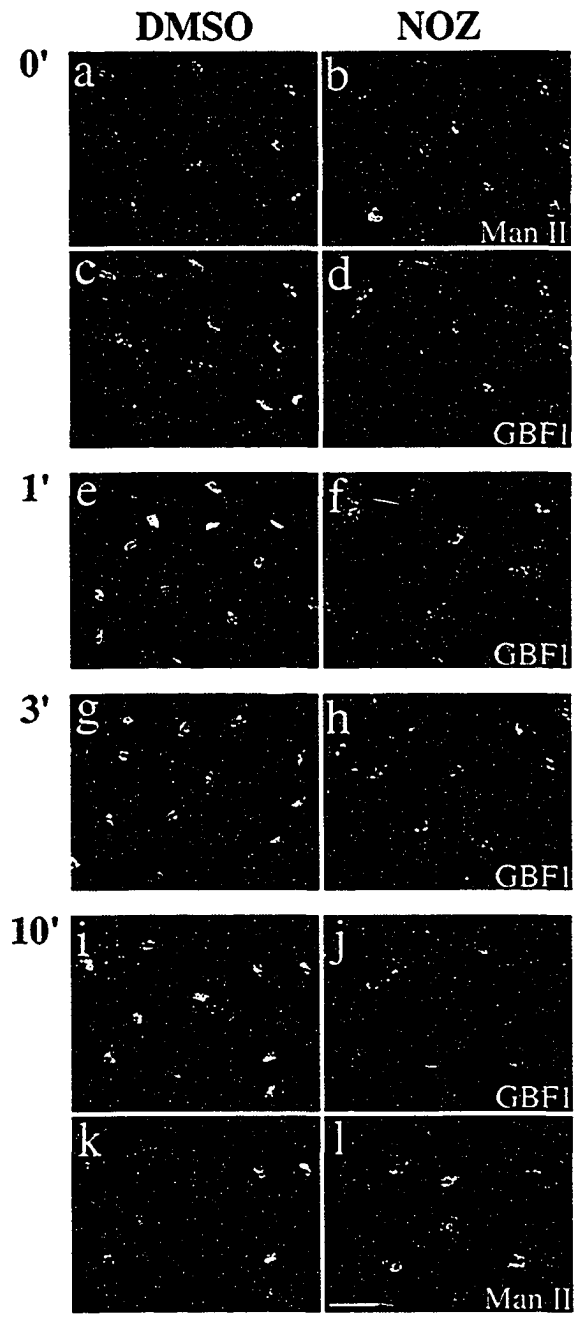

Figure 3.9. Redistribution of GBF1 from the 15°C peripheral compartments upon warm-up to 37°C is microtubule-dependent. NRK cells were transferred to DME containing HEPES (pH 7.4) and either 0.1% DMSO vehicle control (**DMSO**) or 5μg/ml Nocodazole (**NOZ**), and then incubated in a 15°C water bath for 2 hours. Cells were either immediately fixed (**0'**) or quickly transferred to 37°C water bath and incubated for additional 1 min (**1'**), 3 min (**3'**) or 10 min (**10'**) before fixation. Coverslips were processed for IF using polyclonal anti-GBF1 (e-h) or double-label IF (a-d and i-l) using polyclonal anti-GBF1 (c-d, and i-j) and monoclonal anti-Man II (53FC3) (a-b, and k-l). Images obtained by standard epifluorescence microscopy are presented. Bar, 20μm. Similar results were obtained in at least two independent experiments.

Furthermore, the association of COPI with Golgi membranes has been shown in several studies to be very sensitive to BFA (Donaldson et al., 1990; Oprins et al., 1993). The demonstration that a BFA-resistant GEF (GBF1) rather than the BFA-sensitive ones (BIGs) are present in *cis*-regions of the Golgi prompted us to examine the relative distributions of the GEFs with known coat components. Double labeling of NRK cells show that GBF1, but not BIG1, overlaps significantly with the COPI coat (Figure 3.10, a-c). Whereas a few punctate peripheral structures positive for β-COP appear to lack GBF1 (Figure 3.10, b and c, arrows), the majority of the perinuclear structures show extensive overlap of these two markers (Figure 3.10b). Close examination revealed that the vast majority of bright β-COP-positive structures also stained for GBF1. However, as illustrated in the inset, a significant amount of β-COP signal often surrounded structures containing both markers. In contrast, BIG1-positive structures although in close apposition, remained largely distinct from those labeled with β-COP antibody (Figure 3.10e, inset).

These results suggest that the primary function of BIGs may be to regulate activation of Arfs for recruitment of other coat proteins such as APs and / or GGAs in *trans*-elements of the Golgi. In agreement with this possibility, double staining with antibodies against clathrin and either of the two Arf-GEFs revealed closer association of clathrin with BIG1 than with GBF1 (Figure 3.10, g-l). The overlap between clathrin and BIG1 remains partial and appears limited to the perinuclear regions. The insets in Figure3.10, panel h and k, illustrate the difference in the degree of overlap of the two GEFs with clathrin.

To better estimate the extent of overlap between GEFs and other proteins, we

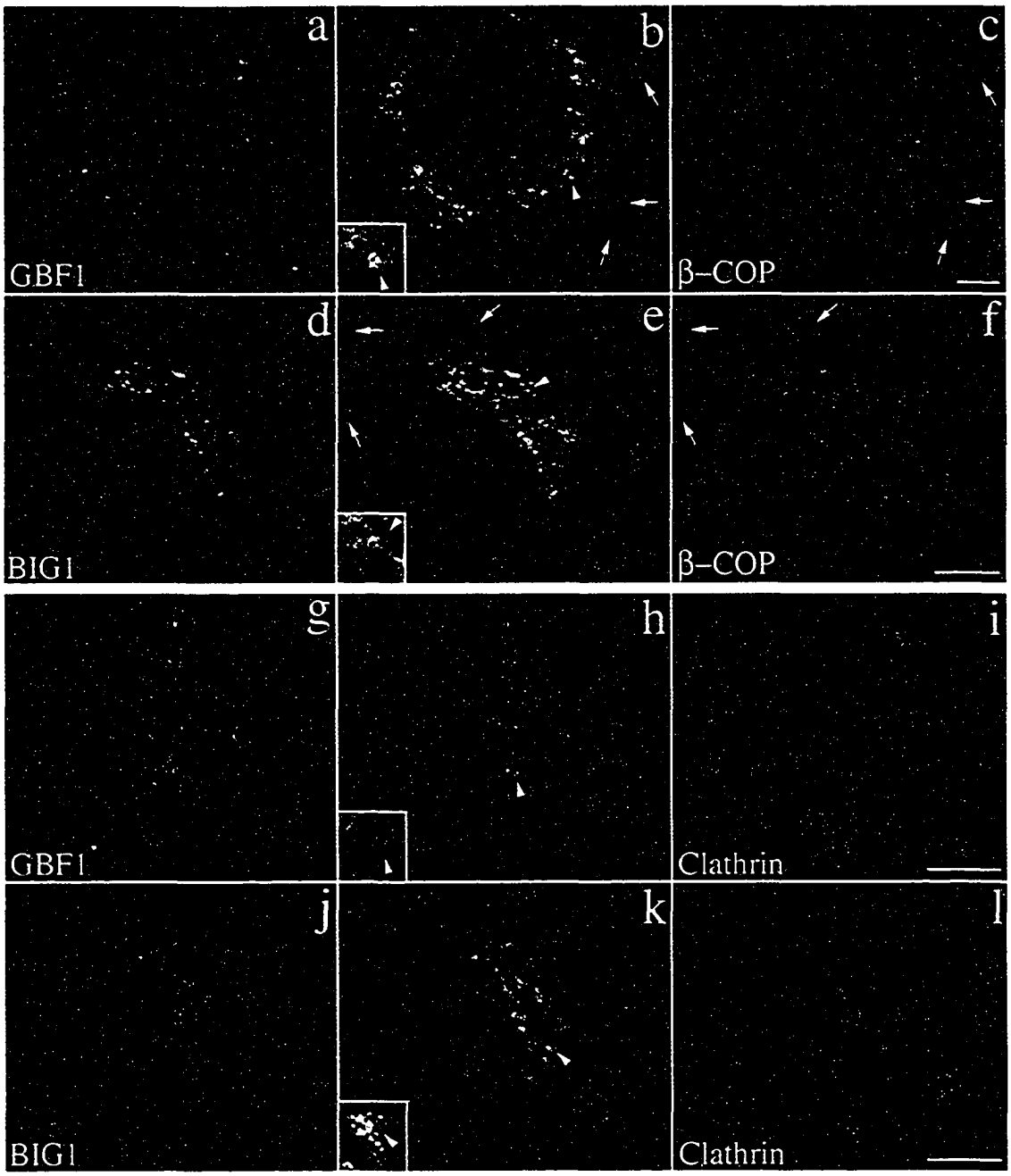

Figure 3.10. GBF1 and BIG1 overlap with distinct sets of coat proteins: GBF1 significantly with β-COP, and BIG1 preferentially with clathrin. NRK cells were fixed and processed for double-label IF using anti-β-COP and anti-GBF1 (a-c), anti-β-COP and anti-BIG1 (d-f), anti-clathrin and anti-GBF1 (g-i) or anti-clathrin and anti-BIG1 (j-l). Shown are single slice confocal images taken in the indicated channel. Middle panels (b, e, h and k) show superimposed left and right images. The inset shows a 4-fold magnification of the area indicated by arrowhead. Arrows in b, c, e and f point to some peripheral structures stained by anti-β-COP only. Bars, 5μm. Shown are representative data from at least two experiments.

developed and tested a quantitative approach that yields the extent of signal intensity from each fluorophore that is present in shared pixels (see section 2.9.1). Application of this method to images similar to those presented in Figures 3.3 and 3.4 confirmed our previous conclusion that GBF1 and BIG1 showed poor overlap with each other, but did colocalize with markers of the *cis*- and *trans*-elements of the Golgi complex, respectively (Figure 3.11). For example, only 15% of the GBF1 signal is present in BIG1-positive structures, while the converse analysis shows only 23% of the BIG1 signal present in GBF1-positive structures. In contrast, the GBF1 and p115 signal overlapped significantly with each other (81 and 86%), while the BIG1 and TGN38 signal showed similarly high degree of overlap (83 and 92%). The small amount of overlap observed between GBF1 and BIG1 (15 and 23%) was similar to that measured for TGN38 and p115 (15 and 29%; see section 2.9.1). Using this method on cells double-stained for β-COP and GBF1, we find that nearly 85% of the GBF1 signal in the perinuclear area was present in β-COP positive pixels. Consistent with images such as shown in inset of Figure 10b, a lower percentage (64%) of the β-COP signal in the perinuclear area overlapped with GBF1. In contrast, the extent of overlap measured with cells stained for BIG1 and β-COP was much lower, in the range of 31-37%. The extensive labeling of clathrin in peripheral structures prevented a meaningful quantitative analysis. The impact of these observation on the mechanism responsible for release of COPI from Golgi membranes by BFA will be discussed in Chapters 4 and 5.

3.8. Summary

The distinct substrate specificities and BFA-sensitivities of members of the GBF1

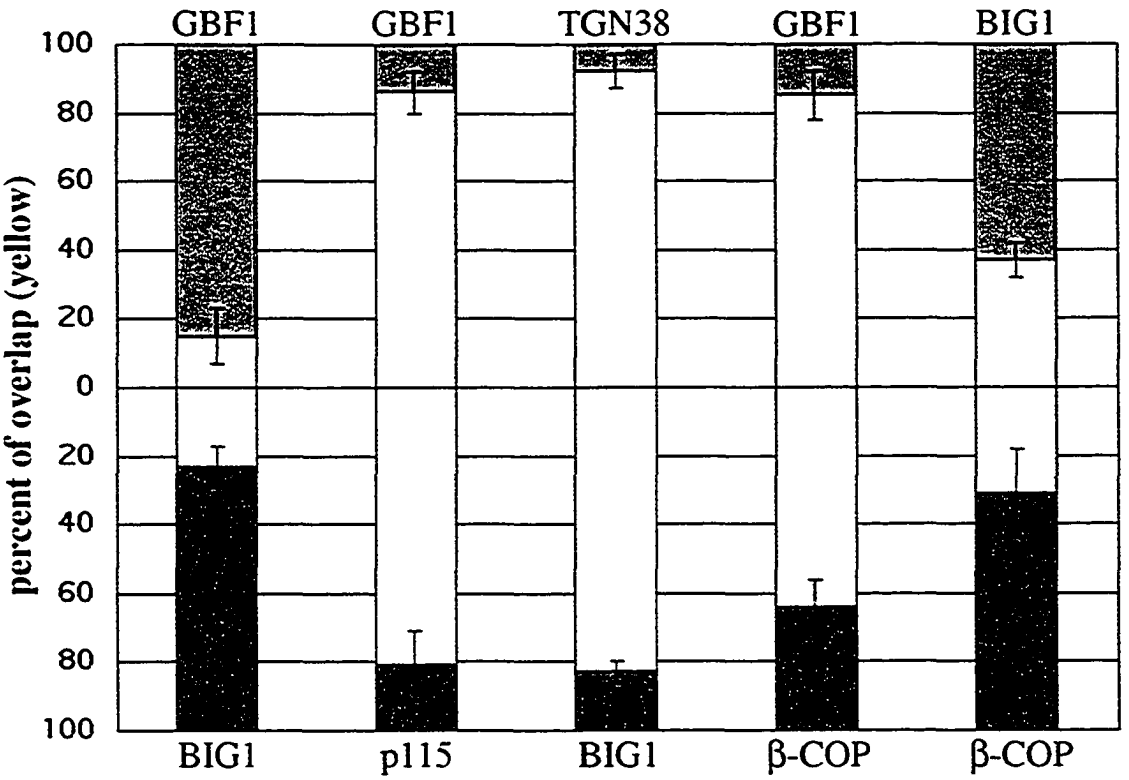

Figure 3.11. Quantitative analysis of the distribution of ARF-GEFs relative to Golgi markers and coat proteins. The extent of overlap observed in the perinuclear area using antibodies to the indicated proteins was measured as described in section 2.9.1. The percent of IF signal intensity present in shared pixels (yellow) relative to total signal was measured for both the red (top) and green (bottom) channels. Red and green only values were defined as the difference between 100% and the overlap measured for the corresponding channel. Red signal was obtained by staining with polyclonal anti-GBF1 or anti-BIG1, while green signal was obtained with monoclonal anti-p115, anti-β-COP or Alexa488-conjugated polyclonal anti-BIG1 (see legends of Figures 3.3, 3.4 and 3.10 for more details). The number of separate images used for quantitation was 5 for GBF1/p115, 4 for TGN38/BIG1, 5 for GBF1/BIG1, 6 for GBF1/β-COP, 6 for BIG1/β-COP. Error bars correspond to the standard deviation of the mean.

and BIG families led us to explore whether these two classes of Arf-GEFs associate with distinct sub-compartments of the Golgi complex. Examination of the steady-state localization and dynamics upon low temperature or BFA treatment revealed dramatic differences. Using p115 and TGN38 as *cis*- and *trans*-Golgi markers, we found that GBF1 and BIG1 associated preferentially with *cis*- and *trans*-compartments, respectively. Consistent with these observations, GBF1 and BIG1 displayed different responses to external treatment. These observations suggest that GBF1 and BIGs may activate distinct subclasses of Arfs in unique locations to regulate different types of reactions. In agreement with this possibility, we found that the COPI coat overlapped to a greater extent with GBF1 than BIG1, while clathrin showed limited overlap with BIG1, and virtually none with GBF1.

The appearance of GBF1 in peripheral structures at 15°C suggests that VTCs produced *de novo* from the ER represent a major site for GBF1 recruitment. As shown in Figure 3.9, these GBF1-labeled peripheral structures cluster very rapidly in the perinuclear area upon warm-up from 15°C and this movement requires microtubules. Therefore, the fact that at steady-state most GBF1 localizes to perinuclear stacks may simply result from the rapid migration of transport complexes along microtubules from the cell periphery to the Golgi area. GBF1 may remain associated with these structures during transport and following their fusion to produce *cis*-compartments of the Golgi complex. However, we cannot exclude the possibility that GBF1 is in constant dynamic equilibrium with a cytoplasmic pool during transport and/or that additional GBF1 is recruited directly on the Golgi stacks. Clearly the mechanism responsible for the recruitment of GBF1 to nascent VTCs, or its release from late Golgi compartments is of

great interest. In next chapter, I will focus on the dynamic association of GBF1 with membranes of both the *cis*-Golgi and peripheral VTCs.

Chapter 4

GBF1, a *cis*-Golgi and VTCs localized Arf-GEF implicated in regulating COPI membrane recruitment

Figure 4.3D was kindly provided by Dr. David Shields (Moores UCSD Cancer center, La Jolla, CA).

4.1. Overview

Recruitment of the various Arf-GEFs to specific intracellular sites likely plays a critical role in regulating protein traffic, because their unique localization may help determine not only when but also where different coat proteins are recruited in the cell. In agreement, our data presented in chapter 3 established that GBF1 and BIGs, large mammalian GEFs that belong to Gea/GBF/GNOM and Sec7/BIG families, respectively, localized to distinct compartments of the Golgi complex (Zhao et al., 2002). While BIG1 and BIG2 localized to *trans*-Golgi elements and partially colocalized with clathrin (refer to Figures 3.4 and 3.10 and (Shinotsuka et al., 2002b)), GBF1 associated with the *cis*-Golgi elements and largely overlapped with COPI (refer to Figures 3.4 and 3.10 and (Garcia-Mata et al., 2003; Kawamoto et al., 2002)). Detailed localization studies revealed that GBF1 cycles between the Golgi and the ER, which suggests its possible involvement in ER-Golgi transport (refer to Figure 3.8 and (Kawamoto et al., 2002)).

Our hypothesis that GBF1 acts as a regulator for COPI recruitment in *cis*-compartments of the Golgi complex and VTCs is supported by several lines of evidence. First, at steady-state, 85% of the GBF1-positive perinuclear structures were also stained with β-COP (refer to Figures 3.10 and 3.11). Second, the recruitment of GBF1 to peripheral VTCs at 15 °C further supports its involvement in regulation of COPI for maturation of those structures (refer to Figure 3.8 and (Kawamoto et al., 2002)). Under normal conditions, formation of VTCs from ER exit sites involves the sequential recruitment of COPII and COPI components onto ER-derived membranes. It seems reasonable to assume that an Arf-GEF would have to be recruited from a cytoplasmic pool *de novo* to initiate COPI recruitment on the nascent structures. The appearance of

GBF1 on peripheral structures at 15°C indicates that GBF1 could have that function. Third, overexpression of GBF1 antagonized the BFA-induced membrane dissociation of COPI (Claude et al., 1999; Kawamoto et al., 2002). Lastly, GBF1 has been linked to the regulation of membrane recruitment of COPI through studies based on overexpression of an inactive GBF1 mutant E794K, which led to COPI dissociation from the membranes (Garcia-Mata et al., 2003). However, direct evidence for the involvement of GBF1 in COPI membrane association remains missing. Furthermore, contrary to this predicted function in the membrane recruitment of COPI that is clearly BFA sensitive (Donaldson et al., 1991; Torii et al., 1995; Yan et al., 1994), GBF1 appeared resistant to BFA in biochemical assays of its GEF activity with purified components (Claude et al., 1999; Kawamoto et al., 2002).

In this chapter, we report that GBF1 dynamically associated not only with membranes of the Golgi complex, but also with those of peripheral VTCs. GBF1 appears sensitive to BFA *in vivo* since treatment with BFA induced rapid accumulation of GBF1 on Golgi and VTC membranes. Furthermore, this recruitment correlated precisely with BFA-induced membrane dissociation of COPI. More importantly, microinjection of anti-GBF1 antibodies caused dissociation of COPI from membranes *in vivo*. These observations suggest that GBF1 is the Arf-GEF that regulates COPI dynamically associated with VTCs and Golgi membrane, and that GBF1/COPI plays an essential role in transport between the ER and the Golgi complex.

4.2. Endogenous GBF1 localizes to β-COP-positive peripheral VTCs at steady state

Our previous IF localization of GBF1 revealed that endogenous GBF1 overlapped extensively with the *cis*-Golgi protein p115, but poorly with the TGN localized Arf-GEF BIG1 (Figure 3.4). Moreover, GBF1 relocalized to β-COP positive peripheral VTCs after incubation at 15°C (Figure 3.8). This observation suggested that GBF1 cycled between the ER and the *cis*-Golgi and could participate at early stages of protein transport between the ER and Golgi complex. To further examine GBF1 function, we raised several additional polyclonal sera against one recombinantly produced N- terminal fragment of hGBF1 (see section 2.3.1). As shown in image b of Figure 4.1A (arrows), one of these sera, 9D2, clearly stained peripheral structures in addition to the juxta-nuclear region in cells at steady state. Although produced with the same immunogen, the antiserum 9D5 yielded primarily juxtanuclear signal (image a of Figure 4.1A), the same pattern as previously observed with serum H-154 raised against a peptide derived from the C-terminus of GBF1 (refer to Figures 3.3, 3.4. 3.5 and 3.10 and (Claude et al., 1999)). Both staining patterns were specific to GBF1 because addition of excess immunizing protein eliminated signal to both the juxtanuclear region and peripheral punctae (images c and e of Figure 4.1A). The neutralization of peripheral punctae and juxta-nuclear staining by excess antigen was specific to GBF1, because it had no effect on the costaining with monoclonal antibodies against β–COP (images d and f of Figure 4.1A). These results suggested that GBF1 binds to peripheral punctae in a conformation slightly different from that found in the juxtanuclear region. The observation that a small but significant amount of GBF1 localizes to peripheral punctate structures first revealed by 9D2 staining has also been confirmed by GFP imaging of a population of a NRK cell line stably expressing N-

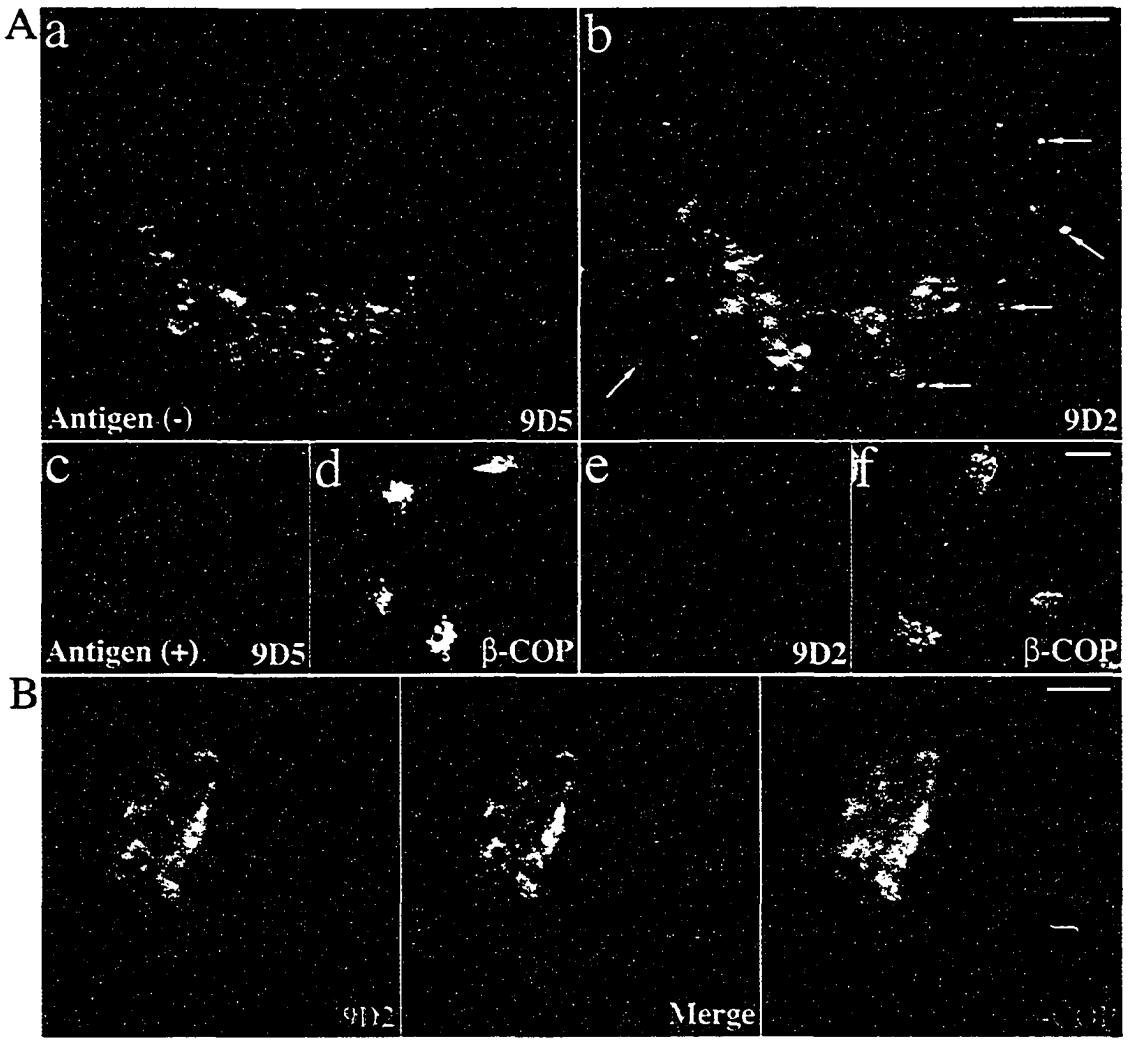

Figure 4.1. Endogenous GBF1 localizes to β-COP positive peripheral VTCs at steady state. (A) Images a and b. NRK cells were fixed and processed for single-label IF using affinity-purified antibodies against GBF1 (9D5 (a) or 9D2 (b)). Peripheral 9D2-positive punctae are indicated by arrows (b). Images shown are single slice confocal images acquired as described in section 2.8. Bar, 5 μm. **Images c-e.** NRK cells were fixed and processed for double-label IF in the presence of 1 μg GBF1 immunizing antigen using 9D5 (c) or 9D2 (f) and monoclonal anti-β-COP antibody (d and f). Images were obtained by standard epifluorescence microscopy. Bar, 10 μm. **(B)** NRK cells were fixed and processed for double-label IF using affinity purified polyclonal antibody against GBF1 (9D2) and monoclonal antibody against β-COP. GBF1 and β-COP colocalize in peripheral punctae. Bar, 5 μm.

terminal GFP tagged GBF1 (Figure 2.1B arrowheads). Unless noted otherwise, we used 9D2 antibodies to localize endogenous GBF1 for the rest of the experiments presented in this chapter.

To characterize the GBF1-positive peripheral punctae, we compared the distribution of GBF1 with that of the early Golgi and VTC marker, β-COP. As shown in Figure 4.1B, GBF1 colocalized significantly with β-COP in peripheral punctae. Since these β-COP positive peripheral structures have been demonstrated previously to represent VTCs (Griffiths et al., 1995; Oprins et al., 1993), our results suggest that GBF1 may regulate COPI recruitment at the VTC structures.

4.3. GBF1 exchanges rapidly between free cytosolic and membrane-bound pools in live cells

GBF1 localized not only to distinct membrane structures but also displayed diffuse staining over the entire cytoplasm. To determine whether this staining corresponded to a free cytosolic pool, or to poorly resolved reticular membrane structures, we performed FRAP experiments using NRK cells stably expressing GFP-GBF1. As described in section 2.5, these cells expressed varied levels of GFP-GBF1, with approximately 70% of GFP-positive cells showing amounts of GFP-GBF1 1 to 1.5 times that of endogenous levels. We photobleached cytoplasmic areas distant from the juxtanuclear region and then followed fluorescence recovery. Signal recovery occurred very rapidly, and appeared complete 10 sec following bleach (Figure 4.2A). Analysis of the recovery kinetics from several such experiments yielded values for the diffusion coefficient of $0.95 \pm 0.13\ \mu m^2\ s^{-1}$ (n=8), consistent with those expected of a free

Figure 4.2. Kinetics of GBF1 binding to and dissociation from Golgi and VTCs membranes in NRK cells stably expressing GFP-GBF1. Live NRK cells stably expressing GFP-GBF1 were examined by confocal microscopy at 37 °C as described in sections 2.8.3 and 2.8.4. **(A)** Cytosol FRAP. An initial prebleach image was taken (prebleach); the cytosol region of interest (ROI) outlined in white was then bleached with high-intensity laser light (bleach). After the bleach, images were taken at 2 sec intervals to monitor exchange between photobleached and non-bleached GFP-GBF1. Shown are still images at the indicated time points. **(B)** Golgi FRAP. Similar to experiment shown in panel A except that the ROI outlined in white corresponds to the Golgi complex and that images were taken at 5 sec intervals after bleach. **(C)** Quantitation of the Golgi FRAP experiment described in panel B. The curve was obtained by fitting the FRAP data to a single exponential using KaleidaGraph v3.6 and corresponds to the equation: $y = 0.520 * (1-e^{-0.055t}) + 0.381$ with an R value of 0.991. **(D)** Golgi FRAP in absence of microtubules. To prevent movement of peripheral VTCs, cells were chilled on ice for 15 min and warmed to 37 °C in the presence of 1 μg/ml nocodazole to depolymerize microtubules. FRAP analysis was then performed as in panel B. **(E)** VTCs FRAP. Similar to experiment shown in panel B except that the ROI was located in the cell periphery and contained VTCs. Bars, 5 μm.

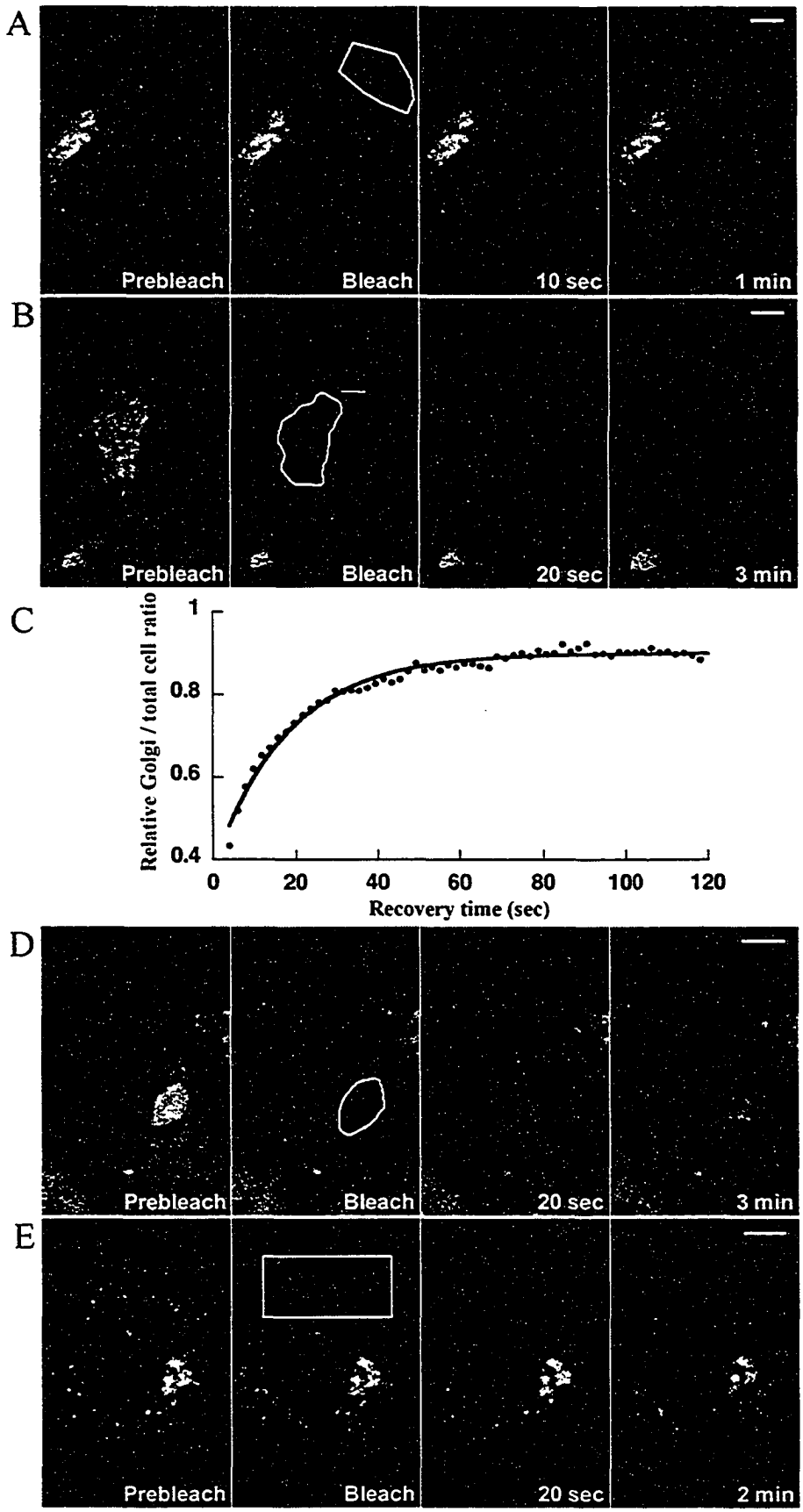

protein, and significantly greater than those reported for a membrane associated protein (Nehls et al., 2000). This observation is consistent with our observations from biochemical assays that a significant pool of GBF1 in homogenates is soluble (refer to Figure 4.3D below; (Claude et al., 1999)).

To determine whether this cytosolic pool is in dynamic equilibrium with the membrane-associated form, we repeated FRAP experiments on membrane bound GFP-GBF1. Following the selective photobleaching of juxtanuclear Golgi-associated signal, we observed rapid fluorescence recovery into the bleached Golgi area (Figure 4.2B). To determine the rate at which GBF1 associates with Golgi membrane, we quantitated the results of several independent FRAP experiments as described in section 2.9.2. The fraction of fluorescence signal present in the juxtanuclear region (termed Golgi-to-cell ratio) averaged about 15:100, a value consistent with the ratio of GBF1 recovered in the microsome fraction of cell homogenates (refer to Figure 4.3D below). The majority (81% ± 1.3%, n=10) of Golgi-bound GBF1 appeared mobile and recovered exponentially to near prebleach levels with an average half-time of 16.0 ± 1.9 sec (n=10) (Figure 4.2C). This recovery rate is similar to that previously reported for Arf1-GFP and slightly faster than measured for COPI (Presley et al., 2002). The FRAP kinetics of Golgi-associated GFP-GBF1 were not affected by disruption of microtubules with nocodazole (Figure 4.2D), a treatment previously shown to block anterograde movement of peripheral VTCs (Presley et al., 1997). This result indicated that recovery was mediated not by delivery via anterograde intermediates but more likely by exchange between Golgi-bound and freely mobile cytosolic pools of GBF1. FRAP experiments examining GFP-GBF1 dynamics on peripheral VTCs revealed that GFP-GBF1 also rapidly exchanged on and

off these structures. As shown in Figure 4.2E, signal recovered quickly after bleach to sites previously labeled with GFP-GBF1. As discussed in more detail below, the dynamic nature of GBF1 recruitment to its sites of action may be particularly critical to regulating coat formation on forming VTCs and ER-Golgi carriers that are themselves very dynamic structures.

4.4. BFA causes accumulation of GBF1 on VTC and Golgi membranes

Previous work established that GBF1 redistributed from the Golgi complex to a diffuse ER pattern in cells treated with BFA for extended periods of time (Garcia-Mata et al., 2003; Kawamoto et al., 2002; Zhao et al., 2002). Time-lapse imaging of NRK cells stably expressing GFP-GBF1 allowed us to examine in more detail the dynamics of GBF1 redistribution following BFA treatment. Surprisingly, GBF1 accumulated on both peripheral punctae and the juxtanuclear Golgi area shortly after BFA addition (Figure 4.3). However, the accumulation of GBF1 at peripheral punctae was transient. At a concentration of 1 μg/ml, BFA caused accumulation of GBF1 in peripheral punctae as early as 10 sec, with maximal signal observed after 1 min and disappearing abruptly from various peripheral sites over the following 4 min (Figure 4.3A). Further analysis of time-lapse movies like that in Figure 4.3A suggests that BFA-induced accumulation occurred on structures positive for GBF1 at steady state prior to drug addition. Subsequent disappearance appears to result from redistribution of GBF1 to a reticular network likely corresponding to the ER (refer to Figure 4.6B below).

To confirm the identity of the peripheral structures where GBF1 accumulated, we

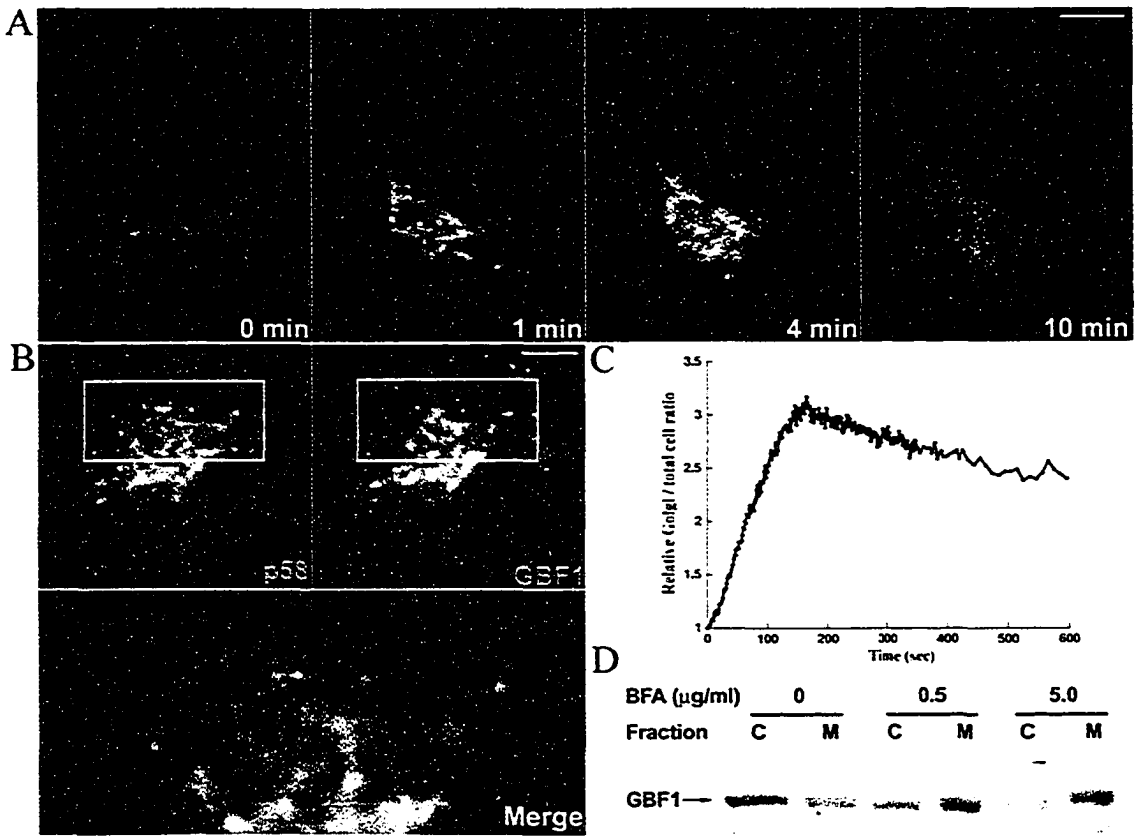

Figure 4.3. GBF1 accumulates on membranes of the Golgi complex and peripheral VTCs upon treatment with BFA. **(A)** Live NRK cells stably expressing GFP-GBF1 were examined by confocal microscopy at 37 °C. Images were captured every 2 sec for 5 min immediately after addition of BFA (1 μg/ml). Still images from the indicated time points illustrate the transient accumulation of GBF1 onto peripheral VTCs and the Golgi complex. Bar, 5 μm. **(B)** NRK cells treated with BFA (5 μg/ml) for 30 seconds were fixed and processed for double IF using Alexa488-conjugated anti-GBF1 rabbit antibody (H-154) and rabbit anti-p58 antibodies. The merged image shows a threefold magnification of the boxed area in the red and green channels above. Bar, 5 μm. **(C)** Quantitation of experiment shown in panel A. Relative Golgi / total ratio calculated as described in section 2.9.2 was plotted against the length of BFA treatment.
(D) Biochemical analysis of BFA-induced recruitment of GBF1 onto membranes. Three plates of NRK cells were washed in ice-cold buffer containing either DMSO vehicle control (0), or 0.5 μg/ml (0.5) or 5 μg/ml (5.0) BFA. Cytosol (C) and microsomes (M) fractions were separated by centrifugation and analyzed for GBF1 content by immunoblot as described in sections 2.11 and 2.12. Dr. David Shields performed the experiment shown in panel D.

compared its distribution to that of a well-characterized VTC marker, p58 (Saraste et al., 1987) using double IF on fixed NRK cells. As shown in Figure 4.3B, brief treatment with BFA caused accumulation of endogenous GBF1 onto peripheral punctae similar to that observed for GFP-GBF1 in live cells. Most GBF1 positive peripheral punctae also stained for p58, and the two proteins co-localized significantly in those structures. To further examine the specificity of the BFA-induced accumulation of GBF1 on peripheral punctae, we examined whether BFA caused similar accumulation of BIG1. This Arf-GEF localizes to late compartments of the Golgi complex at steady-state (refer to Figures 3.4 and 3.6) and should not be trapped on VTCs. As predicted, no BIG1 accumulated in peripheral structures (Figure 4.4, image a) under conditions where endogenous GBF1 appeared in punctae throughout the cell (Figure 4.4, image b). These results suggest that GBF1 normally functions at VTCs where it gets trapped transiently by BFA.

In contrast to the rapid and transient accumulation of GBF1 at peripheral VTCs, accumulation of GBF1 in the juxtanuclear region proceeded more slowly and over a longer time period (Figure 4.3A). Quantitation of Golgi-to-cell ratio as a function of time after BFA addition revealed a gradual 3-fold increase of the Golgi signal within 3 min of 1 μg/ml BFA treatment (Figure 4.3C). The subsequent decrease in signal coincided with redistribution of GFP-GBF1 from the Golgi complex to an ER-like reticular pattern (Figure 4.3A and C). Raising the BFA concentration in range of 0.3 to 1 μg/ml greatly increased the rate of accumulation and, as previously reported for Golgi resident enzymes (Lippincott-Schwartz et al., 1989), significantly shortened the lag before redistribution of GFP-GBF1 to a reticular ER pattern (Figure 4.5).

To confirm the BFA-induced recruitment of GBF1 onto membranes, we

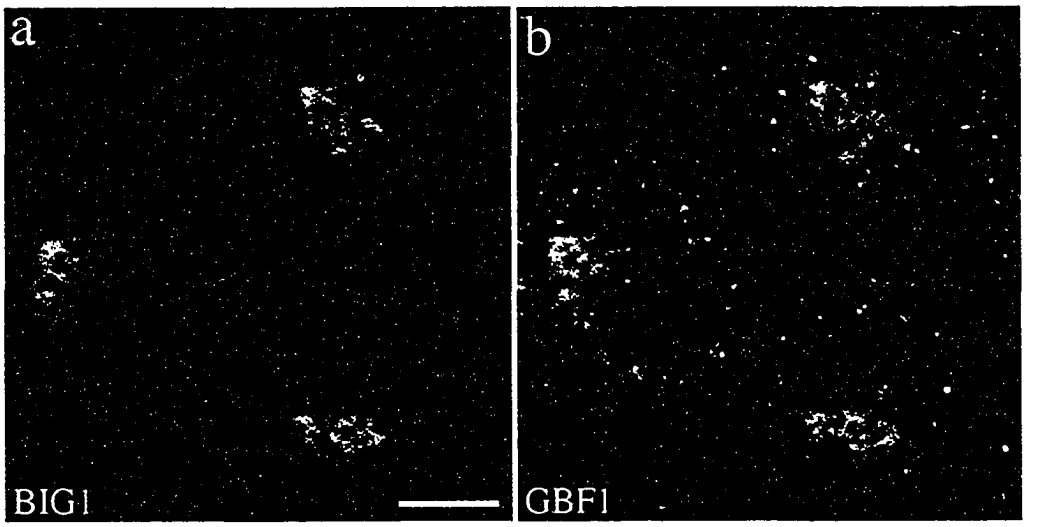

Figure 4.4. BIG1, unlike GBF1, does not accumulate on membranes of peripheral VTCs upon treatment with BFA. NRK cells were treated with 5 μg/ml BFA for 1 min before fixation and processed for double-label IF using polyclonal antibodies against BIG1 (Alexa488-conjugated 9D3, a) and GBF1 (H154). Shown are single-slice confocal images. Bar, 10 μm.

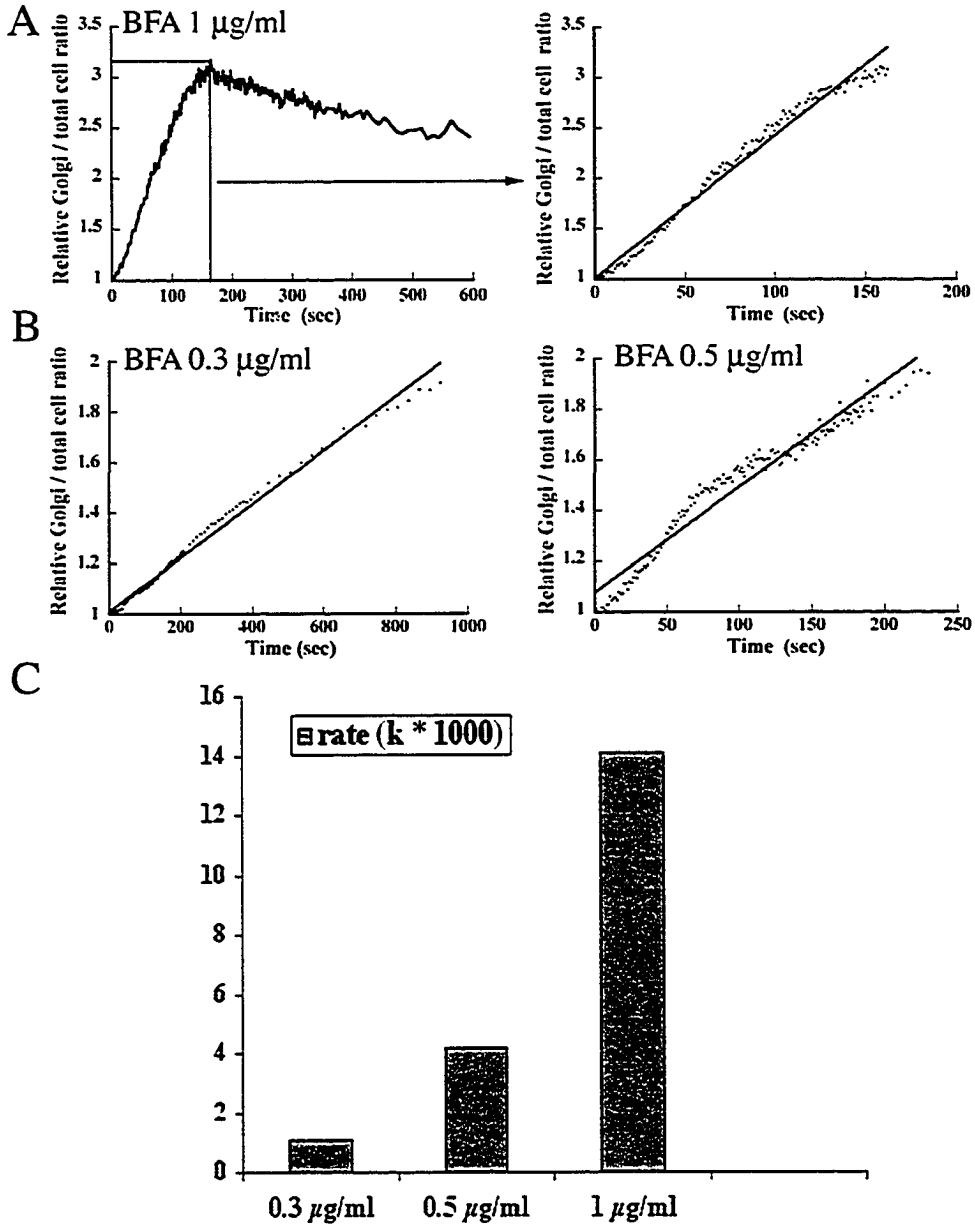

Figure 4.5. Raising BFA concentration increases the rate of GBF1 accumulation on Golgi membranes. **(A)** Left panel is the same as Figure 4.3C, and shows the relative Golgi / total ratio calculated from the experiment shown in Figure 4.3A. Early time points corresponding to GBF1 accumulation in the Golgi complex prior to collapse are indicated by a box. The boxed data were re-plotted in the right panel and fit to the general equation y=kx+b to obtain the initial rate (k) of accumulation. **(B)** Live NRK cells stably expressing GFP-GBF1 were treated with either 0.3 µg/ml or 0.5 µg/ml BFA and examined by confocal microscopy as described in Figure 4.3A. Initial accumulation data were plotted and fit to the equation y=kx+b as in panel A. **(C)** Chart displays the rate of GBF1 accumulation on Golgi membranes ($k*10^3$) measured at three different BFA concentrations.

performed sub-cellular fractionation on homogenates prepared from NRK cells treated with various concentrations of BFA prior to disruption. As previously reported with CHO cell homogenates (Claude et al., 1999), the cytosolic fraction of mock-treated cells contained the vast majority (>80%) of GBF1 (Figure 4.3D). Treatment with BFA for a few min on ice at a concentration as low as 0.5 μg/ml caused a dramatic change in distribution. As predicted from the FRAP data on live cells, treatment with a higher concentration of BFA caused near complete association of GBF1 with the microsomal pellet.

4.5. BFA prevents dynamic exchange between cytosolic and membrane-bound GBF1 pools

The BFA-induced accumulation of GBF1 on membranes likely resulted from prolonged residence time on Golgi membranes. The FRAP experiments presented in Figure 4.2 established that GBF1 normally resides on Golgi membranes only transiently and exchanges dynamically with a cytoplasmic pool. To determine whether the effect of BFA on GBF1 distribution resulted from faster association or slower dissociation, we examined the recovery rate after Golgi photobleaching in the presence of BFA. These FRAP experiments were performed with cells pre-treated with nocodazole for 15 min on ice to disrupt microtubules before BFA addition. This brief nocodazole treatment on its own had no impact on recovery kinetics (refer to Figure 4.2D above), but delayed the microtubule dependent BFA-induced redistribution of GBF1 to the ER long enough to allow measurement of recovery kinetics (Sciaky et al., 1997). A series of images from representative time points is shown in Figure 4.6A. While the majority of GFP-GBF1

signal returned to the bleached Golgi area within a min in the absence of BFA (Figure 4.2D), very little recovery occurred even after 6 min in the presence of BFA (Figure 4.6A). Quantitative analysis of the FRAP data presented in Figure 4.2D and Figure 4.5A further confirmed the much slower exchange rate upon BFA treatment (Figure 4.6C).

After prolonged BFA treatment, GBF1 redistributed to a diffuse pattern throughout the cell that could represent either free or ER-bound GBF1. Measuring diffusion rates under these conditions should resolve this issue since previous work established that free cytosolic proteins are mobile and diffuse much faster than the membrane-bound ones (Cole et al., 1996; Presley et al., 2002). We therefore photobleached areas of cells treated with 5 μg/ml BFA for 30 min (Figure 4.6B) and then measured fluorescence recovery into the bleached area. Whereas we had observed almost immediate recovery for untreated cells (Figure 4.2A), it took as long as 3 min for less than 50% recovery in BFA treated cells (Figure 4.6B). Note that the size of the photobleached areas in BFA-treated cells was similar to those used for untreated cells in Figure 4.2A. The dramatic difference in recovery kinetics was confirmed by quantitative analysis of the FRAP data from Figures 4.2A and 4.6B shown below the images in Figure 4.6D. Whereas GBF1 diffused with a rate of 0.95 ± 0.13 (n=8) consistent with that of a soluble protein in untreated cells (refer to Figure 4.3D above), analysis of several FRAP experiments similar to that shown in Figure 4.6B yielded a rate of 0.21 ± 0.03 (n=8). Such a dramatic decrease in mobility is consistent with GBF1 remaining membrane-associated after prolonged BFA treatment.

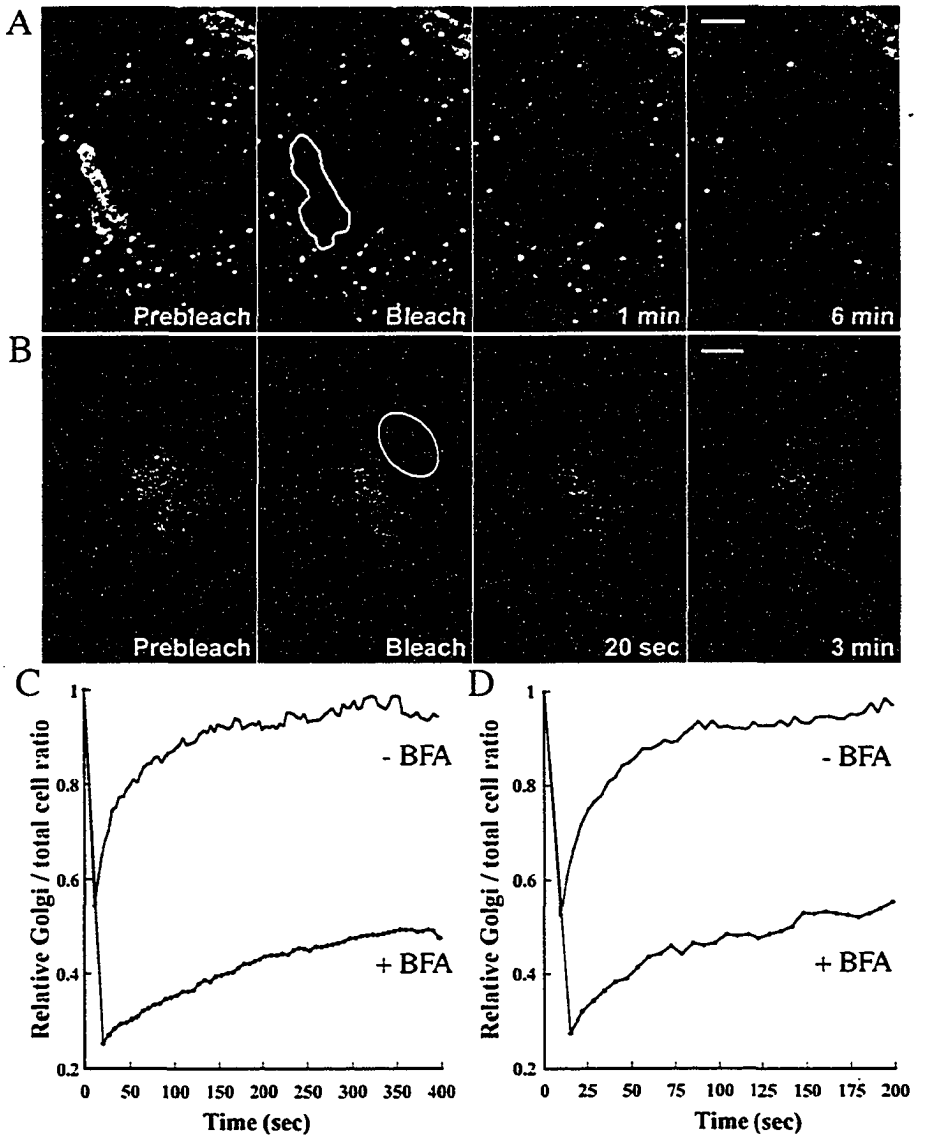

Figure 4.6. BFA treatment traps GBF1 on membranes. (A) NRK cells stably expressing GFP-GBF1 were incubated on ice for 15 min with 5 μg/ml nocodazole prior to transfer onto a microscope stage pre-heated to 37°C. Following equilibration, BFA (5 μg/ml) was added. FRAP was performed as for Figure 4.2D. Bar, 5 μm. **(B)** NRK cells stably expressing GFP-GBF1 were held at 37°C on the Zeiss LSM510 microscope stage and then treated with 5 μg/ml BFA for 10 min. GFP fluorescence associated with the ER-like reticular membrane was photobleached with high-intensity laser light. The subsequent recovery of fluorescence to the bleached area was monitored as for Figure 4.2A. Bar, 5 μm. **(C)** Quantitation of panel A (**+BFA**) and panel D of Figure 4.2 (**-BFA**). Relative Golgi / total ratio was plotted against the length of buffer control or BFA (5 μg/ml) treatment. **(D)** Quantitation of panel B (**+BFA**) and panel A of Figure 4.2 (**-BFA**). Relative Golgi / total ratio was plotted against the length of treatment with buffer control or BFA (5 μg/ml).

4.6. BFA-induced accumulation of GBF1 coincides with loss of COPI from peripheral VTCs

Dissociation of coatomer from Golgi membranes occurs rapidly and constitutes the earliest published response to BFA treatment (Donaldson et al., 1990). The similarly rapid recruitment of GBF1 onto membranes upon treatment with BFA described above strongly suggests that GBF1 is a BFA-sensitive Arf-GEF under in vivo conditions, and could explain COPI loss from membranes. To investigate whether this effect of BFA on GBF1 might account for the rapid dissociation of COPI, we directly compared the kinetics of BFA-induced redistribution of both GBF1 and β-COP by double IF. Consistent with previous observations (Donaldson et al., 1990) (Scheel et al., 1997) and a measured $t_{1/2}$ for dissociation of 30 sec (Presley et al., 2002), most COPI dissociated from membranes after 1 min. Importantly, GBF1 accumulation occurred on structures actively recruiting COPI, and this accumulation coincided with the subsequent loss of COPI (Figure 4.7A). For example, at early time points (10 sec) following BFA addition when β-COP still largely remains membrane-associated, some GBF1 already accumulated both at the Golgi complex and on β-COP-positive peripheral punctae (Figure 4.7A). Further accumulation of GBF1 correlated with loss of β-COP. These observations support the hypothesis that GBF1 is responsible for regulating COPI recruitment in early compartment of the secretory pathway.

4.7. GBF1- positive peripheral structures lie close to but appear physically separate from ERES

Previous work suggested that COPII and COPI act sequentially to produce and

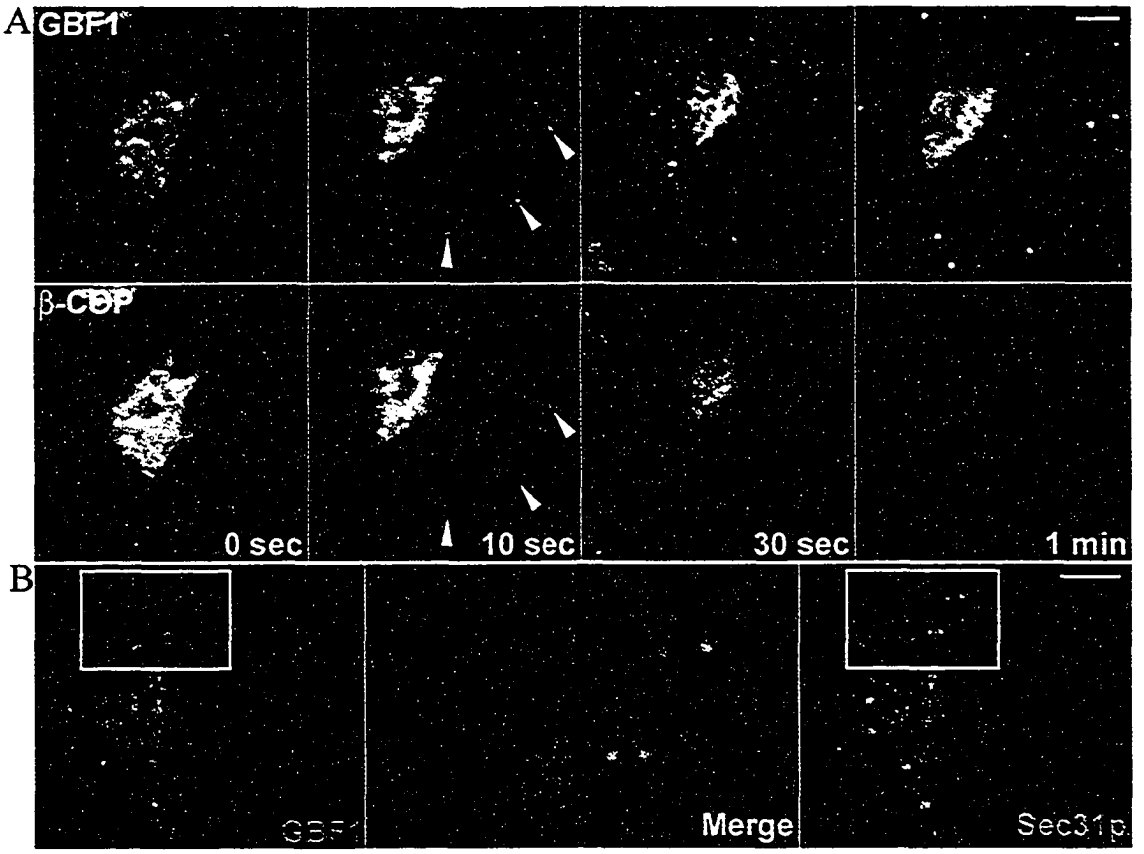

Figure 4.7. BFA-induced accumulation of GBF1 coincides with loss of COPI from peripheral VTCs that lie in close proximity to Sec31p-positive structures. (A) NRK cells treated with BFA (5 μg/ml) for various times (0; 10 sec; 30 sec and 1 min) were fixed and processed for double IF using anti-GBF1 rabbit antibody (9D2) and anti-β-COP mouse antibodies (M3A5). Peripheral punctae containing both GBF1 and β-COP in 10 sec image are indicated by white arrowheads. **(B)** NRK cells treated with BFA (5 μg/ml) for 30 seconds were fixed and processed for double IF using Alexa488-conjugated anti-GBF1 rabbit antibody (H-154) and rabbit anti-sec31p antibodies. The merged image shows a threefold magnification of the boxed areas in the red and green channels. Bars, 5 μm.

mature cargo carriers between the ER and Golgi complex (Aridor et al., 1995; Barlowe, 2000). Whereas COPII functions at ER cargo exit sites and appears stationary (Stephens et al., 2000), COPI decorates VTCs that can be motile but are often tightly juxtaposed to COPII-positive structures (Presley et al., 2002; Scales et al., 1997). To probe in more detail the identity of the peripheral structures containing GBF1, we compared its distribution to that of the COPII subunit Sec31p. As shown in Figure 4.7B, GBF1-positive punctae appeared not to overlap with, but instead lie in close proximity to Sec31p-positive structures. Indeed, the vast majority of structures showed clear separation of the red and green signals. These results suggest that GBF1 is recruited to VTCs shortly after their formation from ER exit cargo sites.

The BFA induced transient accumulation of GBF1 onto nascent VTCs allowed us to address the possibility raised by Mironov and colleagues that VTCs arise through direct en bloc protrusion of specialized ER domains in the vicinity of COPII-coated ERES with which they would be physically connected (Mironov et al., 2003). Shortly following their formation, VTCs are thought to attach to microtubules for rapid movement towards the MTOC and juxtanuclear Golgi complex (Presley et al., 1997; Scales et al., 1997). We reasoned that disruption of the microtubule network by brief treatment with nocodazole would prevent separation of VTCs from ERES and accelerate the collapse of transient GBF1-positive peripheral punctae. To our surprise, microtubule disruption had the opposite effect. In cells treated briefly with NOZ, endogenous GBF1 accumulated as before, but rather than dispersing into the ER within 2 minutes of BFA addition, it remained associated with peripheral structures (Figure 4.8A). More detailed experiments using nocodazole-treated live COS-1 cells transiently overexpressing GFP-

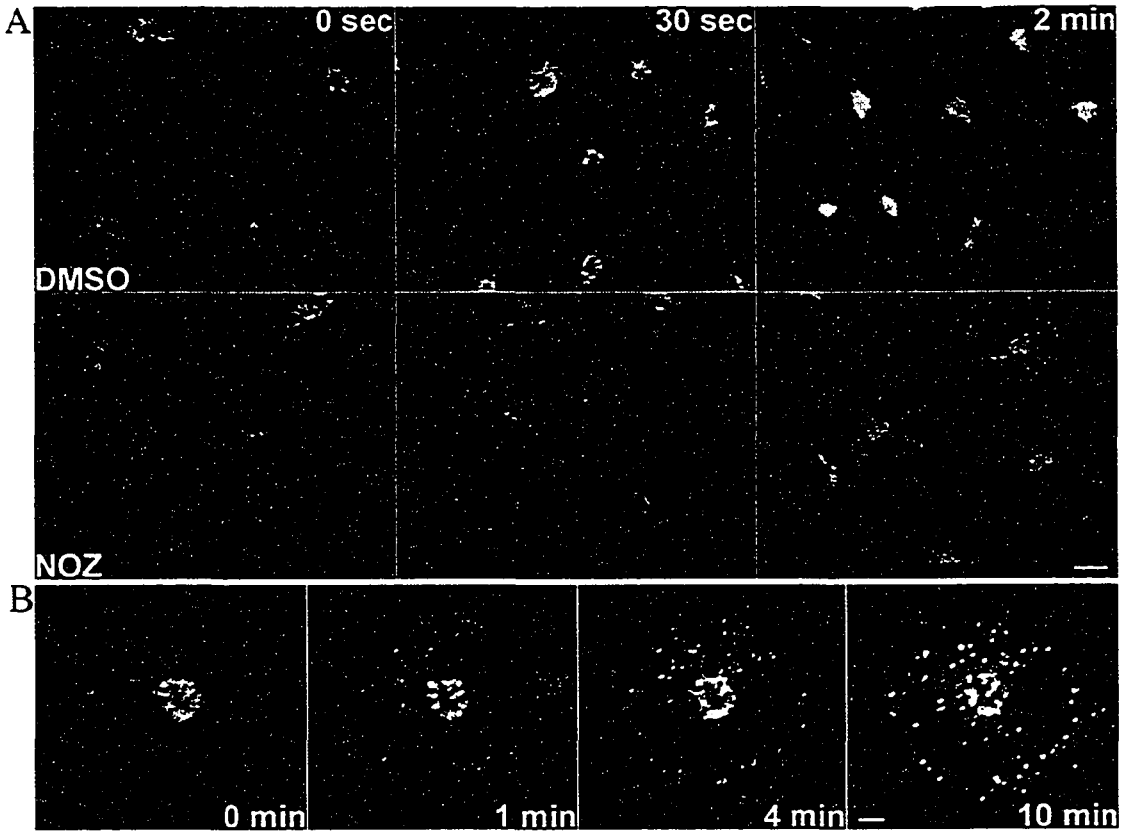

Figure 4.8. Nocodazole treatment stabilizes the BFA-induced accumulation of GBF1 on peripheral VTC membranes. (A) NRK cells treated with either 0.5% DMSO vehicle control (**DMSO**) or 5 μg /ml nocodazole (**NOZ**) were incubated on ice for 15 min before a 3 min warm-up at 37°C to depolymerize microtubules. Cells from both groups were then either immediately fixed (**0 sec**) or treated with 5 μg/ml BFA for 30 sec or 2 min before fixation. All cells were processed for IF with anti-GBF1 antibody 9D2. Bar, 10 μm. **(B)** Live COS-1 cells transiently transfected with GFP-GBF1 pre-incubated on ice for 10 min in the presence of 5 μg/ml nocodazole were examined by confocal microscopy at 37°C. Images were captured every 3 sec immediately after addition of BFA (5 μg /ml). Still images from the representative time points are shown. Bar, 5 μm.

GBF1 confirmed that BFA treatment caused rapid accumulation onto structures that did not collapse on the ER and remained stable for longer than 10 minutes (Figure 4.8B). These observations suggest that most peripheral VTC structures onto which GBF1 accumulates are physically separate from ERES.

4.8. BFA causes accumulation of Arf4 with GBF1 on peripheral VTCs membranes

The identities of the Arf isoforms activated by GBF1 at VTCs or the Golgi complex remain unclear. *In vitro* observations suggest that GBF1 preferentially uses Class II Arfs (Arf5) as substrate (Claude et al., 1999), although recent *in vivo* data support the idea that GBF1 interacts also with class I Arfs (Kawamoto et al., 2002; Niu et al., 2005). To test this directly *in vivo*, we examined the impact of a brief BFA treatment on the distribution of HA-tagged forms of Arf1, Arf4 and Arf5 by taking advantage of the fact that BFA traps GBF1 and its Arf substrate in a complex on the membrane. We found that Arf4, but not Arf1 or Arf5, accumulated with GBF1 on peripheral VTCs membranes upon 30 sec of BFA treatment (Figure 4.9). Higher magnification of a selected region of the merged image for Arf4-HA and GBF1 is presented in a boxed inset to better illustrate the extensive overlap of these two proteins in peripheral punctae (Figure 4.9, image b). Interestingly, significant Arf4 and Arf5 signal remained on the juxta-nuclear Golgi region (Figure 4.9, images a and g). On the other hand, we observed much weaker Arf1 signal on Golgi membranes (Figure 4.9, image d), indicating that recruitment of Arf1 to Golgi membranes is more sensitive to BFA than that of either Arf4 or Arf5 and that the majority of Arf1 is rapidly released from Golgi membranes upon BFA treatment. This agrees with previous *in vitro* observation that Arf 5, but not Arf1 and Arf3, remained

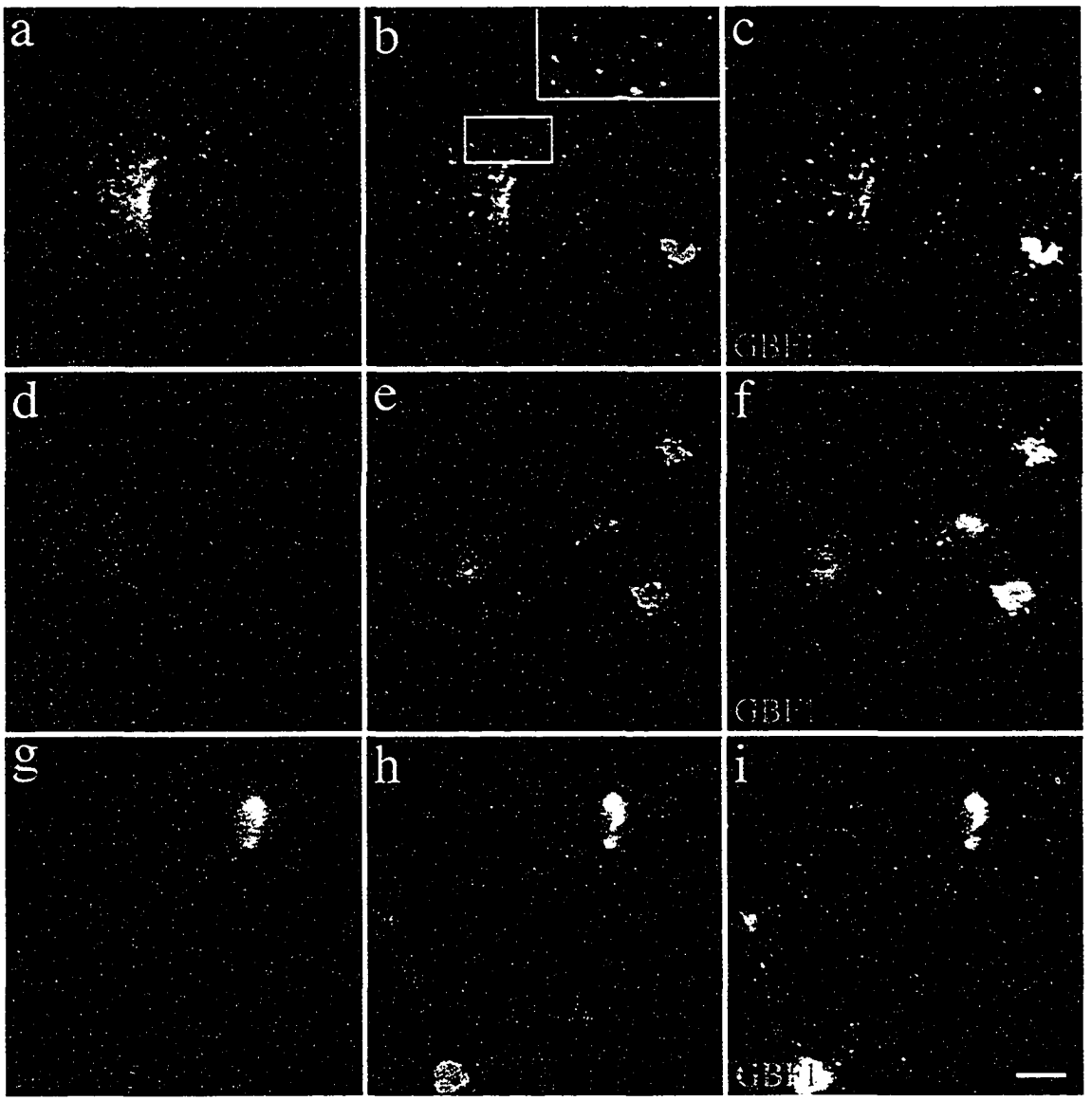

Figure 4.9. HA-Arf4, but not HA-Arf1 or HA-Arf5, accumulated with GBF1 on peripheral VTCs membranes upon brief BFA treatment. COS-1 cells, transfected with a plasmid encoding HA-tagged Arf4, Arf1 or Arf5, were treated with BFA (5 μg/ml) for 30 sec before fixation and processing for double IF using antibodies against the HA epitope (3F10) (a, d and g) and GBF1 (9D2) (c, f and i). Middle panels (b, e and h) show merged left and right images. The inset in image b shows a twofold magnification of the boxed area in this merged image. Bars, 10 μm.

associated with Golgi membrane upon BFA treatment (Tsai et al., 1992). The observation that Arf4 specifically accumulated with GBF1 on peripheral VTCs membranes suggests that GBF1 may activate Arf4 at peripheral VTCs.

4.9. GBF1 participates in ER-Golgi traffic by regulating COPI recruitment

To investigate in more detail when GBF1 is recruited for anterograde cargo transport, we next examined the appearance of GBF1 on transport carriers containing ts-O45-G, a temperature-sensitive mutant viral glycoprotein produced by VSV. This mutant glycoprotein accumulates in the ER at the restrictive temperature, can be synchronously released for export by temperature shift, and has been used extensively to dissect the molecular machinery of ER-to-Golgi transport (Bergmann, 1989; Kreis and Lodish, 1986). VSV-G, like other cargo molecules, is initially sorted into COPII-coated ER export carriers and then transported from the ER to the Golgi in mobile VTCs that contain COPI (Presley et al., 2002; Scales et al., 1997). Indeed, quantitative analysis of triply labeled cells (Scales et al., 1997) revealed that the peak of colocalization between ts-O45-G and COPII occurred earlier (~1 min after temperature shift) than that with COPI (>6 min).

To compare the localization of GBF1 with ts-O45-G during its export from the ER, COS-1 cells infected with tsO45-VSV were kept at the restrictive temperature (40°C) for 3 h, and then shifted to the permissive temperature (32°C) for either 1 min or 6 min to allow synchronized ER export. As shown in Figure 4.10, GBF1, like COPI, co-localized with VSV-G in peripheral structures at later time points (6 min, image k) after temperature shift, but not at earlier time points (1 min, image h), when COPII-dependent

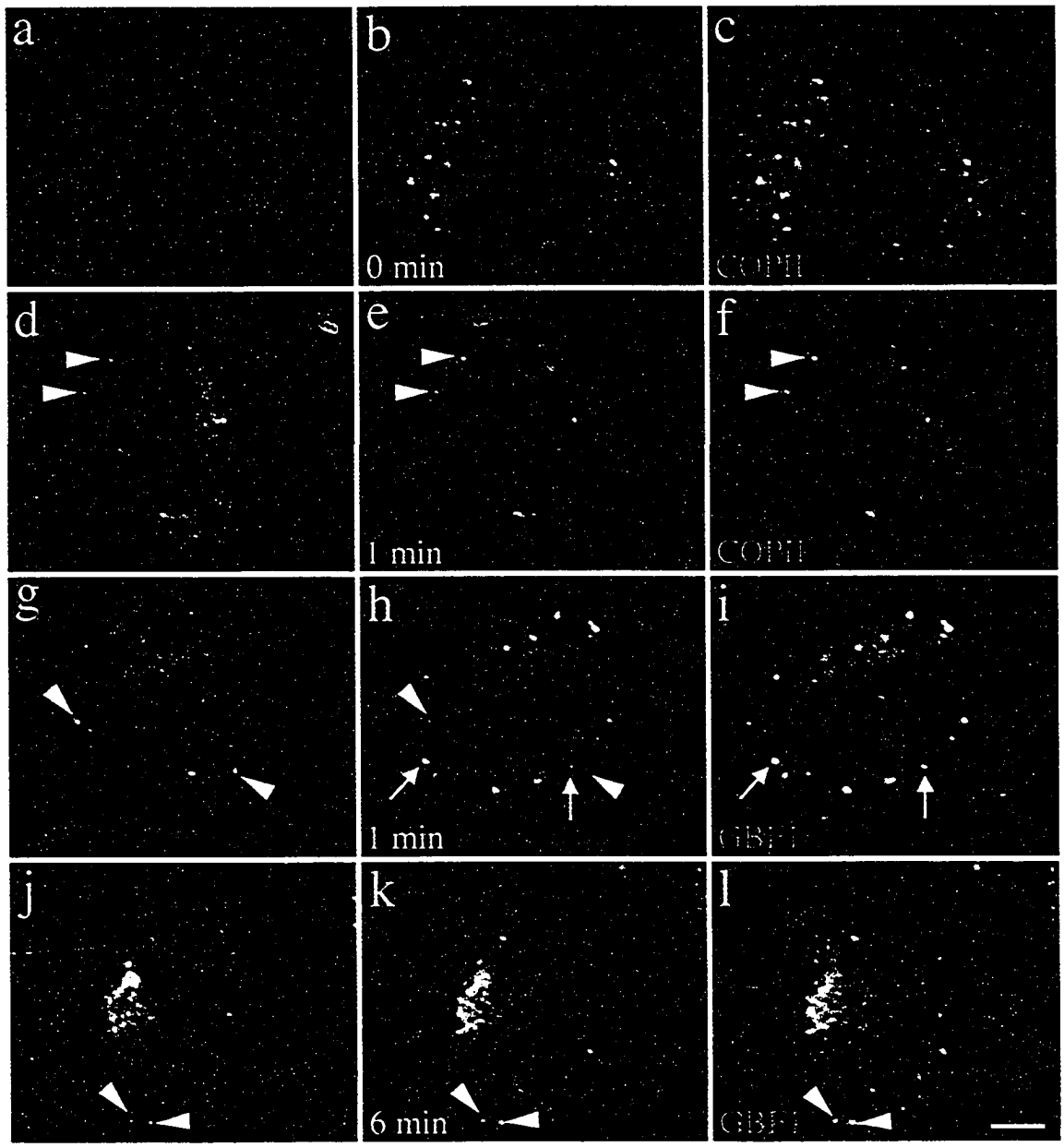

Figure 4.10. Matured VTCs labeled by VSVGtsO45 contain GBF1. COS-1 cells infected with VSV tsO45 virus were incubated at 40°C for 3hr (0 min) (a-c) and then shifted to permissive temperature 32°C for either 1 min (d-i) or 6 min (j-l). Cells were fixed and then processed for double IF using monoclonal antibodies against VSV-G (a, d, g and j) and polyclonal antibodies against either COPII (c and f) or GBF1 (i and l). Middle panels (b, e, h and k) show merged left and right images. At time "1 min", COPII-positive peripheral punctae (indicated by white arrowheads), but not GBF1-positive peripheral punctae (indicated by white arrows), colocalize with VSV-G-positive peripheral punctae (indicated by white arrowheads). At time "6 min", the peripheral punctae containing both VSV-G and GBF1 are indicated by white arrowheads. Bar, 5 μm.

events lead to VTC formation. These observations suggest that GBF1 is recruited to the cargo-containing VTCs rather than to the earlier ER-associated cargo exit sites.

To further investigate the functional link between GBF1 and COPI, we inhibited GBF1 function by microinjection of neutralizing antibody and analyzed its effect on COPI membrane association. Several anti-GBF1 polyclonal antibodies were affinity-purified, concentrated and microinjected into the cytoplasm of HeLa cells. Microinjected cells were identified by staining with a conjugated anti-rabbit antibody and the potential effects on COPI recruitment were assayed by staining with an anti-β-COP monoclonal antibody 2 h post-microinjection. Only two of the four concentrated antibody preparations, 9D2 and 9D7, caused dissociation of COPI from the membrane. As shown in Figure 4.11, antibody 9D7 caused COPI dissociation but only in cells that received a relatively high level of microinjected anti-GBF1 antibodies (Figure 4.11, a-b). In contrast, antibody 9D2 was particularly effective, causing complete dissociation of COPI even at low levels of microinjected antibodies (Figure 4.11, c-d). This effect is COPI-specific because microinjection of anti-GBF1 antibodies did not disrupt the distribution of clathrin coats (Figure 4.11, e-f). Furthermore, this effect is not an artifact of microinjection because, another anti-GBF1 antibody 9D5 microinjected at the same concentration as 9D2 and 9D7 did not cause membrane dissociation of COPI (Figure 4.12). These results argue strongly that GBF1 is the Arf-GEF responsible for activating a particular Arf to initiate COPI membrane recruitment, and suggest that the GBF1/COPI system participates in ER-to-Golgi protein transport.

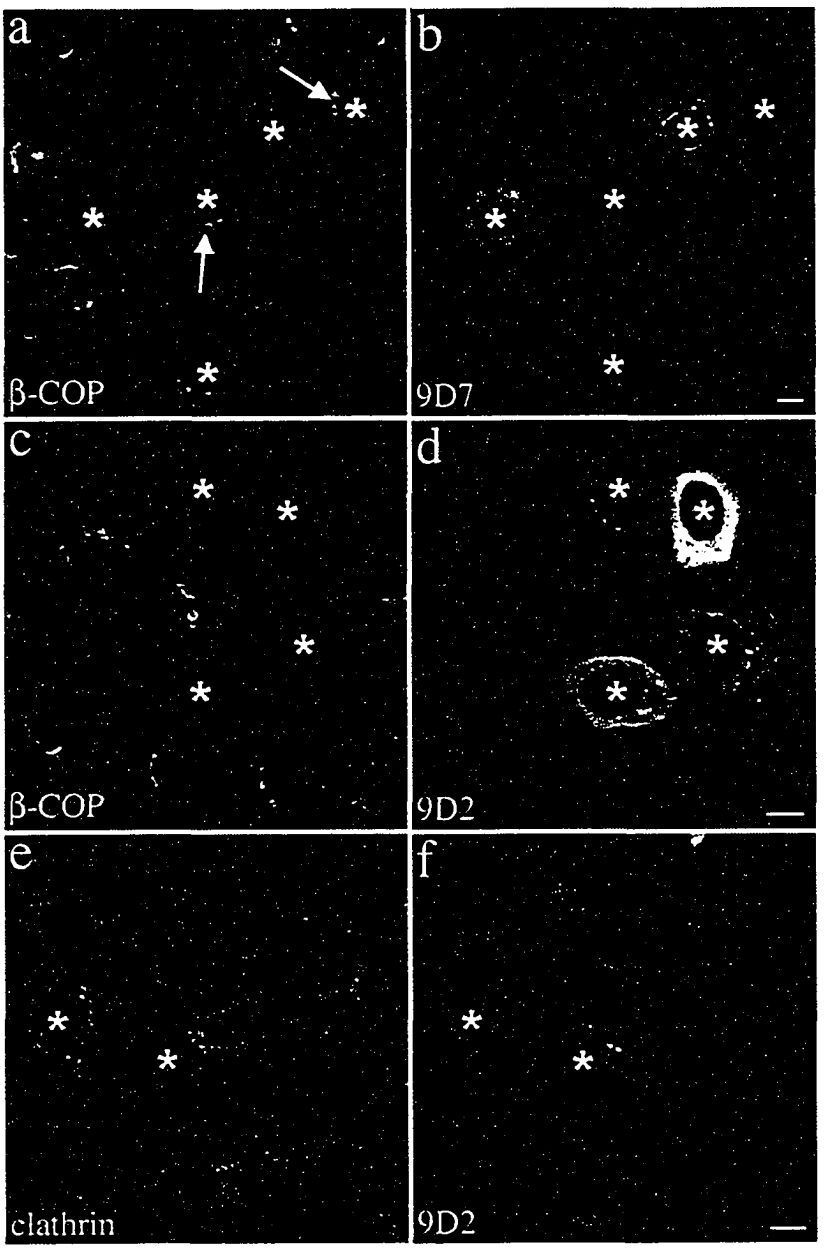

Figure 4.11. Microinjection of anti-GBF1 antibodies specifically causes membrane dissociation of the COPI but not the clathrin coat. Hela cells were microinjected with affinity-purified polyclonal anti-GBF1 antibodies, 9D7 (a-b) or 9D2 (c-f), and fixed 2 hours post-injection. Microinjected cells were identified using goat anti-rabbit antibody (b, d and f) and indicated by white asterisks. Coat proteins were revealed by staining for either COPI or clathrin using anti-β-COP (M3A5) (a and c) or anti-clathrin (X22) (e) monoclonal antibodies. In image a, cells that received a lower level of microinjected 9D7 antibodies and displayed a normal membrane-associated staining pattern of β-COP are indicated by white arrows. Bars, 10 μm.

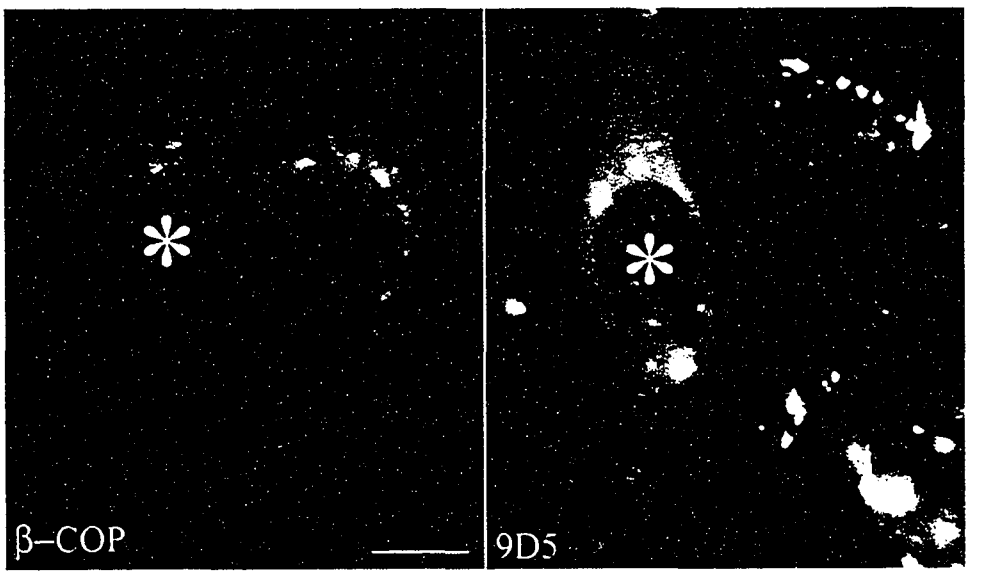

Figure 4.12. Microinjection of anti-GBF1 antibody 9D5 does not cause membrane dissociation of COPI. Hela cells were microinjected with affinity-purified polyclonal anti-GBF1 antibodies 9D5 and fixed 2 hours post-injection. Microinjected cells were identified using goat anti-rabbit antibody and indicated by white asterisks. COPI coat proteins were revealed by staining with anti-β-COP (M3A5) antibody. Bar, 10 μm.

4.10. Summary

The recycling properties of GBF1 between *cis*-Golgi and VTCs led us to further explore GBF1's function in protein transport between the ER and Golgi complex. Examination of the steady-state localization of GBF1 revealed that endogenous GBF1 localized not only to juxtanuclear *cis*-Golgi, but also to peripheral VTCs. Live cell FRAP studies established that binding of GBF1 to both membranes was extremely dynamic with rapid exchange between free cytosolic and membrane-bound GBF1. The dynamic membrane recruitment of GBF1 is important for its function. Treatment of cells with the drug BFA, which inhibits Arf-GEF activity, significantly slowed down exchange of GBF1, resulting in transient accumulation of GBF1 on both Golgi and VTCs membranes before its eventual redistribution to ER membranes. This effect of BFA on GBF1 could account for the rapid dissociation of COPI by BFA treatment, since BFA-induced accumulation of GBF1 coincides well with loss of COPI from peripheral VTCs membranes. These observations suggest that GBF1 may be the Arf-GEF responsible for regulating COPI membrane recruitment in early secretory pathway. In agreement with this possibility, we found that when GBF1 was recruited to cargo-containing VTC structures, COPI, but not COPII concurrently recruited to the same membranes. Strikingly, microinjection of neutralizing anti-GBF1 antibodies specifically caused dissociation of COPI from the membrane.

Chapter 5

General Discussion

5.1. Overview

Since the identification of the first Arf-GEF, ARNO, less than 10 years ago (Chardin et al., 1996), this class of enzymes has attracted much attention. This interest largely resulted from the profound effects of BFA on the secretory pathway in eukaryotic cells, which demonstrated that Arf-GEFs, its major targets, are important regulators of organelle structure and function. Initial studies that led to the identification of a great number of Arf-GEFs (refer to Figure 1.3) provided the foundation of this emerging Arf-GEF field, and now the challenge is to elucidate how each Arf-GEF participates at a particular stage of protein transport. Characterization of the sub-cellular localization of each Arf-GEF constitutes a reasonable first step in this direction.

Recently, one of the main focuses of our laboratory has been the identification and characterization of a large mammalian Arf-GEF, GBF1 (Claude et al., 1999), and the characterization of two previously identified large mammalian Arf-GEFs, BIG1 (Morinaga et al., 1996) and BIG2 (Togawa et al., 1999). The goal of my doctoral work was to characterize the relative sub-cellular localizations and functions of these three large Arf-GEFs.

The experimental results presented in Chapter 3 provided novel information regarding the distinct Golgi sub-compartment localizations of GBF1 and BIGs. They established, for the first time, that GBF1 and BIGs associate with *cis*- and *trans*- Golgi compartments, respectively, where they overlap preferentially with the COPI and clathrin coats, respectively. These observations suggest that the function of GBF1 and BIGs may not be limited to Arf activation but may also include selection of protein coats for recruitment at unique locations.

In Chapter 4, I focused on the further characterization of GBF1: its membrane binding dynamics, its BFA sensitivity and its role in regulating COPI coat recruitment. Live cell FRAP analysis revealed that GBF1 rapidly cycles between the cytosol and the membranes of both juxtanuclear *cis*-Golgi and the peripheral VTCs. This dynamic membrane recruitment of GBF1 is blocked by BFA treatment, and the BFA-induced membrane accumulation of GBF1 appeared to coincide with the BFA-induced membrane dissociation of COPI. The possibility that GBF1 regulates COPI membrane recruitment was confirmed by the striking observation that microinjection of anti-GBF1 antibodies specifically caused dissociation of COPI, but not clathrin, from the membranes.

The following sections will discuss the significance of the experimental results presented in my doctoral thesis in light of the current literature. This analysis will also include additional results obtained in the course of my graduate work that have important implications for Arf-GEF function but did not fit easily into those two chapters. For convenience and ease of reading, these results were included as figures in this chapter rather than as separate appendices. Finally, some questions raised by my doctoral work, as well as potential experimental approaches that could address these issues will be also discussed.

5.2. Subcellular localization of large Arf -GEFs

5.2.1. Localization of large Arf- GEFs to distinct Golgi sub-compartments

Large Arf-GEFs of the GBF1 and BIG sub-families were localized using confocal microscopy. Despite multiple attempts, we were not able to use available antibodies to examine the relative localization of endogenous Arf-GEFs using immuno-EM.

Fortunately, the significant differences in localization of the two GEF families made assignment to distinct sub-compartments of the Golgi complex possible even at the light microscope level. Co-staining for endogenous GBF1 and either HA-tagged or endogenous BIG1 revealed very clear separation in staining pattern for these two Arf-GEF classes. Such separation between GBF1 and BIGs was observed in at least two cell types and with various combinations of endogenous GEFs, GFP tagged GBF1 or HA-tagged BIGs. Furthermore, the observation that GBF1 staining extensively overlaps with that of *cis*- Golgi marker p115 or p58, and BIG1 staining largely overlaps with that of *trans*-Golgi marker TGN38 suggests that GBF1 and BIG1 localizes to *cis*- and *trans*-subcompartments of the Golgi complex, respectively.

The estimation of the degree of overlap is subject to nonobjective judgment, which is further complicated by the extent to which an image is processed to improve presentation and facilitate interpretation. Image quantitation is one way to solve this problem. In this project, we collaborated with Dr X. Sun (Cross Cancer Institute, University of Alberta) to develop a quantitative approach to yield a more accurate estimate of overlap. In this approach, overlap was defined as the percentage of total signal "intensity" presented in shared pixels by each of two fluorophores, rather than simply comparing the "number" of shared pixels to the total. This method weighed preferentially those pixels that have greater intensity and therefore yielded a more accurate of the extent of signal overlap. After this work published (Zhao et al., 2002), this method became available in an updated module of the MetaMorph software. Quantitative analysis of confocal images presented in chapter 3 confirmed the separation between

GBF1 and BIG1 and revealed a large degree of overlap of these two Arf-GEFs with either *cis*- or *trans*-Golgi markers.

Our localization of GBF1 to early compartments of the secretory pathway was not limited to quantitative confocal microscopy, but it was also based on its response to various treatments. As expected of a *cis*-Golgi protein, GBF1 partially redistributed from the Golgi complex to peripheral sites following incubation at 15°C; in addition it appeared in a diffuse reticular ER pattern following prolonged treatment with BFA. Shortly after publication of our work (Zhao et al., 2002), several groups reported observations that similarly established that GBF1 associates primarily with *cis*-Golgi membranes. For example, Nakayama and colleagues reported that in response to nocodazole treatment or 15 °C incubation, GBF1 redistributes similarly to proteins cycling between the *cis*-Golgi and the ER (Kawamoto et al., 2002), while Sztul and colleagues confirmed our observation that GBF1 overlaps extensively with the *cis*- Golgi proteins p115 and β–COP (Garcia-Mata et al., 2003).

Similarly, our localization of BIGs to *trans*-elements of the Golgi complex was based on both their distribution and their response to various treatments. At steady state, BIG1 separated well from GBF1 (refer to Figure 3.3) and p115 (refer to Figure 3.4), and overlapped to a large extent with TGN38 (refer to Figure 3.4), while BIG2 also clearly separated from the *cis*-Golgi localized p58 and GBF1 (refer to Figure 3.6). As expected of a *trans*-Golgi protein, the juxtanuclear localization of BIG1 was not altered at 15°C. Furthermore, BFA treatment caused its redistribution to a dense collection of fine punctate structures in the perinuclear area as observed for TGN38 (refer to Figure 3.7). These results significantly extend the previous demonstration by Vaughan and colleagues

that BIG1 and BIG2 exist in a large complex that localizes in the perinuclear region (Yamaji et al., 2000). These observations are also consistent with our previous report that BIG1 overlaps better with ManII than with ERGIC-53 (Mansour et al., 1999). The apparent discrepancy with the conclusion of Vaughan and colleagues that BFA causes little change in BIGs' distribution (Yamaji et al., 2000) most likely reflects the slow kinetics of BFA's effect on the TGN and the short 10-min treatment used by those authors (Figure 3.7, image d). In agreement with our observation that BIGs concentrate on the *trans* side of the Golgi complex, Nakayama and colleagues reported shortly after our work had been published (Zhao et al., 2002) that BIG2 likely regulates membrane recruitment of AP-1 and GGA through activating Arf in the TGN. This conclusion was based on the fact that BIG2 overexpression blocked BFA-induced membrane dissociation of Arf1 and AP1 (Shinotsuka et al., 2002b), and that a dominant-negative mutant of BIG2 causes redistribution of AP-1 and GGA but not of COPI (Shinotsuka et al., 2002a).

5.2.2. Localization of GBF1 to peripheral VTCs

The recruitment of GBF1 to peripheral VTCs first revealed by 15°C incubation could be confirmed to occur at steady state under normal physiological conditions using one of our newly prepared anti-GBF1 sera. This antibody, 9D2, revealed that endogenous GBF1 localized not only to juxtanuclear *cis*-Golgi, but also to peripheral VTCs. The observation that VTC-localized GBF1 can be recognized well by one anti-GBF1 antibody, but poorly by another is interesting as it suggests that GBF1 binds to peripheral VTCs in a conformation slightly different from that found in the juxtanuclear Golgi region. It is possible that GBF1 associates with different membranes by forming different protein complexes with distinct membrane receptors in either peripheral VTC or

juxtanuclear Golgi membranes (see section below 5.2.5). The identification and localization of membrane receptors and binding partners for GBF1 may one day provide an explanation for the unique pattern revealed by 9D2.

Our observation that GBF1 associates with peripheral VTC membranes is consistent with several studies. First, our previous EM study with rat hepatocytes (Claude et al., 1999), revealed that GBF1 appeared at the highest concentration in stacked regions, but also at significant levels on smooth tubules corresponding to VTCs in these cells (Dahan et al., 1994; Lavoie et al., 1999). Second, an EM study by Nakayama and colleagues (Kawamoto et al., 2002) similarly revealed that GBF1 localizes mainly to vesicular and tubular structures apposed to the *cis*-face of the Golgi stacks. Third, an IF study by Sztul and colleagues (Garcia-Mata et al., 2003) showed that GBF1 localizes to COPI-coated VTCs in addition to the Golgi complex. Furthermore, their observation that 66% of GBF1-positive peripheral structures contained the COPII subunit Sec31p while another 13% laid near such Sec31p-structures, led them conclude that GBF1 localizes to ERES as well. The latter observation appears in conflict with our observation that GBF1-positive peripheral punctae appeared not to overlap with, but instead lie in close proximity to Sec31p-positive structures (refer to Figure 4.7). It may be important to note that our analysis of the relative distribution of GBF1 and Sec31p was performed on cells treated briefly with BFA. The resulting increase in GBF1 signal at peripheral VTCs greatly facilitated comparison of its distribution relative to Sec31p. We think it unlikely that brief BFA treatment altered VTCs but cannot exclude this possibility.

5.2.3. Microtubule-dependent fusion of GBF1 coated VTCs with ER membranes

Due to the extremely dynamic nature of peripheral VTCs, their biogenesis

remains somewhat controversial. Whereas it is generally assumed that VTCs arise by homotypic fusion of uncoated COPII vesicles, Mironov and colleagues (Mironov et al., 2003) reported experimental evidence, which suggests that VTCs arise through cargo concentration and direct en bloc protrusion of specialized ER domains in the vicinity of COPII-coated exit sites. This formation process is apparently COPII-dependent but does not involve budding and fusion of COPII-dependent vesicles (Mironov et al., 2003). The transient BFA-induced accumulation of GBF1 on nascent VTCs allowed us to examine this potential physical connection between COPII-positive ERES and the GBF1- and COPI-positive peripheral VTCs. Our observation that nocodazole treatment does not accelerate but rather blocks the fusion of the GBF1-positive VTCs with the ER suggests that VTCs and the ER are not connected. This observation not only provides the first experimental evidence for this lack of VTC-ER continuity, but also uncovers the existence of a potential microtubule-dependent mechanism for retrograde movement of material from peripheral VTCs back to the ER.

5.2.4. Dynamic membrane association of GBF1

Subcellular fractionation studies established that the vast majority of GBF1 appears in the cytosolic fraction of cellular homogenates, suggesting it is a weakly associated membrane protein (refer to Figure 4.3D and (Claude et al., 1999)). However, since there are a series of *in vitro* procedures involved in preparing homogenates, this approach may yield an underestimate of the fraction of GBF bound to membranes under *in vivo* conditions. Imaging of GFP-GBF1 in live cells revealed approximately 85% of GBF1 in a diffuse pattern throughout the entire cytoplasm. FRAP analysis of this diffuse fraction yielded an estimated value of diffusion coefficient for GBF1 that is consistent

with a freely diffusing protein, suggesting that indeed a significant pool of GBF1 is soluble. Recently published studies by the Jackson and Stzul groups revealed similar cytosolic pools of GFP-tagged forms of GBF1, but those authors did not provide quantitative estimates of either its abundance or mobility (Niu et al., 2005; Szul et al., 2005).

FRAP experiments examining GFP-GBF1 dynamics in the juxta-nuclear Golgi region revealed that GFP-GBF1 rapidly exchanged on and off the membranes of the Golgi complex. While this thesis was in preparation, similar results showing GBF1 membrane dynamics were reported (Niu et al., 2005; Szul et al., 2005). The $t_{1/2}$ of 16 seconds for GBF1 recovery determined by our FRAP analysis is similar to the $t_{1/2}$ (17 seconds) reported by one group (Szul et al., 2005), and both are significantly faster than the $t_{1/2}$ (30 seconds) reported by another group (Niu et al., 2005). This variance could result from differences in experimental systems, especially actual temperature, different cell lines, type of GFP chimera and/or expression levels. We carried our FRAP analysis using a cell line stably expressing low to moderate amounts of GFP tagged GBF1 that is closer to physiological conditions, while the other two groups used transiently transfected cells with a wide range of expression levels that need to be carefully selected to find cells with low to moderate overexpression of GBF1. High overexpression of GBF1 might have altered GBF1 membrane dynamics and caused the slower $t_{1/2}$ determined by one group (Niu et al., 2005). Indeed, most transfected cells acquired resistance to BFA-induced Golgi disassembly under their experimental condition, as expected of cells overexpressing high levels of GBF1 (Niu et al., 2005). Nevertheless, it is clear that all of

the above observations demonstrate that, similar to Arf1, ArfGAP1 and COPI, GBF1 is also continuously cycling on and off the membranes.

FRAP analysis of GFP-GBF1 dynamics at peripheral VTCs established that GFP-GBF1 exchanged on and off these structures within seconds, a rate similar to that observed at the Golgi complex. Since peripheral VTCs transit to the Golgi region in a few minutes on average (Presley et al., 1997; Scales et al., 1997), it is tempting to speculate that multiple binding and release of GBF1 events should take place during VTCs movement. Interestingly, we failed to observe any movement of GBF1-positive peripheral VTCs towards the Golgi complex. GBF1 differs significantly from COPI in this respect, since the coat remains on the surface of VTCs during their central movement (Presley et al., 2002). The longer average residence time for coatomer on membranes ($t_{1/2}$ = 30 sec.) could account for this difference (Presley et al., 2002).

5.2.5. Mechanism of Arf-GEF Recruitment to Specific Membranes

Greater than 90% of GBF1 and BIGs are recovered in the soluble fraction of cellular homogenates (refer to Figure 4.3D and (Claude et al., 1999; Yamaji et al., 2000). Even under *in vivo* conditions, nearly 85% of GFP-GBF1 resides in cytosol and exchanges dynamically with the membrane-bound pool. Our localization of these proteins to distinct Golgi sub-compartment in intact cells therefore predicts that the interaction of Arf-GEFs with membranes is regulated. The localization of putative receptors for Arf-GEFs must be tightly maintained to localize GBF1 and BIGs to separate compartments. Alternatively, the activity of the receptors could be altered when present in the "wrong" compartment. Asymmetric distribution of phosphoinositides is unlikely to play a direct role in localizing these Arf-GEFs since contrary to CYH family members,

which have a PH domain that preferentially binds to membranes containing PtdIns(3,4,5)P_3, GBF1 and BIGs lack recognizable PH domains. We conclude that membrane recruitment of large Arf-GEFs may involve tightly regulated membrane-localized receptor-like proteins, interaction with other types of lipids, or both.

Recently, several membrane-localized binding partners have been identified for GBF1 or its yeast Gea1/2 homolog, including p115 (Garcia-Mata and Sztul, 2003), Gmh1p (Chantalat et al., 2003) and Drs2 (Chantalat et al., 2004). GBF1 has been shown to interact with the tethering protein p115, yet these two proteins display distinct responses to external treatment, such as BFA. As shown in Figure 5.1, BFA caused GBF1, but not p115, to accumulate to peripheral VTCs at early time points (Figure 5.1, b and g). Upon prolonged BFA treatment, GBF1 relocalized to the ER (Figure 5.1, e, also refer to Figure 3.7, e), while p115 appeared at punctate peripheral structures (Figure 5.1, j), presumably as arrested ER sites and immature VTCs (Ward et al., 2001). Furthermore, interaction with p115 is not required for targeting GBF1 to membranes because a GBF1 mutant that lacks the proline-rich p115 binding domain, targeted to membranes in a pattern indistinguishable from that of wt GBF1 (Garcia-Mata and Sztul, 2003). Similar conclusions were reached in the case of Gmh1p, an integral Golgi membrane protein identified by Jackson's group as a binding partner of Gea1p and Gea2p (Chantalat et al., 2003). Interestingly, both yeast Gmh1p and its human homolog associate preferentially with early Golgi cisternae like yeast Gea1/2p and mammalian GBF1(Spang et al., 2001; Zhao et al., 2002). However, membrane association of Gea2p is only slightly affected in *gmh1Δ* cells (Chantalat et al., 2003). The same group has reported that Gea2p also

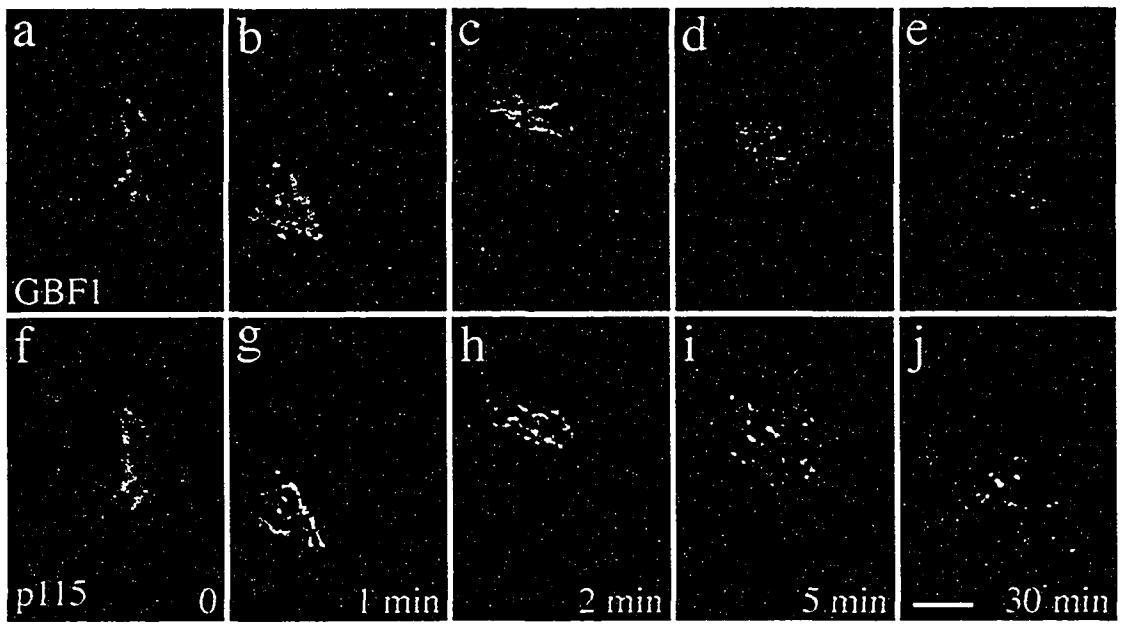

Figure 5.1. GBF1 and p115 redistribute to different membrane compartments upon treatment with BFA. NRK cells treated with BFA (5 μg/ml) for various times (0; 1 min; 2 min; 5 min and 30 min) were fixed and processed for double IF using anti-GBF1 rabbit antibody (9D2, a-e) and anti-p115 mouse antibodies (3A10, f-j). Shown are single-slice confocal images. Bar, 5 μm.

interacts directly with another transmembrane protein Drs2p at the Golgi (Chantalat et al., 2004). However, as was the case for *gmh1Δ*, cells deleted for *DRS2* show only a mild effect on Gea2p localization (Chantalat et al., 2004). In summary, none of the interactions between GBF/GEA members and their binding partners have been shown to be essential for GEF association with membranes. Thus, it seems unlikely that p115, Gmh1p or *DRS2* function as the only Golgi receptor for the GBF1/Gea proteins. Ongoing efforts in our lab and other groups to identify physiological binding partners for these Arf-GEFs, will certainly be helpful in understanding the mechanisms by which large Arf-GEFs are recruited to specific membranes.

The work presented in Chapter 3 provides interesting starting points to analyze the regulation of recruitment of BIGs to the TGN. We established that HA-tagged fragments containing the N-terminal third of either BIG1 (refer to Figure 3.1B) or BIG2 (refer to Figure 3.6) localized to the Golgi complex. Further analysis established, in the case of BIG1, that a HA-tagged fragment co-localized with endogenous BIG1 at the TGN (refer to Figure 3.2C). The information present within the N- terminal domain is therefore necessary and sufficient to direct the protein to the correct Golgi sub-compartment. We cannot at this point determine whether the N- terminal third contains targeting information or is responsible for interaction with a partner in a hetero-oligomeric complex that contains such targeting information. However, it may be important to note that Vaughan's group recently reported that BIG2 interacts with regulatory subunits of protein kinase A (PKA) through PKA-anchoring domains within its N-terminal region (Li et al., 2003).

Although there are many parallels in the molecular events regulated by Sar1p and Arfs, the fact that the GEF for Sar1p, Sec12p, is constitutively membrane-bound, whereas Arf-GEFs are largely cytosolic and are recruited to specific membranes, provides a striking difference. What is more interesting is that Sec12p is not the sole spatial determinant for tER-localized COPII buds (Mancias and Goldberg, 2005), because Sec12p is not concentrated at ERES/tER sites in eukaryotes other than *Pichia pastoris* (Weissman et al., 2001). Thus, while we propose that specific Arf-GEF membrane recruitment is important for determining where Arfs are activated and in consequence where COPI-coated structures or CCVs are formed, we cannot rule out the existence of other regulating molecules.

5.3. GBF1 is a BFA sensitive Arf-GEF

5.3.1. Sequence comparison predicts that GBF1 is a BFA sensitive Arf-GEF

Among all of the Arf-GEFs identified to date, only some can be inhibited by BFA (Cox et al., 2004). Mutagenesis studies have identified critical amino acid residues within the Sec7d that determine BFA sensitivity (YS-M-D-M) or resistance (FA-L-S-P) of Arf-GEFs (Baumgartner et al., 2001; Peyroche et al., 1999; Sata et al., 1999). GBF1 is predicted to be BFA sensitive because its sec7 domain contains the sequence YA-M-D-P, which contains key Yx-**M-D**-x, BFA-sensitive residues (Melançon *et al.*, 2004). Furthermore, if the effects of BFA on the early secretory pathway result from inhibition of an Arf-GEF, logic would dictate this GEF to be GBF1 since the other two Golgi-localized mammalian Arf-GEFs, BIG1 and BIG2, have been convincingly localized to *trans*-element of the Golgi (Zhao et al., 2002) and shown to be involved in late Golgi

events (Shinotsuka et al., 2002a; Shinotsuka et al., 2002b). In addition, the yeast homologues of GBF1, Gea1p and Gea2p are the major targets of BFA in the yeast secretory pathway (Peyroche et al., 1999).

Contrary to this prediction, GBF1 was originally identified as a BFA-resistant GEF based on its BFA-resistant GEF activity toward Arf5 in an *in vitro* GEF assay (Claude et al., 1999). In addition, overexpression of GBF1 allowed cell growth in the presence of BFA at concentrations toxic to wild type cells. The apparent BFA-resistance observed *in vitro* may have resulted from low concentrations of GBF1 and Arf substrate used in the *in vitro* GEF assays (Claude et al., 1999) and the uncompetitive nature of BFA inhibition. Indeed, our laboratory subsequently discovered that reducing levels of Arfs in *in vitro* GEF assays caused an apparent increase in the amount of BFA needed to observe inhibition (Mansour et al., 1999). Alternatively, it is possible that GBF1 activates different Arf isoforms *in vivo*, such as class I Arfs (Arf1 / 3) and that BFA shows specificity towards Arf1/3, but not toward Arf5. Finally, the BFA resistance conferred by GBF1 overexpression could simply result from antagonizing BFA-induced reduction in activity by increasing total enzyme level, rather than arise from BFA-resistant GEF activities. This latter possibility is strongly supported by a recent study showing that overexpression of another BFA-sensitive Arf-GEF, BIG2, does prevent BFA-induced membrane dissociation of Arf1 and AP-1 at the TGN (Shinotsuka et al., 2002b).

5.3.2. Experimental results confirm that GBF1 is a BFA sensitive Arf-GEF in vivo

Our data presented in Chapter 4, together with results obtained from other groups (Niu et al., 2005; Szul et al., 2005), strongly suggest that GBF1 is a BFA target at the

early secretory pathway.

First, three separate studies showed that BFA altered the dynamic exchange of GBF1 between cytosolic and membrane-bound pools, resulting in transient accumulation of GBF1 on both Golgi and VTCs membranes before they eventually redistributed to ER membranes. This accumulation resulted from slower dissociation rather than increased association since all three groups report much longer residence time for GBF1 on Golgi membranes in the presence of BFA (refer to Figure 4.6 and (Niu et al., 2005; Szul et al., 2005)).

Second, dissociation of coatomer from Golgi membranes occurs rapidly and has been reported to be the earliest response to BFA treatment (Donaldson et al., 1990; Orci et al., 1991), but its mechanism remains unknown. Here we found that BFA-induced accumulation of GBF1 displays kinetics similar to those reported for the loss of COPI from peripheral VTCs membranes (refer to Figure 4.7A). Taking the fact that activated Arf1 plays an essential role in coatomer membrane recruitment into consideration, the inhibitory effect of BFA on GBF1 could account for the rapid BFA-induced membrane dissociation of COPI following Arf1 inactivation.

Third, Jackson and colleagues reported that BFA no longer altered the dynamics of a GFP-GBF1 mutant lacking potential contact sites with the BFA molecule (Niu et al., 2005). This observation strongly indicated that GBF1 formed a non-functional complex with BFA and was a direct target of the drug (Niu et al., 2005). Using an *in vivo* assay that monitors Arf-GTP levels, the same group confirmed that BFA indeed inhibits GBF1 exchange activity on Arf1 (Niu et al., 2005).

5.3.3. A model for BFA-induced stabilization of membrane-bound complex

Structural studies demonstrated that BFA blocks the GEF activity of the Sec7d by trapping the Arf-GEF in an abortive Arf-GDP-Sec7d-BFA complex (Mossessova et al., 2003b; Renault et al., 2003). These observations predict that some Arf(s) should be trapped with GBF1 on the membrane. However, contrary to this prediction, BFA causes rapid release of Arf1 from Golgi membranes (Presley et al., 2002). This apparent discrepancy could be readily explained since Arf1 is in large excess compared to GBF1 and thus relocalizes to cytosol in its GDP form in the presence of BFA. As discussed below (section 5.4.2), we observed that Arf4 accumulated transiently like GBF1 on BFA-induced peripheral VTCs membranes upon BFA treatment. This observation supports our model that BFA causes formation of an abortive complex and that this abortive Arf-GDP-GBF1-BFA complex somehow has enhanced affinity for *cis*-Golgi and VTC membranes (Figure 5.2). In agreement with this model, Sztul and colleagues demonstrated that using GBF1 (E794K) and Arf (T31N) mutants, known to stabilize the GBF1-Arf complex, also promoted membrane association and led to decreases in exchange rates (Szul et al., 2005).

Interestingly, the BFA-sensitive BIG1, like GBF1, was clearly not released from membranes upon BFA treatment but redistributed instead to a pattern distinct from GBF1. While GBF1 eventually redistributed to ER membranes, BIG1 appeared in a hybrid organelle that clusters near the MTOC in the presence of BFA. Although the mechanisms regulating the association of GBF1 and BIG1 with Golgi membranes remain poorly understood, it is tempting to speculate that BFA traps these two GEFs onto distinct membranes through their specific membrane receptors. In this model, the

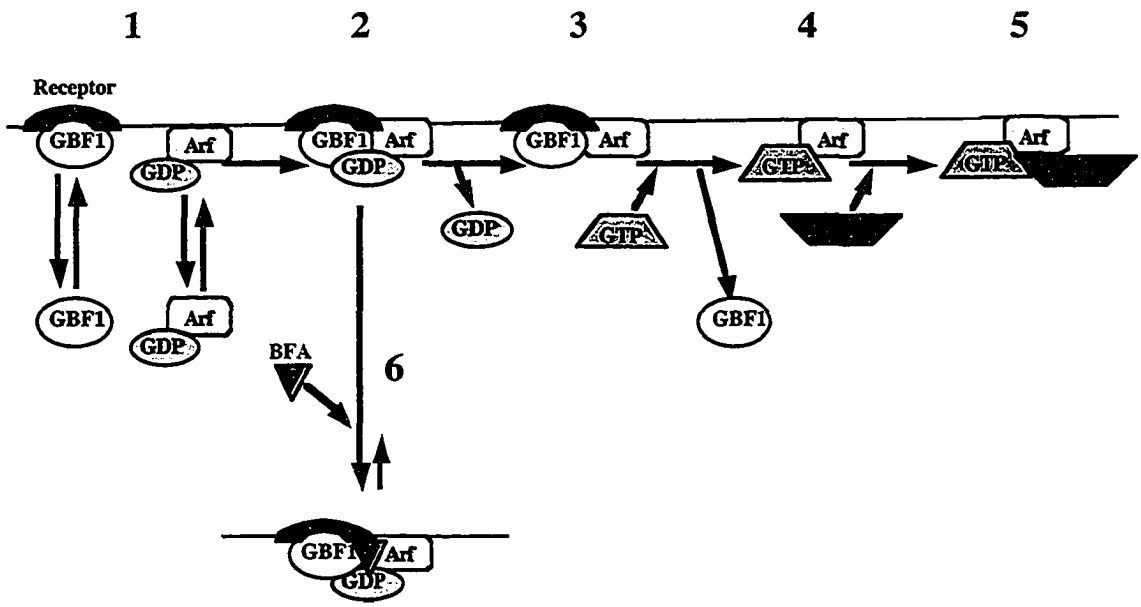

Figure 5.2. Model for GBF1 cycling at the membrane. GBF1 and Arf-GDP dynamically associate with the membrane and their membrane association is independent of each other **(Step 1)**. Once on the membrane, these two proteins interact and GBF1 catalyzes displacement of GDP from Arf **(Step 2)**. A complex of GBF1 and the apo-form of Arf remains on the membrane **(Step 3)** until Arf binds GTP **(Step 4)**. GTP binding triggers complex dissociation, and GBF1 dissociates from membranes, but Arf-GTP remains on membranes. It then interacts with effectors **(Step 5)**, such as a variety of coat proteins (refer to section 1.4.1). GBF1 cycling is inhibited by BFA, which forms a trimeric complex with GBF1 and Arf-GDP **(Step 6)** and inhibits GDP displacement. This prevents GTP binding to the Arf, and subsequently prevents the dissociation of GBF1 from the membrane. The complex remains membrane bound presumably associated with the receptor(s) that normally facilitate GBF1 membrane association (refer to section 5.2.4). (Adapted from (Szul, et al., 2005)).

abortive Arf-GDP-GEF-BFA complex would acquire enhanced affinity for receptors on the membrane, whose selection would depend on the GEF present in the complex.

5.3.4. Mechanism of resistance to BFA in mutant BFY cells

Whereas the present studies confirmed GBF1 as one of the cellular targets of BFA, this analysis does not yet fully explain the full range of effects of BFA on cell physiology. We previously isolated several CHO mutant lines, termed BFY1-22, which acquired the ability to grow in the presence of BFA (Yan et al., 1994). Interestingly, all BFY lines displayed Golgi-specific BFA resistance, since BFA treatment no longer disrupted the Golgi complex but still caused dispersal of the TGN and endosomes (Yan et al., 1994). Based on our results on the distribution of GBF1 and its involvement in recruitment of the COP1 coat, we would have expected BFY cells to contain GBF1 that was either mutated or overexpressed. However, comparison of wt CHO cells and BFY-1 or BFY-2 cells established that GBF1 cDNAs in these two cell lines had identical sequences and were present at similar levels (Claude et al., 2003), suggesting that BFA resistance in BFY cells did not arise from changes in GBF1.

We consider it unlikely that resistance in BFY cells arose from mutations or overexpression of a yet-to-be-identified BFA sensitive Arf-GEFs involved in the early secretory pathway. Analysis of the completed human genome identified only 5 classes of Arf-GEFs, only two of which convincingly localize to the Golgi complex (Cox et al., 2004; Mouratou et al., 2005). Alternatively, the candidate could be a BFA target other than Arf-GEFs, for example CtBP3/BARS (refer to section 1.6.3). This possibility is supported by the observation that drugs that prevent the BFA-induced ADP-ribosylation of CtBP3/BARS such as coumermicyn or dicumerol, stabilize the Golgi complex and

prevent its redistribution to the ER (Mironov et al., 1997). Further analysis of the BFY cells should elucidate the resistance mechanism.

5.4. Function of large Arf-GEFs

5.4.1. GBF1 regulates COPI membrane recruitment

Although several observations summarized in section 4.1 suggested that GBF1 is responsible for COPI membrane recruitment (Claude et al., 1999) (Garcia-Mata et al., 2003; Kawamoto et al., 2002; Zhao et al., 2002), our microinjection experiments with anti-GBF1 neutralizing antibodies most convincingly support this conclusion. Affinity-purified 9D2 specifically caused dissociation of COPI from VTCs and Golgi membranes, while leaving clathrin intact on TGN membranes (refer to Figure 4.11) within 2 hours of microinjection. In contrast, previous experiments with the E794K mutant required 12-14 h incubation to allow accumulation of sufficient levels of mutant proteins in cells transiently transfected with E794 constructs (Garcia-Mata et al., 2003). The phenotype observed under these conditions could have resulted from indirect effects. Clear loss of COP1 staining within 2 hours of microinjection greatly enhances the likelihood that the specific dissociation of COPI from membranes resulted directly from blocking GBF1 function. The *cis*-Golgi localized COPI (Oprins et al., 1993) has been implicated in bi-directional traffic between ER and Golgi (Orci et al., 1997). However, our studies to date cannot resolve whether GBF1 participates primarily in one or in both directions.

5.4.2. Activation of Arf4 by GBF1 may regulate COPI recruitment at VTCs

The identity of the Arf isoforms activated by GBF1 at VTCs or the Golgi complex remains unclear. *In vitro* observations suggest that GBF1 preferentially uses Class II Arfs

(Arf5) as substrate (Claude et al., 1999). On the other hand, overexpression of GBF1 *in vivo* protects both Class I Arfs (Arf1 and Arf3) and Class II Arfs from BFA-induced release (Kawamoto et al., 2002). Furthermore, GBF1 was shown to bind all Arfs except Arf6 *in vivo* and catalyze Arf1 activation in vivo (Niu et al., 2005). In agreement with these observations, both Class I and Class II Arfs have been localized to the Golgi complex (Hosaka et al., 1996; Stearns et al., 1990; Tsai et al., 1992) and *in vitro* studies showed that Arf 1, 3 and 5 facilitate, with similar efficiencies, the recruitment of COPI and AP-1 onto Golgi-enriched membranes (Liang and Kornfeld, 1997).

However, the observations summarized above do not preclude the possibility that GBF1 acts on different Arf isoforms at distinct membranes sites. The results I presented in Figure 4.9 provide interesting starting points to investigate the substrate specificity of GBF1 at peripheral VTC structures. Our observation established that Arf4, but not Arf1 or Arf5, accumulated with GBF1 on peripheral VTCs membrane upon brief BFA treatment. The lack of BFA-induced accumulation Arf5 and Arf1 at VTCs cannot be unambiguously interpreted at this point. For example, it may simply be that BFA forms stable abortive Arf-GEF complex preferentially with Arf4 (step 6 in Figure 5.2). What our observation does clearly suggest is that GBF1 may activate Arf4 at peripheral VTCs. Note that the function of Arf4 cannot be limited to VTCs since involvement of Arf4 in post-Golgi sorting and endosomal trafficking has been reported (Deretic et al., 2005). This would explain why ARF4 accumulated not only at VTCs but also in the juxtanuclear Golgi region. Further efforts will be directed towards confirming Arf4 substrate specificity of GBF1 at VTCs and determining which Arf isoforms GBF1 activates at Golgi membranes.

5.4.3. Function of BIGs in the TGN

Several proteins implicated in the assembly of clathrin have been identified in *trans*-elements of the Golgi complex. These include the adaptins AP-1 and AP-3, as well as a new class of proteins termed GGAs that appear to function in sorting cargo into nascent clathrin coated vesicles (Bonifacino, 2004; Robinson, 2004). Interestingly, the recruitment of these proteins to Golgi membranes is sensitive to BFA (Robinson, 2004) and is most likely regulated by the BFA-sensitive and TGN-localized BIGs. As expected, we observed clear but limited overlap in the distribution of clathrin and BIG1 (refer to Figure 3.10). Our observation that many clathrin-positive structures lacked BIGs was not really surprising since much of the clathrin pool is involved in endocytosis. In agreement with our observation, BIG2 has been shown to regulate the membrane recruitment of the clathrin adaptor complexes AP-1 and GGA1 (Shinotsuka et al., 2002a). Most recently, BIG2 has also been found in the recycling endosomes in addition to the TGN and is implicated in the endosomal integrity, because expression of catalytically inactive E738K mutant of BIG2 induces membrane tubules from the recycling endosomes (Shin et al., 2004).

Previous evidence suggests that greater than 75% of BIG1 and BIG2 form a hetero-dimer complex in mammalian cells (Morinaga et al., 1996; Yamaji et al., 2000). However, we, and others identified several differences between BIG1 and BIG2, suggesting that their functions may not completely overlap. For example, BIG2, but not BIG1 accumulated in TGN38-containing tubules extending from the TGN in BFA treated cells (Figure 5.3 and (Shinotsuka et al., 2002b)). Likewise, a large fraction of BIG1, but not BIG2, accumulated in the nucleus when cells were cultured under serum-starved

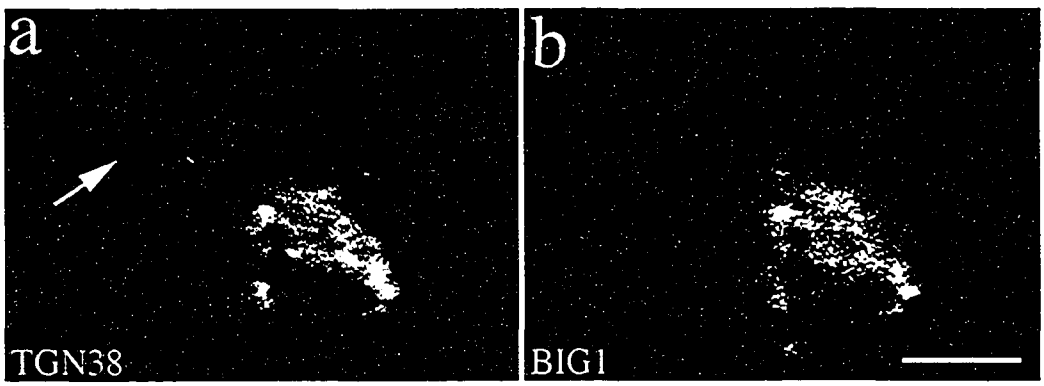

Figure 5.3. BFA-induced tubules from the TGN contain TGN 38 but lack BIG1. NRK cells treated with BFA (5 μg/ml) for 10 min were fixed and processed for double IF using anti-TGN rabbit antibody (a) and anti-BIG1 rabbit antibody (Alexa488- conjugated 9D3, b). BFA-induced tubules containing TGN 38 in image a are indicated by a white arrow. Bar, 5 μm.

conditions (Padilla et al., 2004). These observations suggest that significant amounts of both BIG1 and BIG2 form homodimers, and that such homodimers have distinct function.

5.4.4. Arf-GEFs may determine the specificity of coat recruitment

Our hypothesis that GBF1 and BIGs perform distinct functions in different environments is consistent with several morphological and functional studies with their yeast homologues, Gea1p / Gea2p and Sec7p. These proteins, like their mammalian homologues, associate preferentially with early and late Golgi cisternae, respectively (Mogelsvang et al., 2003; Spang et al., 2001). Furthermore, Gea1p and Gea2p have non-redundant but overlapping functions in retrograde traffic between the Golgi complex and the ER, while Sec7 mutants do not show defects in this step of traffic (Spang et al., 2001). In addition, recent work from Jackson and colleagues revealed that Gea2p plays a role in the formation of secretory granules/vesicles through interaction with the P-type ATPase Drs2p (Chantalat et al., 2004). Sec7p, like BIGs, probably works at the *trans*-Golgi and its reported involvement in ER-Golgi traffic (Deitz et al., 2000) may result from indirect effects.

How each class of Arf-GEF regulates the recruitment of different types of coat components on their respective compartments remains unclear. It seems unlikely that activation of distinct classes of Arfs is sufficient to account for coat selectivity. Whereas both Arf1 and Arf5 have been found associated with Golgi membranes (Cavenagh et al., 1996; Morinaga et al., 2001; Tsai et al., 1992), to date neither has been localized to a specific sub-compartment at either the light or EM level. ARNOs catalyze exchange on both Arf1 and Arf6 (Donaldson and Jackson, 2000), and recent reports localize these

small GEFs to the Golgi complex in some cells (Lee et al., 2000); Class I and Class II Arfs may therefore not show a polarized distribution that match coat proteins. On the other hand, the striking similarity between the polarized distribution of the two large Arf-GEF classes and the two main type of protein coats on the Golgi complex suggest that the GEFs may actually participate directly in effector and/or coat selection. By acting as transient molecular scaffolds, the large Arf-GEFs could provide some of the required specificity to direct specific interactions between GEFs and downstream effectors in a spatially and temporally regulated manner. Ongoing efforts in several laboratories to identify partners for Arfs and their regulators will, in time, test this hypothesis.

5.5. Future perspectives

Since the identification of the first Arf-GEF (Chardin et al., 1996), much progress has been made in characterizing their biochemical and molecular properties. As described in this thesis, subcellular localizations of some Arf-GEFs have been determined, and the sensitivity to BFA and regulation of some particular type(s) of coat protein recruitment have been discovered. However, some important questions remain unanswered. For example, what is the specificity of a given Arf-GEF for a particular Arf protein in vivo, especially for those Arf-GEFs with multiple membrane locations? How is it determined where different coat proteins are recruited? Since some Arf-GEF family members have been localized to specific membrane compartments as presented in this thesis, it is likely that Arf-GEFs determine where Arfs are activated, and activated Arfs in turn determine where distinct coated structures are formed. Then the next question is how these Arf-GEFs are recruited to specific membrane locations. Answers to this question will be

obtained by identifying the physiological interaction partners of Arf-GEFs, which will certainly help us to ultimately understand the function of each Arf-GEF in membrane trafficking.

Chapter 6

References

Achstetter, T., A. Franzusoff, C. Field, and R. Schekman. 1988. SEC7 encodes an unusual, high molecular weight protein required for membrane traffic from the yeast Golgi apparatus. *J Biol Chem.* 263:11711-7.

Allan, V.J., and T.E. Kreis. 1986. A microtubule-binding protein associated with membranes of the Golgi apparatus. *J Cell Biol.* 103:2229-39.

Altan-Bonnet, N., R. Sougrat, and J. Lippincott-Schwartz. 2004. Molecular basis for Golgi maintenance and biogenesis. *Curr Opin Cell Biol.* 16:364-72.

Alvarez, C., H. Fujita, A. Hubbard, and E. Sztul. 1999. ER to Golgi transport: Requirement for p115 at a pre-Golgi VTC stage. *J Cell Biol.* 147:1205-22.

Antonny, B., S. Beraud-Dufour, P. Chardin, and M. Chabre. 1997. N-terminal hydrophobic residues of the G-protein ADP-ribosylation factor-1 insert into membrane phospholipids upon GDP to GTP exchange. *Biochemistry.* 36:4675-84.

Antonny, B., D. Madden, S. Hamamoto, L. Orci, and R. Schekman. 2001. Dynamics of the COPII coat with GTP and stable analogues. *Nat Cell Biol.* 3:531-7.

Aoe, T., E. Cukierman, A. Lee, D. Cassel, P.J. Peters, and V.W. Hsu. 1997. The KDEL receptor, ERD2, regulates intracellular traffic by recruiting a GTPase-activating protein for ARF1. *Embo J.* 16:7305-16.

Aoe, T., I. Huber, C. Vasudevan, S.C. Watkins, G. Romero, D. Cassel, and V.W. Hsu. 1999. The KDEL receptor regulates a GTPase-activating protein for ADP-ribosylation factor 1 by interacting with its non-catalytic domain. *J Biol Chem.* 274:20545-9.

Appenzeller, C., H. Andersson, F. Kappeler, and H.P. Hauri. 1999. The lectin ERGIC-53 is a cargo transport receptor for glycoproteins. *Nat Cell Biol.* 1:330-4.

Aridor, M., S.I. Bannykh, T. Rowe, and W.E. Balch. 1995. Sequential coupling between COPII and COPI vesicle coats in endoplasmic reticulum to Golgi transport. *J Cell Biol.* 131:875-93.

Aridor, M., J. Weissman, S. Bannykh, C. Nuoffer, and W.E. Balch. 1998. Cargo selection by the COPII budding machinery during export from the ER. *J Cell Biol.* 141:61-70.

Bannykh, S.I., and W.E. Balch. 1997. Membrane dynamics at the endoplasmic reticulum-Golgi interface. *J Cell Biol.* 138:1-4.

Bannykh, S.I., T. Rowe, and W.E. Balch. 1996. The organization of endoplasmic reticulum export complexes. *J Cell Biol.* 135:19-35.

Barlowe, C. 2000. Traffic COPs of the early secretory pathway. *Traffic.* 1:371-7.

Barlowe, C. 2003a. Molecular recognition of cargo by the COPII complex: a most accommodating coat. *Cell.* 114:395-7.

Barlowe, C. 2003b. Signals for COPII-dependent export from the ER: what's the ticket out? *Trends Cell Biol.* 13:295-300.

Barlowe, C., L. Orci, T. Yeung, M. Hosobuchi, and S. Hamamoto, et al. 1994. COP II: a membrane coat formed by sec proteins that drive vesicle budding from the endoplasmic reticulum. *Cell.* 77:895-907.

Barr, F.A., and B. Short. 2003. Golgins in the structure and dynamics of the Golgi apparatus. *Curr Opin Cell Biol.* 15:405-13.

Baumgartner, F., S. Wiek, K. Paprotka, S. Zauner, and K. Lingelbach. 2001. A point mutation in an unusual Sec7 domain is linked to brefeldin A resistance in a Plasmodium falciparum line generated by drug selection. *Mol Microbiol.* 41:1151-8.

Becker, B., B. Bolinger, and M. Melkonian. 1995. Anterograde transport of algal scales through the Golgi complex is not mediated by vesicles. *Trends Cell Biol.* 5:305-7.

Bell, A.W., M.A. Ward, W.P. Blackstock, H.N. Freeman, J.S. Choudhary, A.P. Lewis, D. Chotai, A. Fazel, J.N. Gushue, J. Paiement, S. Palcy, E. Chevet, M. Lafreniere-Roula, R. Solari, D.Y. Thomas, A. Rowley, and J.J. Bergeron. 2001. Proteomics characterization of abundant Golgi membrane proteins. *J Biol Chem.* 276:5152-65.

Beraud-Dufour, S., S. Robineau, P. Chardin, S. Paris, M. Chabre, J. Cherfils, and B. Antonny. 1998. A glutamic finger in the guanine nucleotide exchange factor ARNO displaces Mg2+ and the beta-phosphate to destabilize GDP on ARF1. *Embo J.* 17:3651-9.

Bergmann, J.E. 1989. Using temperature-sensitive mutants of VSV to study membrane protein biogenesis. *Methods Cell Biol.* 32:85-110.

Bi, X., R.A. Corpina, and J. Goldberg. 2002. Structure of the Sec23/24-Sar1 pre-budding complex of the COPII vesicle coat. *Nature.* 419:271-7.

Bigay, J., P. Gounon, S. Robineau, and B. Antonny. 2003. Lipid packing sensed by ArfGAP1 couples COPI coat disassembly to membrane bilayer curvature. *Nature.* 426:563-6.

Boman, A.L., and R.A. Kahn. 1995. Arf proteins: the membrane traffic police? *Trends Biochem Sci.* 20:147-50.

Bonazzi, M., S. Spano, G. Turacchio, C. Cericola, C. Valente, A. Colanzi, H.S. Kweon, V.W. Hsu, E.V. Polishchuck, R.S. Polishchuck, M. Sallese, T. Pulvirenti, D. Corda, and A. Luini. 2005. CtBP3/BARS drives membrane fission in dynamin-independent transport pathways. *Nat Cell Biol.* 7:570-80.

Bonfanti, L., A.A. Mironov, Jr., J.A. Martinez-Menarguez, O. Martella, A. Fusella, M. Baldassarre, R. Buccione, H.J. Geuze, A.A. Mironov, and A. Luini. 1998. Procollagen traverses the Golgi stack without leaving the lumen of cisternae: evidence for cisternal maturation. *Cell.* 95:993-1003.

Bonifacino, J.S. 2004. The GGA proteins: adaptors on the move. *Nat Rev Mol Cell Biol.* 5:23-32.

Bonifacino, J.S., and B.S. Glick. 2004. The mechanisms of vesicle budding and fusion. *Cell.* 116:153-66.

Bonifacino, J.S., and J. Lippincott-Schwartz. 2003. Coat proteins: shaping membrane transport. *Nat Rev Mol Cell Biol.* 4:409-14.

Bremser, M., W. Nickel, M. Schweikert, M. Ravazzola, M. Amherdt, C.A. Hughes, T.H. Sollner, J.E. Rothman, and F.T. Wieland. 1999. Coupling of coat assembly and vesicle budding to packaging of putative cargo receptors. *Cell.* 96:495-506.

Bretscher, M.S., and S. Munro. 1993. Cholesterol and the Golgi apparatus. *Science.* 261:1280-1.

Brown, F.D., A.L. Rozelle, H.L. Yin, T. Balla, and J.G. Donaldson. 2001. Phosphatidylinositol 4,5-bisphosphate and Arf6-regulated membrane traffic. *J Cell Biol.* 154:1007-17.

Brown, H.A., S. Gutowsk, C.R. Moomaw, C. Slaughter, and P.C. Sternweis. 1993. ADP-ribosylation factor, a small GTP-dependent regulatory protein, stimulates phospholipase D activity. *Cell.* 75:1137-44.

Brugger, B., R. Sandhoff, S. Wegehingel, K. Gorgas, J. Malsam, J.B. Helms, W.D. Lehmann, W. Nickel, and F.T. Wieland. 2000. Evidence for segregation of sphingomyelin and cholesterol during formation of COPI-coated vesicles. *J Cell Biol.* 151:507-18.

Burke, B., G. Griffiths, H. Reggio, D. Louvard, and G. Warren. 1982. A monoclonal antibody against a 135-K Golgi membrane protein. *Embo J.* 1:1621-8.

Cavenagh, M.M., J.A. Whitney, K. Caroll, C. Zhang, A.L. Boman, A.G. Rosenwald, I. Melman, and R.A. Kahn. 1996. Intracellular distribution of ARF proteins in mammalian cells. ARF6 is uniquely localized to the plasma membrane. *J. Biol Chem.* 271:21786-84.

Chantalat, S., R. Courbeyrette, F. Senic-Matuglia, C.L. Jackson, B. Goud, and A. Peyroche. 2003. A novel Golgi membrane protein is a partner of the ARF exchange factors Gea1p and Gea2p. *Mol Biol Cell.* 14:2357-71.

Chantalat, S., S.K. Park, Z. Hua, K. Liu, R. Gobin, A. Peyroche, A. Rambourg, T.R. Graham, and C.L. Jackson. 2004. The Arf activator Gea2p and the P-type ATPase Drs2p interact at the Golgi in Saccharomyces cerevisiae. *J Cell Sci.* 117:711-22.

Chardin, P., S. Paris, B. Antonny, S. Robineau, S. Beraud-Dufour, C.L. Jackson, and M. Chabre. 1996. A human exchange factor for ARF contains Sec7- and pleckstrin-homology domains. *Nature.* 384:481-4.

Chen, E.H., B.A. Pryce, J.A. Tzeng, G.A. Gonzalez, and E.N. Olson. 2003. Control of myoblast fusion by a guanine nucleotide exchange factor, loner, and its effector ARF6. *Cell.* 114:751-62.

Cherfils, J., and P. Chardin. 1999. GEFs: structural basis for their activation of small GTP-binding proteins. *Trends Biochem Sci.* 24:306-11.

Cherfils, J., J. Menetrey, M. Mathieu, G. Le Bras, S. Robineau, S. Beraud-Dufour, B. Antonny, and P. Chardin. 1998. Structure of the Sec7 domain of the Arf exchange factor ARNO. *Nature.* 392:101-5.

Claude, A., B.P. Zhao, C.E. Kuziemsky, S. Dahan, S.J. Berger, J.P. Yan, A.D. Armold, E.M. Sullivan, and P. Melancon. 1999. GBF1: A novel Golgi-associated BFA-resistant guanine nucleotide exchange factor that displays specificity for ADP-ribosylation factor 5. *J Cell Biol.* 146:71-84.

Claude, A., B.P. Zhao, and P. Melancon. 2003. Characterization of alternatively spliced and truncated forms of the Arf guanine nucleotide exchange factor GBF1 defines regions important for activity. *Biochem Biophys Res Commun.* 303:160-9.

Cole, N.B., C.L. Smith, N. Sciaky, M. Terasaki, M. Edidin, and J. Lippincott-Schwartz. 1996. Diffusional mobility of Golgi proteins in membranes of living cells. *Science.* 273:797-801.

Cosson, P., C. Demolliere, S. Hennecke, R. Duden, and F. Letourneur. 1996. Delta- and zeta-COP, two coatomer subunits homologous to clathrin- associated proteins, are involved in ER retrieval. *Embo J.* 15:1792-8.

Cosson, P., and F. Letourneur. 1994. Coatomer interaction with di-lysine endoplasmic reticulum retention motifs. *Science.* 263:1629-31.

Cox, R., R.J. Mason-Gamer, C.L. Jackson, and N. Segev. 2004. Phylogenetic analysis of Sec7-domain-containing Arf nucleotide exchangers. *Mol Biol Cell.* 15:1487-505.

Dahan, S., J.P. Ahluwalia, L. Wong, B.I. Posner, and J.J. Bergeron. 1994. Concentration of intracellular hepatic apolipoprotein E in Golgi apparatus saccular distensions and endosomes. *J Cell Biol.* 127:1859-69.

Dascher, C., and W.E. Balch. 1994. Dominant inhibitory mutants of ARF1 block endoplasmic reticulum to Golgi transport and trigger disassembly of the Golgi apparatus. *J Biol Chem.* 269:1437-48.

De Matteis, M.A., M. Di Girolamo, A. Colanzi, M. Pallas, G. Di Tullio, L.J. McDonald, J. Moss, G. Santini, S. Bannykh, D. Corda, and a. et. 1994. Stimulation of endogenous ADP-ribosylation by brefeldin A. *Proc Natl Acad Sci U S A.* 91:1114-8.

De Matteis, M.A., A. Luna, G. Di Tullio, D. Corda, J.W. Kok, A. Luini, and G. Egea. 1999. PDMP blocks the BFA-induced ADP-ribosylation of BARS-50 in isolated Golgi membranes. *FEBS Lett.* 459:310-2.

Deitz, S.B., A. Rambourg, F. Kepes, and A. Franzusoff. 2000. Sec7p directs the transitions required for yeast Golgi biogenesis. *Traffic.* 1:172-83.

Deitz, S.B., C. Wu, S. Silve, K.E. Howell, P. Melancon, R.A. Kahn, and A. Franzusoff. 1996. Human ARF4 expression rescues sec7 mutant yeast cells. *Mol Cell Biol.* 16:3275-84.

Deretic, D., A.H. Williams, N. Ransom, V. Morel, P.A. Hargrave, and A. Arendt. 2005. Rhodopsin C terminus, the site of mutations causing retinal disease, regulates trafficking by binding to ADP-ribosylation factor 4 (ARF4). *Proc Natl Acad Sci U S A.* 102:3301-6.

Derrien, V., C. Couillault, M. Franco, S. Martineau, P. Montcourrier, R. Houlgatte, and P. Chavrier. 2002. A conserved C-terminal domain of EFA6-family ARF6-guanine nucleotide exchange factors induces lengthening of microvilli-like membrane protrusions. *J Cell Sci.* 115:2867-79.

Di Girolamo, M., M.G. Silletta, M.A. De Matteis, A. Braca, A. Colanzi, D. Pawlak, M.M. Rasenick, A. Luini, and D. Corda. 1995. Evidence that the 50-kDa substrate of brefeldin A-dependent ADP- ribosylation binds GTP and is modulated by the G-protein beta gamma subunit complex. *Proc Natl Acad Sci U S A.* 92:7065-9.

Dominguez, M., K. Dejgaard, J. Fullekrug, S. Dahan, A. Fazel, J.P. Paccaud, D.Y. Thomas, J.J. Bergeron, and T. Nilsson. 1998. gp25L/emp24/p24 protein family members of the cis-Golgi network bind both COP I and II coatomer. *J Cell Biol.* 140:751-65.

Donaldson, J.G. 2003. Multiple roles for Arf6: sorting, structuring, and signaling at the plasma membrane. *J Biol Chem.* 278:41573-6.

Donaldson, J.G., D. Cassel, R.A. Kahn, and R.D. Klausner. 1992a. ADP-ribosylation factor, a small GTP-binding protein, is required for binding of the coatomer protein beta-COP to Golgi membranes. *Proc Natl Acad Sci U S A.* 89:6408-12.

Donaldson, J.G., D. Finazzi, and R.D. Klausner. 1992b. Brefeldin A inhibits Golgi membrane-catalysed exchange of guanine nucleotide onto ARF protein. *Nature.* 360:350-2.

Donaldson, J.G., and C.L. Jackson. 2000. Regulators and effectors of the ARF GTPases. *Curr Opin Cell Biol.* 12:475-82.

Donaldson, J.G., S.J. Lippincott, and R.D. Klausner. 1991. Guanine nucleotides modulate the effects of brefeldin A in semipermeable cells: regulation of the association of a 110-kD peripheral membrane protein with the Golgi apparatus. *J Cell Biol.* 112:579-88.

Donaldson, J.G., J. Lippincott-Schwartz, G.S. Bloom, T.E. Kreis, and R.D. Klausner. 1990. Dissociation of a 110-kD peripheral membrane protein from the Golgi apparatus is an early event in brefeldin A action. *J Cell Biol.* 111:2295-306.

Doray, B., P. Ghosh, J. Griffith, H.J. Geuze, and S. Kornfeld. 2002. Cooperation of GGAs and AP-1 in packaging MPRs at the trans-Golgi network. *Science.* 297:1700-3.

Duden, R., G. Griffiths, R. Frank, P. Argos, and T.E. Kreis. 1991. Beta-COP, a 110 kd protein associated with non-clathrin-coated vesicles and the Golgi complex, shows homology to beta-adaptin. *Cell.* 64:649-65.

Elsner, M., H. Hashimoto, J.C. Simpson, D. Cassel, T. Nilsson, and M. Weiss. 2003. Spatiotemporal dynamics of the COPI vesicle machinery. *EMBO Rep.* 4:1000-4.

Farquhar, M.G., and G.E. Palade. 1981. The Golgi apparatus (complex)-(1954-1981)-from artifact to center stage. *J Cell Biol.* 91:77s-103s.

Farquhar, M.G., and G.E. Palade. 1998. The Golgi apparatus: 100 years of progress and controversy. *Trends Cell Biol.* 8:2-10.

Franco, M., P. Chardin, M. Chabre, and S. Paris. 1995. Myristoylation of ADP-ribosylation factor 1 facilitates nucleotide exchange at physiological Mg^{2+} levels. *J. Biol. Chem.* 270:1337-41.

Franco, M., P. Chardin, M. Chabre, and S. Paris. 1996. Myristoylation-facilitated binding of the G protein ARF1GDP to membrane phospholipids is required for its activation by a soluble nucleotide exchange factor. *J Biol Chem.* 271:1573-8.

Franco, M., P.J. Peters, J. Boretto, E. van Donselaar, A. Neri, C. D'Souza-Schorey, and P. Chavrier. 1999. EFA6, a sec7 domain-containing exchange factor for ARF6, coordinates membrane recycling and actin cytoskeleton organization. *Embo J.* 18:1480-91.

Frank, S., S. Upender, S.H. Hansen, and J.E. Casanova. 1998. ARNO is a guanine nucleotide exchange factor for ADP-ribosylation factor 6. *J Biol Chem.* 273:23-7.

Franzusoff, A., K. Redding, J. Crosby, R.S. Fuller, and R. Schekman. 1991. Localization of components involved in protein transport and processing through the yeast Golgi apparatus. *J Cell Biol.* 112:27-37.

Futai, E., S. Hamamoto, L. Orci, and R. Schekman. 2004. GTP/GDP exchange by Sec12p enables COPII vesicle bud formation on synthetic liposomes. *Embo J.* 23:4146-55.

Garcia-Mata, R., and E. Sztul. 2003. The membrane-tethering protein p115 interacts with GBF1, an ARF guanine-nucleotide-exchange factor. *EMBO Rep.* 4:320-5.

Garcia-Mata, R., T. Szul, C. Alvarez, and E. Sztul. 2003. ADP-ribosylation factor/COPI-dependent events at the endoplasmic reticulum-Golgi interface are regulated by the guanine nucleotide exchange factor GBF1. *Mol Biol Cell.* 14:2250-61.

Geldner, N., N. Anders, H. Wolters, J. Keicher, W. Kornberger, P. Muller, A. Delbarre, T. Ueda, A. Nakano, and G. Jurgens. 2003. The Arabidopsis GNOM ARF-GEF mediates endosomal recycling, auxin transport, and auxin-dependent plant growth. *Cell.* 112:219-30.

Girod, A., B. Storrie, J.C. Simpson, L. Johannes, B. Goud, L.M. Roberts, J.M. Lord, T. Nilsson, and R. Pepperkok. 1999. Evidence for a COP-I-independent transport route from the Golgi complex to the endoplasmic reticulum. *Nat Cell Biol.* 1:423-30.

Godi, A., A. Di Campli, A. Konstantakopoulos, G. Di Tullio, D.R. Alessi, G.S. Kular, T. Daniele, P. Marra, J.M. Lucocq, and M.A. De Matteis. 2004. FAPPs control Golgi-to-cell-surface membrane traffic by binding to ARF and PtdIns(4)P. *Nat Cell Biol.* 6:393-404.

Godi, A., P. Pertile, R. Meyers, P. Marra, G. Di Tullio, C. Iurisci, A. Luini, D. Corda, and M.A. De Matteis. 1999. ARF mediates recruitment of PtdIns-4-OH kinase-beta and stimulates synthesis of PtdIns(4,5)P2 on the Golgi complex. *Nat Cell Biol.* 1:280-7.

Goldberg, J. 1998. Structural basis for activation of ARF GTPase: mechanisms of guanine nucleotide exchange and GTP-myristoyl switching. *Cell.* 95:237-48.

Grasse, P.P. 1957. [Ultrastructure, polarity and reproduction of Golgi apparatus.]. *C R Hebd Seances Acad Sci.* 245:1278-81.

Grebe, M., J. Gadea, T. Steinmann, M. Kientz, J.U. Rahfeld, K. Salchert, C. Koncz, and G. Jurgens. 2000. A conserved domain of the arabidopsis GNOM protein mediates subunit interaction and cyclophilin 5 binding. *Plant Cell.* 12:343-56.

Griffiths, G., R. Pepperkok, J.K. Locker, and T.E. Kreis. 1995. Immunocytochemical localization of beta-COP to the ER-Golgi boundary and the TGN. *J Cell Sci.* 108:2839-56.

Guo, Q., E. Vasile, and M. Krieger. 1994. Disruptions in Golgi structure and membrane traffic in a conditional lethal mammalian cell mutant are corrected by epsilon-COP. *J Cell Biol.* 125:1213-24.

Guo, W., M. Sacher, J. Barrowman, S. Ferro-Novick, and P. Novick. 2000. Protein complexes in transport vesicle targeting. *Trends Cell Biol.* 10:251-5.

Hammond, A.T., and B.S. Glick. 2000. Dynamics of transitional endoplasmic reticulum sites in vertebrate cells. *Mol Biol Cell.* 11:3013-30.

Hara-Kuge, S., O. Kuge, L. Orci, M. Amherdt, M. Ravazzola, F.T. Wieland, and J.E. Rothman. 1994. En bloc incorporation of coatomer subunits during the assembly of COP-coated vesicles. *J Cell Biol.* 124:883-92.

Harlan, J.E., H.S. Yoon, P.J. Hajduk, and S.W. Fesik. 1995. Structural characterization of the interaction between a pleckstrin homology domain and phosphatidylinositol 4,5-bisphosphate. *Biochemistry.* 34:9859-64.

Harlow, E., and D. Lane. 1988. Antibodies, A laboratory Manual. Cold Spring Harbor Laboratory, Cold Spring Harbor. 726 pp.

Hauri, H.P., and A. Schweizer. 1992. The endoplasmic reticulum-Golgi intermediate compartment. *Curr Opin Cell Biol.* 4:600-8.

Helms, J.B., and J.E. Rothman. 1992. Inhibition by brefeldin A of a Golgi membrane enzyme that catalyzes exchange of guanine nucleotide bound to ARF. *Nature.* 360:352-354.

Hemmings, B.A. 1997. PH domains--a universal membrane adapter. *Science.* 275:1899.

Hidalgo Carcedo, C., M. Bonazzi, S. Spano, G. Turacchio, A. Colanzi, A. Luini, and D. Corda. 2004. Mitotic Golgi partitioning is driven by the membrane-fissioning protein CtBP3/BARS. *Science.* 305:93-6.

Hoffman, G.R., P.B. Rahl, R.N. Collins, and R.A. Cerione. 2003. Conserved structural motifs in intracellular trafficking pathways: structure of the gammaCOP appendage domain. *Mol Cell.* 12:615-25.

Holthuis, J.C., and T.P. Levine. 2005. Lipid traffic: floppy drives and a superhighway. *Nat Rev Mol Cell Biol.* 6:209-20.

Hosaka, M., K. Toda, H. Takatsu, S. Torii, K. Murakami, and K. Nakayama. 1996. Structure and intracellular localization of mouse ADP-ribosylation factors type 1 to type 6 (ARF1-ARF6). *J Biochem.* 120:813-9.

Itoh, T., and P. De Camilli. 2004. Membrane trafficking: dual-key strategy. *Nature.* 429:141-3.

Jackson, C.L., and J.E. Casanova. 2000. Turning on ARF: the Sec7 family of guanine-nucleotide-exchange factors. *Trends Cell Biol.* 10:60-7.

Jones, S., G. Jedd, R.A. Kahn, A. Franzusoff, F. Bartolini, and N. Segev. 1999. Genetic interactions in yeast between Ypt GTPases and Arf guanine nucleotide exchangers. *Genetics.* 152:1543-56.

Kahn, R.A., and A.G. Gilman. 1984. Purification of a protein cofactor required for ADP-ribosylation of the stimulatory regulatory component of adenylate cyclase by cholera toxin. *J Biol Chem.* 259:6228-34.

Kawamoto, K., Y. Yoshida, H. Tamaki, S. Torii, C. Shinotsuka, S. Yamashina, and K. Nakayama. 2002. GBF1, a guanine nucleotide exchange factor for ADP-ribosylation factors, is localized to the cis-Golgi and involved in membrane association of the COPI coat. *Traffic.* 3:483-95.

Klarlund, J.K., A. Guilherme, J.J. Holik, J.V. Virbasius, A. Chawla, and M.P. Czech. 1997. Signaling by phosphoinositide-3,4,5-trisphosphate through proteins containing pleckstrin and Sec7 homology domains. *Science.* 275:1927-30.

Klausner, R.D., J.G. Donaldson, and J. Lippincott-Schwartz. 1992. Brefeldin A: insights into the control of membrane traffic and organelle structure. *J Cell Biol.* 116:1071-80.

Klumperman, J., A. Schweizer, H. Clausen, B.L. Tang, W. Hong, V. Oorschot, and H.P. Hauri. 1998. The recycling pathway of protein ERGIC-53 and dynamics of the ER-Golgi intermediate compartment. *J Cell Sci.* 111:3411-25.

Kreis, T.E., and H.F. Lodish. 1986. Oligomerization is essential for transport of vesicular stomatitis viral glycoprotein to the cell surface. *Cell.* 46:929-37.

Kuehn, M.J., J.M. Herrmann, and R. Schekman. 1998. COPII-cargo interactions direct protein sorting into ER-derived transport vesicles. *Nature.* 391:187-90.

Ladinsky, M.S., J.R. Kremer, P.S. Furcinitti, R.J. MaIntosh, and K.E. Howell. 1994. HVEM tomograpgy of the *trans*-Golgi network: structural insights and identification of a lace-like vesicle coat. *J. Cell Biol.* 127:29-38.

Ladinsky, M.S., D.N. Mastronarde, J.R. McIntosh, K.E. Howell, and L.A. Staehelin. 1999. Golgi structure in three dimensions: functional insights from the normal rat kidney cell. *J Cell Biol.* 144:1135-49.

Ladinsky, M.S., C.C. Wu, S. McIntosh, J.R. McIntosh, and K.E. Howell. 2002. Structure of the Golgi and distribution of reporter molecules at 20 degrees C reveals the complexity of the exit compartments. *Mol Biol Cell.* 13:2810-25.

Langille, S.E., V. Patki, J.K. Klarlund, J.M. Buxton, J.J. Holik, A. Chawla, S. Corvera, and M.P. Czech. 1999. ADP-ribosylation factor 6 as a target of guanine nucleotide exchange factor GRP1. *J Biol Chem.* 274:27099-104.

Lanoix, J., J. Ouwendijk, C.C. Lin, A. Stark, H.D. Love, J. Ostermann, and T. Nilsson. 1999. GTP hydrolysis by arf-1 mediates sorting and concentration of Golgi resident enzymes into functional COP I vesicles. *Embo J.* 18:4935-48.

Lavoie, C., J. Paiement, M. Dominguez, L. Roy, S. Dahan, J.N. Gushue, and J.J. Bergeron. 1999. Roles for alpha(2)p24 and COPI in endoplasmic reticulum cargo exit site formation. *J Cell Biol.* 146:285-99.

Lee, S.Y., M. Mansour, and B. Pohajdak. 2000. B2-1, a Sec7- and pleckstrin homology domain-containing protein, localizes to the Golgi complex. *Exp Cell Res.* 256:515-21.

Lee, S.Y., and B. Pohajdak. 2000. N-terminal targeting of guanine nucleotide exchange factors (GEF) for ADP ribosylation factors (ARF) to the Golgi. *J Cell Sci.* 113:1883-9.

Letourneur, F., E.C. Gaynor, S. Hennecke, C. Demolliere, R. Duden, S.D. Emr, H. Riezman, and P. Cosson. 1994. Coatomer is essential for retrival of dilysine-tagged proteins to the endoplasmic reticulum. *Cell.* 79:1199-1207.

Li, H., R. Adamik, G. Pacheco-Rodriguez, J. Moss, and M. Vaughan. 2003. Protein kinase A-anchoring (AKAP) domains in brefeldin A-inhibited guanine nucleotide-exchange protein 2 (BIG2). *Proc Natl Acad Sci U S A.* 100:1627-32.

Liang, J.O., and S. Kornfeld. 1997. Comparative activity of ADP-ribosylation factor family members in the early steps of coated vesicle formation on rat liver Golgi membranes. *J Biol Chem.* 272:4141-8.

Lippincott-Schwartz, J. 2001. The secretory membrane system studied in real-time. Robert Feulgen Prize Lecture, 2001. *Histochem Cell Biol.* 116:97-107.

Lippincott-Schwartz, J., N.B. Cole, and J.G. Donaldson. 1998. Building a secretory apparatus: role of ARF1/COPI in Golgi biogenesis and maintenance. *Histochem Cell Biol.* 109:449-62.

Lippincott-Schwartz, J., J.G. Donaldson, A. Schweizer, E.G. Berger, H.P. Hauri, L.C. Yuan, and R.D. Klausner. 1990. Microtubule-dependent retrograde transport of proteins into the ER in the presence of brefeldin A suggests an ER recycling pathway. *Cell.* 60:821-36.

Lippincott-Schwartz, J., L. Yuan, C. Tipper, M. Amherdt, L. Orci, and R.D. Klausner. 1991. Brefeldin A's effects on endosomes, lysosomes, and the TGN suggest a general mechanism for regulating organelle structure and membrane traffic. *Cell.* 67:601-16.

Lippincott-Schwartz, J., L.C. Yuan, J.S. Bonifacino, and R.D. Klausner. 1989. Rapid redistribution of Golgi proteins into the ER in cells treated with brefeldin A: evidence for membrane cycling from Golgi to ER. *Cell.* 56:801-13.

Lupashin, V., and E. Sztul. 2005. Golgi tethering factors. *Biochim Biophys Acta.* 1744:325-39.

Macia, E., M. Chabre, and M. Franco. 2001. Specificities for the small g proteins arf1 and arf6 of the guanine nucleotide exchange factors arno and efa6. *J Biol Chem.* 276:24925-30.

Majoul, I., K. Sohn, F.T. Wieland, R. Pepperkok, M. Pizza, J. Hillemann, and H.D. Soling. 1998. KDEL receptor (Erd2p)-mediated retrograde transport of the cholera toxin A subunit from the Golgi involves COPI, p23, and the COOH terminus of Erd2p. *J Cell Biol.* 143:601-12.

Majoul, I., M. Straub, S.W. Hell, R. Duden, and H.D. Soling. 2001. KDEL-cargo regulates interactions between proteins involved in COPI vesicle traffic: measurements in living cells using FRET. *Dev Cell.* 1:139-53.

Mancias, J.D., and J. Goldberg. 2005. Exiting the endoplasmic reticulum. *Traffic.* 6:278-85.

Mansour, S.J., J. Skaug, X.H. Zhao, J. Giordano, S.W. Scherer, and P. Melancon. 1999. p200 ARF-GEP1: a Golgi-localized guanine nucleotide exchange protein whose Sec7 domain is targeted by the drug brefeldin A. *Proc Natl Acad Sci U S A.* 96:7968-73.

Marsh, B.J., and K.E. Howell. 2002. The mammalian Golgi--complex debates. *Nat Rev Mol Cell Biol.* 3:789-95.

Marsh, B.J., D.N. Mastronarde, K.F. Buttle, K.E. Howell, and J.R. McIntosh. 2001. Organellar relationships in the Golgi region of the pancreatic beta cell line, HIT-T15, visualized by high resolution electron tomography. *Proc Natl Acad Sci U S A.* 98:2399-406.

Martinez-Menarguez, J.A., H.J. Geuze, J.W. Slot, and J. Klumperman. 1999. Vesicular tubular clusters between the ER and Golgi mediate concentration of soluble secretory proteins by exclusion from COPI-coated vesicles. *Cell.* 98:81-90.

Martinez-Menarguez, J.A., R. Prekeris, V.M. Oorschot, R. Scheller, J.W. Slot, H.J. Geuze, and J. Klumperman. 2001. Peri-Golgi vesicles contain retrograde but not anterograde proteins consistent with the cisternal progression model of intra-Golgi transport. *J Cell Biol.* 155:1213-24.

Matanis, T., A. Akhmanova, P. Wulf, E. Del Nery, T. Weide, T. Stepanova, N. Galjart, F. Grosveld, B. Goud, C.I. De Zeeuw, A. Barnekow, and C.C. Hoogenraad. 2002. Bicaudal-D regulates COPI-independent Golgi-ER transport by recruiting the dynein-dynactin motor complex. *Nat Cell Biol.* 4:986-92.

Matsuoka, K., L. Orci, M. Amherdt, S.Y. Bednarek, S. Hamamoto, R. Schekman, and T. Yeung. 1998. COPII-coated vesicle formation reconstituted with purified coat proteins and chemically defined liposomes. *Cell.* 93:263-75.

McNew, J.A., F. Parlati, R. Fukuda, R.J. Johnston, K. Paz, F. Paumet, T.H. Sollner, and J.E. Rothman. 2000. Compartmental specificity of cellular membrane fusion encoded in SNARE proteins. *Nature.* 407:153-9.

Meacci, E., S.C. Tsai, R. Adamik, J. Moss, and M. Vaughan. 1997. Cytohesin-1, a cytosolic guanine nucleotide-exchange protein for ADP- ribosylation factor. *Proc Natl Acad Sci U S A.* 94:1745-8.

Melançon, P., B.S. Glick, V. Malhotra, P.J. Weidman, T. Serafini, M.L. Gleason, L. Orci, and J.E. Rothman. 1987. Involvement of GTP-binding "G" proteins in transport through the Golgi stack. *Cell.* 51:1053-62.

Melançon, P. Zhao, X. and Lasell, T.R. (2004)) Large Arf-GEFs of the Golgi complex: In search of mechanisms for the cellular effects of BFA. In "ARF Family GTPases" Anne Ridley, Jon Frampton, Series Editors; Richard A. Kahn, Volume Editor), pp. 101-119, Kluwer Academic Publishers, 3300 AA Dordrecht, The Netherlands.

Miesenbock, G., and J.E. Rothman. 1995. The capacity to retrieve escaped ER proteins extends to the trans- most cisterna of the Golgi stack. *J Cell Biol.* 129:309-19.

Miller, E., B. Antonny, S. Hamamoto, and R. Schekman. 2002. Cargo selection into COPII vesicles is driven by the Sec24p subunit. *Embo J.* 21:6105-13.

Miller, E.A., T.H. Beilharz, P.N. Malkus, M.C. Lee, S. Hamamoto, L. Orci, and R. Schekman. 2003. Multiple cargo binding sites on the COPII subunit Sec24p ensure capture of diverse membrane proteins into transport vesicles. *Cell.* 114:497-509.

Mironov, A., A. Colanzi, M.G. Silletta, G. Fiucci, S. Flati, A. Fusella, R. Polishchuk, A. Mironov, Jr., G. Di Tullio, R. Weigert, V. Malhotra, D. Corda, M.A. De Matteis, and A. Luini. 1997. Role of NAD+ and ADP-ribosylation in the maintenance of the Golgi structure. *J Cell Biol.* 139:1109-18.

Mironov, A.A., G.V. Beznoussenko, P. Nicoziani, O. Martella, A. Trucco, H.S. Kweon, D. Di Giandomenico, R.S. Polishchuk, A. Fusella, P. Lupetti, E.G. Berger, W.J. Geerts, A.J. Koster, K.N. Burger, and A. Luini. 2001. Small cargo proteins and large aggregates can traverse the Golgi by a common mechanism without leaving the lumen of cisternae. *J Cell Biol.* 155:1225-38.

Mironov, A.A., A.A. Mironov, Jr., G.V. Beznoussenko, A. Trucco, P. Lupetti, J.D. Smith, W.J. Geerts, A.J. Koster, K.N. Burger, M.E. Martone, T.J. Deerinck, M.H. Ellisman, and A. Luini. 2003. ER-to-Golgi carriers arise through direct en bloc protrusion and multistage maturation of specialized ER exit domains. *Dev Cell.* 5:583-94.

Misumi, Y., Y. Misumi, K. Miki, A. Takatsuki, G. Tamura, and Y. Ikehara. 1986. Novel blockade by brefeldin A of intracellular transport of secretory proteins in cultured rat hepatocytes. *J Biol Chem.* 261:11398-403.

Miura, K., K.M. Jacques, S. Stauffer, A. Kubosaki, K. Zhu, D.S. Hirsch, J. Resau, Y. Zheng, and P.A. Randazzo. 2002. ARAP1: a point of convergence for Arf and Rho signaling. *Mol Cell.* 9:109-19.

Mogelsvang, S., N. Gomez-Ospina, J. Soderholm, B.S. Glick, and L.A. Staehelin. 2003. Tomographic evidence for continuous turnover of Golgi cisternae in Pichia pastoris. *Mol Biol Cell.* 14:2277-91.

Mogelsvang, S., B.J. Marsh, M.S. Ladinsky, and K.E. Howell. 2004. Predicting function from structure: 3D structure studies of the mammalian Golgi complex. *Traffic.* 5:338-45.

Morinaga, N., R. Adamik, J. Moss, and M. Vaughan. 1999. Brefeldin A inhibited activity of the sec7 domain of p200, a mammalian guanine nucleotide-exchange protein for ADP-ribosylation factors. *J Biol Chem.* 274:17417-23.

Morinaga, N., Y. Kaihou, N. Vitale, J. Moss, and M. Noda. 2001. Involvement of ADP-ribosylation factor 1 in cholera toxin-induced morphological changes of Chinese hamster ovary cells. *J Biol Chem.* 276:22838-43.

Morinaga, N., S.C. Tsai, J. Moss, and M. Vaughan. 1996. Isolation of a brefeldin A-inhibited guanine nucleotide-exchange protein for ADP ribosylation factor (ARF) 1 and ARF3 that contains a Sec7-like domain. *Proc Natl Acad Sci U S A.* 93:12856-60.

Moss, J., and M. Vaughan. 1998. Molecules in the ARF orbit. *J Biol Chem.* 273:21431-4.

Mossessova, E., L.C. Bickford, and J. Goldberg. 2003a. SNARE selectivity of the COPII coat. *Cell.* 114:483-95.

Mossessova, E., R.A. Corpina, and J. Goldberg. 2003b. Crystal structure of ARF1*Sec7 complexed with Brefeldin A and its implications for the guanine nucleotide exchange mechanism. *Mol Cell.* 12:1403-11.

Mossessova, E., J.M. Gulbis, and J. Goldberg. 1998. Structure of the guanine nucleotide exchange factor Sec7 domain of human arno and analysis of the interaction with ARF GTPase. *Cell.* 92:415-23.

Mouratou, B., V. Biou, A. Joubert, J. Cohen, D.J. Shields, N. Geldner, G. Jurgens, P. Melancon, and J. Cherfils. 2005. The domain architecture of large guanine nucleotide exchange factors for the small GTP-binding protein Arf. *BMC Genomics.* 6:20.

Muniz, M., C. Nuoffer, H.P. Hauri, and H. Riezman. 2000. The Emp24 complex recruits a specific cargo molecule into endoplasmic reticulum-derived vesicles. *J Cell Biol.* 148:925-30.

Munro, S. 1995. An investigation of the role of transmembrane domains in Golgi protein retention. *Embo J.* 14:4695-704.

Munro, S. 2003. Lipid rafts: elusive or illusive? *Cell.* 115:377-88.

Nagel, W., L. Zeitlmann, P. Schilcher, C. Geiger, J. Kolanus, and W. Kolanus. 1998. Phosphoinositide 3-OH kinase activates the beta2 integrin adhesion pathway and induces membrane recruitment of cytohesin-1. *J Biol Chem.* 273:14853-61.

Nehls, S., E.L. Snapp, N.B. Cole, K.J. Zaal, A.K. Kenworthy, T.H. Roberts, J. Ellenberg, J.F. Presley, E. Siggia, and J. Lippincott-Schwartz. 2000. Dynamics and retention of misfolded proteins in native ER membranes. *Nat Cell Biol.* 2:288-95.

Nickel, W., J. Malsam, K. Gorgas, M. Ravazzola, N. Jenne, J.B. Helms, and F.T. Wieland. 1998. Uptake by COPI-coated vesicles of both anterograde and retrograde cargo is inhibited by GTPgammaS in vitro. *J Cell Sci.* 111 (Pt 20):3081-90.

Nickel, W., and F.T. Wieland. 1998. Biosynthetic protein transport through the early secretory pathway. *Histochem Cell Biol.* 109:477-86.

Nie, Z., D.S. Hirsch, and P.A. Randazzo. 2003. Arf and its many interactors. *Curr Opin Cell Biol.* 15:396-404.

Niu, T.K., A.C. Pfeifer, J. Lippincott-Schwartz, and C.L. Jackson. 2005. Dynamics of GBF1, a Brefeldin A-Sensitive Arf1 Exchange Factor at the Golgi. *Mol Biol Cell.* 16:1213-22.

Novick, P., C. Field, and R. Schekman. 1980. Identification of 23 complementation groups required for post- translational events in the yeast secretory pathway. *Cell.* 21:205-15.

Oka, T., and M. Krieger. 2005. Multi-component protein complexes and Golgi membrane trafficking. *J Biochem (Tokyo).* 137:109-14.

Oprins, A., R. Duden, T.E. Kreis, H.J. Geuze, and J.W. Slot. 1993. Beta-COP localizes mainly to the cis-Golgi side in exocrine pancreas. *J Cell Biol.* 121:49-59.

Oprins, A., C. Rabouille, G. Posthuma, J. Klumperman, H.J. Geuze, and J.W. Slot. 2001. The ER to Golgi interface is the major concentration site of secretory proteins in the exocrine pancreatic cell. *Traffic.* 2:831-8.

Orci, L., B.S. Glick, and J.E. Rothman. 1986. A new type of coated vesicular carrier that appears not to contain clathrin: its possible role in protein transport within the Golgi stack. *Cell.* 46:171-84.

Orci, L., D.J. Palmer, M. Ravazzola, A. Perrelet, M. Amherdt, and J.E. Rothman. 1993. Budding from Golgi membranes requires the coatomer complex of non- clathrin coat proteins. *Nature.* 362:648-52.

Orci, L., M. Ravazzola, M. Amherdt, A. Perrelet, S.K. Powell, D.L. Quinn, and H.P. Moore. 1987. The trans-most cisternae of the Golgi complex: a compartment for sorting of secretory and plasma membrane proteins. *Cell.* 51:1039-51.

Orci, L., M. Stamnes, M. Ravazzola, M. Amherdt, A. Perrelet, T.H. Sollner, and J.E. Rothman. 1997. Bidirectional transport by distinct populations of COPI-coated vesicles. *Cell.* 90:335-49.

Orci, L., M. Tagaya, M. Amherdt, A. Perrelet, J.G. Donaldson, S.J. Lippincott, R.D. Klausner, and J.E. Rothman. 1991. Brefeldin A, a drug that blocks secretion, prevents the assembly of non-clathrin-coated buds on Golgi cisternae. *Cell.* 64:1183-95.

Ostermann, J., L. Orci, K. Tani, M. Amherdt, M. Ravazzola, Z. Elazar, and J.E. Rothman. 1993. Stepwise assembly of functionally active transport vesicles. *Cell.* 75:1015-25.

Padilla, P.I., G. Pacheco-Rodriguez, J. Moss, and M. Vaughan. 2004. Nuclear localization and molecular partners of BIG1, a brefeldin A-inhibited guanine nucleotide-exchange protein for ADP-ribosylation factors. *Proc Natl Acad Sci U S A.* 101:2752-7.

Palade, G. 1975. Intracellular aspects of the process of protein synthesis. *Science.* 189:347-58.

Paris, S., S. Beraud-Dufour, S. Robineau, J. Bigay, B. Antonny, M. Chabre, and P. Chardin. 1997. Role of protein-phospholipid interactions in the activation of ARF1 by the guanine nucleotide exchange factor Arno. *J Biol Chem.* 272:22221-6.

Pasqualato, S., L. Renault, and J. Cherfils. 2002. Arf, Arl, Arp and Sar proteins: a family of GTP-binding proteins with a structural device for 'front-back' communication. *EMBO Rep.* 3:1035-41.

Pelham, H.R. 2001. Traffic through the Golgi apparatus. *J Cell Biol.* 155:1099-101.

Pepperkok, R., J. Scheel, H. Horstmann, H.P. Hauri, G. Griffiths, and T.E. Kreis. 1993. Beta-COP is essential for biosynthetic membrane transport from the endoplasmic reticulum to the Golgi complex in vivo. *Cell.* 74:71-82.

Pepperkok, R., J.A. Whitney, M. Gomez, and T.E. Kreis. 2000. COPI vesicles accumulating in the presence of a GTP restricted arf1 mutant are depleted of anterograde and retrograde cargo. *J Cell Sci.* 113 (Pt 1):135-44.

Peter, F., H. Plutner, H. Zhu, T.E. Kreis, and W.E. Balch. 1993. Beta-COP is essential for transport of protein from the endoplasmic reticulum to the Golgi in vitro. *J Cell Biol.* 122:1155-67.

Peters, P.J., V.W. Hsu, C.E. Ooi, D. Finazzi, S.B. Teal, V. Oorschot, J.G. Donaldson, and R.D. Klausner. 1995. Overexpression of wild-type and mutant ARF1 and ARF6: distinct perturbations of nonoverlapping membrane compartments. *J Cell Biol.* 128:1003-17.

Peyroche, A., B. Antonny, S. Robineau, J. Acker, J. Cherfils, and C.L. Jackson. 1999. Brefeldin A acts to stabilize an abortive ARF-GDP-Sec7 domain protein complex: involvement of specific residues of the Sec7 domain. *Mol Cell.* 3:275-85.

Peyroche, A., R. Courbeyrette, A. Rambourg, and C.L. Jackson. 2001. The ARF exchange factors Gea1p and Gea2p regulate Golgi structure and function in yeast. *J Cell Sci.* 114:2241-53.

Peyroche, A., Paris, S., Jackson, C. 1996. Nucleotide exchange on ARF mediated by yeast Gea1 protein. *Nature.* 384:479-481.

Pfeffer, S. 2001. Vesicle tethering factors united. *Mol Cell.* 8:729-30.

Pfeffer, S., and D. Aivazian. 2004. Targeting Rab GTPases to distinct membrane compartments. *Nat Rev Mol Cell Biol.* 5:886-96.

Poon, P.P., D. Cassel, A. Spang, M. Rotman, E. Pick, R.A. Singer, and G.C. Johnston. 1999. Retrograde transport from the yeast Golgi is mediated by two ARF GAP proteins with overlapping function. *Embo J.* 18:555-64.

Presley, J.F., N.B. Cole, T.A. Schroer, K. Hirschberg, K.J. Zaal, and J. Lippincott-Schwartz. 1997. ER-to-Golgi transport visualized in living cells. *Nature*. 389:81-5.

Presley, J.F., T.H. Ward, A.C. Pfeifer, E.D. Siggia, R.D. Phair, and J. Lippincott-Schwartz. 2002. Dissection of COPI and Arf1 dynamics in vivo and role in Golgi membrane transport. *Nature*. 417:187-93.

Puertollano, R., R.C. Aguilar, I. Gorshkova, R.J. Crouch, and J.S. Bonifacino. 2001a. Sorting of mannose 6-phosphate receptors mediated by the GGAs. *Science*. 292:1712-6.

Puertollano, R., P.A. Randazzo, J.F. Presley, L.M. Hartnell, and J.S. Bonifacino. 2001b. The GGAs promote ARF-dependent recruitment of clathrin to the TGN. *Cell*. 105:93-102.

Rambourg, A., and Y. Clermont. 1990. Three-dimensional electron microscopy: structure of the Golgi apparatus. *Eur J Cell Biol*. 51:189-200.

Randazzo, P.A., and D.S. Hirsch. 2004. Arf GAPs: multifunctional proteins that regulate membrane traffic and actin remodelling. *Cell Signal*. 16:401-13.

Randazzo, P.A., Z. Nie, K. Miura, and V.W. Hsu. 2000. Molecular aspects of the cellular activities of ADP-ribosylation factors. *Sci STKE*. 2000:RE1.

Randazzo, P.A., Y.C. Yang, C. Rulka, and R.A. Kahn. 1993. Activation of ADP-ribosylation factor by Golgi membranes. *J. Biol. Chem.* 268:9555-9563.

Rein, U., U. Andag, R. Duden, H.D. Schmitt, and A. Spang. 2002. ARF-GAP-mediated interaction between the ER-Golgi v-SNAREs and the COPI coat. *J Cell Biol*. 157:395-404.

Renault, L., P. Christova, B. Guibert, S. Pasqualato, and J. Cherfils. 2002. Mechanism of domain closure of Sec7 domains and role in BFA sensitivity. *Biochemistry*. 41:3605-12.

Renault, L., B. Guibert, and J. Cherfils. 2003. Structural snapshots of the mechanism and inhibition of a guanine nucleotide exchange factor. *Nature*. 426:525-30.

Robinson, M.S. 2004. Adaptable adaptors for coated vesicles. *Trends Cell Biol*. 14:167-74.

Robinson, M.S., and T.E. Kreis. 1992. Recruitment of coat proteins onto Golgi membranes in intact and permeabilized cells: effects of brefeldin A and G protein activators. *Cell*. 69:129-38.

Roth, M.G. 1999. Lipid regulators of membrane traffic through the Golgi complex. *Trends Cell Biol.* 9:174-9.

Rothman, J.E. 1994. Mechanisms of intracellular protein transport. *Nature.* 372:55-63.

Rothman, J.E., and L. Orci. 1992. Molecular dissection of the secretory pathway. *Nature.* 355:409-15.

Rothman, J.E., and G. Warren. 1994. Implications of the SNARE hypothesis for intracellular membrane topology and dynamics. *Curr Biol.* 4:220-33.

Rothman, J.E., and F.T. Wieland. 1996. Protein sorting by transport vesicles. *Science.* 272:227-34.

Sandvig, K., and B. van Deurs. 2002. Membrane traffic exploited by protein toxins. *Annu Rev Cell Dev Biol.* 18:1-24.

Sannerud, R., J. Saraste, and B. Goud. 2003. Retrograde traffic in the biosynthetic-secretory route: pathways and machinery. *Curr Opin Cell Biol.* 15:438-45.

Saraste, J., and E. Kuismanen. 1992. Pathways of protein sorting and membrane traffic between the rough endoplasmic reticulum and the Golgi complex. *Semin Cell Biol.* 3:343-55.

Saraste, J., G.E. Palade, and M.G. Farquhar. 1986. Temperature-sensitive steps in the transport of secretory proteins through the Golgi complex in exocrine pancreatic cells. *Proc Natl Acad Sci U S A.* 83:6425-9.

Saraste, J., G.E. Palade, and M.G. Farquhar. 1987. Antibodies to rat pancreas Golgi subfractions: identification of a 58- kD cis-Golgi protein. *J Cell Biol.* 105:2021-9.

Sata, M., J.G. Donaldson, J. Moss, and M. Vaughan. 1998. Brefeldin A-inhibited guanine nucleotide-exchange activity of Sec7 domain from yeast Sec7 with yeast and mammalian ADP ribosylation factors. *Proc Natl Acad Sci U S A.* 95:4204-8.

Sata, M., J. Moss, and M. Vaughan. 1999. Structural basis for the inhibitory effect of brefeldin A on guanine nucleotide-exchange proteins for ADP-ribosylation factors. *Proc Natl Acad Sci U S A.* 96:2752-7.

Sato, K. 2004. COPII Coat Assembly and Selective Export from the Endoplasmic Reticulum. *J Biochem (Tokyo).* 136:755-60.

Scales, S.J., R. Pepperkok, and T.E. Kreis. 1997. Visualization of ER-to-Golgi transport in living cells reveals a sequential mode of action for COPII and COPI. *Cell.* 90:1137-48.

Scheel, J., R. Pepperkok, M. Lowe, G. Griffiths, and T.E. Kreis. 1997. Dissociation of coatomer from membranes is required for brefeldin A-induced transfer of Golgi enzymes to the endoplasmic reticulum. *J Cell Biol.* 137:319-33.

Sciaky, N., J. Presley, C. Smith, K.J. Zaal, N. Cole, J.E. Moreira, M. Terasaki, E. Siggia, and J. Lippincott-Schwartz. 1997. Golgi tubule traffic and the effects of brefeldin A visualized in living cells. *J Cell Biol.* 139:1137-55.

Seabra, M.C., and C. Wasmeier. 2004. Controlling the location and activation of Rab GTPases. *Curr Opin Cell Biol.* 16:451-7.

Serafini, T., G. Stenbeck, A. Brecht, F. Lottspeich, L. Orci, J.E. Rothman, and F.T. Wieland. 1991. A coat subunit of Golgi-derived non-clathrin-coated vesicles with homology to the clathrin-coated vesicle coat protein beta-adaptin. *Nature.* 349:215-20.

Shima, D.T., S.J. Scales, T.E. Kreis, and R. Pepperkok. 1999. Segregation of COPI-rich and anterograde-cargo-rich domains in endoplasmic-reticulum-to-Golgi transport complexes. *Curr Biol.* 9:821-4.

Shin, H.W., N. Morinaga, M. Noda, and K. Nakayama. 2004. BIG2, a guanine nucleotide exchange factor for ADP-ribosylation factors: its localization to recycling endosomes and implication in the endosome integrity. *Mol Biol Cell.* 15:5283-94.

Shin, H.W., and K. Nakayama. 2004. Dual control of membrane targeting by PtdIns(4)P and ARF. *Trends Biochem Sci.* 29:513-5.

Shin, O.H., A.D. Couvillon, and J.H. Exton. 2001. Arfophilin is a common target of both class II and class III ADP- ribosylation factors. *Biochemistry.* 40:10846-52.

Shin, O.H., and J.H. Exton. 2001. Differential binding of arfaptin 2/POR1 to ADP-ribosylation factors and Rac1. *Biochem Biophys Res Commun.* 285:1267-73.

Shinotsuka, C., S. Waguri, M. Wakasugi, Y. Uchiyama, and K. Nakayama. 2002a. Dominant-negative mutant of BIG2, an ARF-guanine nucleotide exchange factor, specifically affects membrane trafficking from the trans-Golgi network through inhibiting membrane association of AP-1 and GGA coat proteins. *Biochem Biophys Res Commun.* 294:254-60.

Shinotsuka, C., Y. Yoshida, K. Kawamoto, H. Takatsu, and K. Nakayama. 2002b. Overexpression of an ADP-ribosylation factor-guanine nucleotide exchange factor, BIG2, uncouples brefeldin A-induced adaptor protein-1 coat dissociation and membrane tubulation. *J Biol Chem.* 277:9468-73.

Short, B., C. Preisinger, J. Schaletzky, R. Kopajtich, and F.A. Barr. 2002. The Rab6 GTPase regulates recruitment of the dynactin complex to Golgi membranes. *Curr Biol.* 12:1792-5.

Siggia, E.D., J. Lippincott-Schwartz, and S. Bekiranov. 2000. Diffusion in inhomogeneous media: theory and simulations applied to whole cell photobleach recovery. *Biophys J.* 79:1761-70.

Someya, A., M. Sata, K. Takeda, G. Pacheco-Rodriguez, V.J. Ferrans, J. Moss, and M. Vaughan. 2001. ARF-GEP100, a guanine nucleotide-exchange protein for ADP-ribosylation factor 6. *Proc Natl Acad Sci U S A.* 98:2413-8.

Spang, A., J.M. Herrmann, S. Hamamoto, and R. Schekman. 2001. The ADP ribosylation factor-nucleotide exchange factors Gea1p and Gea2p have overlapping, but not redundant functions in retrograde transport from the Golgi to the endoplasmic reticulum. *Mol Biol Cell.* 12:1035-45.

Spang, A., K. Matsuoka, S. Hamamoto, R. Schekman, and L. Orci. 1998. Coatomer, Arf1p, and nucleotide are required to bud coat protein complex I-coated vesicles from large synthetic liposomes. *Proc Natl Acad Sci U S A.* 95:11199-204.

Spano, S., M.G. Silletta, A. Colanzi, S. Alberti, G. Fiucci, C. Valente, A. Fusella, M. Salmona, A. Mironov, A. Luini, D. Corda, and S. Spanfo. 1999. Molecular cloning and functional characterization of brefeldin A-ADP- ribosylated substrate. A novel protein involved in the maintenance of the Golgi structure. *J Biol Chem.* 274:17705-10.

Springer, S., A. Spang, and R. Schekman. 1999. A primer on vesicle budding. *Cell.* 97:145-8.

Stearns, T., M.C. Willingham, D. Botstein, and R.A. Kahn. 1990. ADP-ribosylation factor is functionally and physically associated with the Golgi complex. *Proc Natl Acad Sci U S A.* 87:1238-42.

Steinmann, T., N. Geldner, M. Grebe, S. Mangold, C.L. Jackson, S. Paris, L. Galweiler, K. Palme, and G. Jurgens. 1999. Coordinated polar localization of auxin efflux carrier PIN1 by GNOM ARF GEF. *Science.* 286:316-8.

Stephens, D.J., N. Lin-Marq, A. Pagano, R. Pepperkok, and J.P. Paccaud. 2000. COPI-coated ER-to-Golgi transport complexes segregate from COPII in close proximity to ER exit sites. *J Cell Sci.* 113:2177-85.

Stephens, D.J., and R. Pepperkok. 2001. Illuminating the secretory pathway: when do we need vesicles? *J Cell Sci.* 114:1053-9.

Stephens, D.J., and R. Pepperkok. 2002. Imaging of procollagen transport reveals COPI-dependent cargo sorting during ER-to-Golgi transport in mammalian cells. *J Cell Sci.* 115:1149-60.

Storrie, B., R. Pepperkok, and T. Nilsson. 2000. Breaking the COPI monopoly on Golgi recycling. *Trends Cell Biol.* 10:385-91.

Stuven, E., A. Porat, F. Shimron, E. Fass, D. Kaloyanova, B. Brugger, F.T. Wieland, Z. Elazar, and J.B. Helms. 2003. Intra-Golgi protein transport depends on a cholesterol balance in the lipid membrane. *J Biol Chem.* 278:53112-22.

Suh, Y.G., J.K. Jung, S.Y. Seo, K.H. Min, D.Y. Shin, Y.S. Lee, S.H. Kim, and H.J. Park. 2002. Total synthesis of (+)-Brefeldin A. *J Org Chem.* 67:4127-37.

Szul, T., R. Garcia-Mata, E. Brandon, S. Shestopal, C. Alvarez, and E. Sztul. 2005. Dissection of membrane dynamics of the ARF-guanine nucleotide exchange factor GBF1. *Traffic.* 6:374-85.

Tang, B.L., T. Zhang, D.Y. Low, E.T. Wong, H. Horstmann, and W. Hong. 2000. Mammalian homologues of yeast sec31p. An ubiquitously expressed form is localized to endoplasmic reticulum (ER) exit sites and is essential for ER-Golgi transport. *J Biol Chem.* 275:13597-604.

Teasdale, R.D., and M.R. Jackson. 1996. Signal-mediated sorting of membrane proteins between the endoplasmic reticulum and the golgi apparatus. *Annu Rev Cell Dev Biol.* 12:27-54.

Togawa, A., N. Morinaga, M. Ogasawara, J. Moss, and M. Vaughan. 1999. Purification and cloning of a brefeldin A-inhibited guanine nucleotide- exchange protein for ADP-ribosylation factors. *J Biol Chem.* 274:12308-15.

Torii, S., T. Banno, T. Watanabe, Y. Ikehara, K. Murakami, and K. Nakayama. 1995. Cytotoxicity of brefeldin A correlates with its inhibitory effect on membrane binding of COP coat proteins. *J Biol Chem.* 270:11574-80.

Trucco, A., R.S. Polishchuk, O. Martella, A. Di Pentima, A. Fusella, D. Di Giandomenico, E. San Pietro, G.V. Beznoussenko, E.V. Polishchuk, M. Baldassarre, R. Buccione, W.J. Geerts, A.J. Koster, K.N. Burger, A.A. Mironov, and A. Luini. 2004. Secretory traffic triggers the formation of tubular continuities across Golgi sub-compartments. *Nat Cell Biol.* 6:1071-81.

Tsai, S.C., R. Adamik, R.S. Haun, J. Moss, and M. Vaughan. 1992. Differential interaction of ADP-ribosylation factors 1, 3, and 5 with rat brain Golgi membranes. *Proc Natl Acad Sci U S A.* 89:9272-6.

van Meer, G. 1998. Lipids of the Golgi membrane. *Trends Cell Biol.* 8:29-33.

Velloso, L.M., K. Svensson, G. Schneider, R.F. Pettersson, and Y. Lindqvist. 2002. Crystal structure of the carbohydrate recognition domain of p58/ERGIC-53, a protein

involved in glycoprotein export from the endoplasmic reticulum. *J Biol Chem.* 277:15979-84.

Venkateswarlu, K., P.B. Oatey, J.M. Tavare, and P.J. Cullen. 1998. Insulin-dependent translocation of ARNO to the plasma membrane of adipocytes requires phosphatidylinositol 3-kinase. *Curr Biol.* 8:463-6.

Wang, Y.J., J. Wang, H.Q. Sun, M. Martinez, Y.X. Sun, E. Macia, T. Kirchhausen, J.P. Albanesi, M.G. Roth, and H.L. Yin. 2003. Phosphatidylinositol 4 phosphate regulates targeting of clathrin adaptor AP-1 complexes to the Golgi. *Cell.* 114:299-310.

Ward, T.H., R.S. Polishchuk, S. Caplan, K. Hirschberg, and J. Lippincott-Schwartz. 2001. Maintenance of Golgi structure and function depends on the integrity of ER export. *J Cell Biol.* 155:557-70.

Waters, M.G., D.O. Clary, and J.E. Rothman. 1992. A novel 115-kD peripheral membrane protein is required for intercisternal transport in the Golgi stack. *J Cell Biol.* 118:1015-26.

Waters, M.G., and S.R. Pfeffer. 1999. Membrane tethering in intracellular transport. *Curr Opin Cell Biol.* 11:453-9.

Waters, M.G., T. Serafini, and J.E. Rothman. 1991. 'Coatomer': a cytosolic protein complex containing subunits of non- clathrin-coated Golgi transport vesicles. *Nature.* 349:248-51.

Watt, S.A., G. Kular, I.N. Fleming, C.P. Downes, and J.M. Lucocq. 2002. Subcellular localization of phosphatidylinositol 4,5-bisphosphate using the pleckstrin homology domain of phospholipase C delta1. *Biochem J.* 363:657-66.

Weigert, R., A. Colanzi, A. Mironov, R. Buccione, C. Cericola, M.G. Sciulli, G. Santini, S. Flati, A. Fusella, J.G. Donaldson, M. Di Girolamo, D. Corda, M.A. De Matteis, and A. Luini. 1997. Characterization of chemical inhibitors of brefeldin A-activated mono-ADP-ribosylation. *J Biol Chem.* 272:14200-7.

Weigert, R., M.G. Silletta, S. Spano, G. Turacchio, C. Cericola, A. Colanzi, S. Senatore, R. Mancini, E.V. Polishchuk, M. Salmona, F. Facchiano, K.N. Burger, A. Mironov, A. Luini, and D. Corda. 1999. CtBP/BARS induces fission of Golgi membranes by acylating lysophosphatidic acid. *Nature.* 402:429-33.

Weissman, J.T., H. Plutner, and W.E. Balch. 2001. The mammalian guanine nucleotide exchange factor mSec12 is essential for activation of the Sar1 GTPase directing endoplasmic reticulum export. *Traffic.* 2:465-75.

White, J., L. Johannes, F. Mallard, A. Girod, S. Grill, S. Reinsch, P. Keller, B. Tzschaschel, A. Echard, B. Goud, and E.H. Stelzer. 1999. Rab6 coordinates a novel Golgi to ER retrograde transport pathway in live cells. *J Cell Biol.* 147:743-60.

Whyte, J.R., and S. Munro. 2002. Vesicle tethering complexes in membrane traffic. *J Cell Sci.* 115:2627-37.

Wood, S.A., J.E. Park, and W.J. Brown. 1991. Brefeldin A causes a microtubule-mediated fusion of the trans-Golgi network and early endosomes. *Cell.* 67:591-600.

Wu, C.C., J.R. Yates, 3rd, M.C. Neville, and K.E. Howell. 2000. Proteomic analysis of two functional states of the Golgi complex in mammary epithelial cells. *Traffic.* 1:769-82.

Xu, D., and J.C. Hay. 2004. Reconstitution of COPII vesicle fusion to generate a pre-Golgi intermediate compartment. *J Cell Biol.* 167:997-1003.

Yamaji, R., R. Adamik, K. Takeda, A. Togawa, G. Pacheco-Rodriguez, V.J. Ferrans, J. Moss, and M. Vaughan. 2000. Identification and localization of two brefeldin A-inhibited guanine nucleotide-exchange proteins for ADP-ribosylation factors in a macromolecular complex. *Proc Natl Acad Sci U S A.* 97:2567-72.

Yan, J.P., M.E. Colon, L.A. Beebe, and P. Melancon. 1994. Isolation and characterization of mutant CHO cell lines with compartment-specific resistance to brefeldin A. *J. Cell. Biol.* 126:65-75.

Yang, J.S., S.Y. Lee, M. Gao, S. Bourgoin, P.A. Randazzo, R.T. Premont, and V.W. Hsu. 2002. ARFGAP1 promotes the formation of COPI vesicles, suggesting function as a component of the coat. *J Cell Biol.* 159:69-78.

Ying, M., S. Grimmer, T.G. Iversen, B. Van Deurs, and K. Sandvig. 2003. Cholesterol loading induces a block in the exit of VSVG from the TGN. *Traffic.* 4:772-84.

Zaal, K.J., C.L. Smith, R.S. Polishchuk, N. Altan, N.B. Cole, J. Ellenberg, K. Hirschberg, J.F. Presley, T.H. Roberts, E. Siggia, R.D. Phair, and J. Lippincott-Schwartz. 1999. Golgi membranes are absorbed into and reemerge from the ER during mitosis. *Cell.* 99:589-601.

Zakrzewska, E., M. Perron, A. Laroche, and D. Pallotta. 2003. A role for GEA1 and GEA2 in the organization of the actin cytoskeleton in Saccharomyces cerevisiae. *Genetics.* 165:985-95.

Zhao, L., J.B. Helms, B. Brugger, C. Harter, B. Martoglio, R. Graf, J. Brunner, and F.T. Wieland. 1997. Direct and GTP-dependent interaction of ADP ribosylation factor 1 with coatomer subunit beta. *Proc Natl Acad Sci U S A.* 94:4418-23.

Zhao, X., T.K. Lasell, and P. Melancon. 2002. Localization of large ADP-ribosylation factor-guanine nucleotide exchange factors to different Golgi compartments: evidence for distinct functions in protein traffic. *Mol Biol Cell.* 13:119-33.

Zhu, Y., B. Doray, A. Poussu, V.P. Lehto, and S. Kornfeld. 2001. Binding of GGA2 to the lysosomal enzyme sorting motif of the mannose 6- phosphate receptor. *Science.* 292:1716-8.